CHAPTER ONE

INTRODUCTION

1.1 Background of the Study

The discovery of new materials with unique properties often leads to new technology. After the discovery of conductive polymers at the end of the 1970s, it opened up a whole new research, which eventually led to new technology of plastic electronics (Chiang *et al*., 1978). When interesting material properties are observed in the laboratory, efforts are made to understand their mechanisms, which lead to the fine control of the fabrication process of this new and potentially important material (Aga and Mu, 2010).

Polymers are known to have good insulating properties and are one of the most used materials in modern world. They are widely used in electrical and electronic applications. In early works, polymers have been used as insulators because of their high resistivity and dielectric properties. Polymer – based insulators are used in electrical equipment to separate electrical conductors without passing current through themselves. The insulator applications of polymers include printed circuit boards, wire encapsulants, corrosion protective electronic devices and cable sheathing materials (Alias *et al*., 2013, Hosseini *et al*., 2011, Hasanov *et al*., 2011)

1.2 Statement of the problem

Traditionally most known conductive materials have been inorganic. Metals such as copper and aluminum are the most common conductive materials and have high electrical conductivity. Since the discovery of conductivity, studies have focused primarily on inorganic conductive materials. The prospect of replacing costly and labour–intensive inorganic device with cheaper and more flexible organic electronic materials entered a new era.

Organic conductive polymers have a higher resistance and therefore conduct electricity poorly and inefficiently as compared to inorganic conductors. Researchers currently are exploring ways of doping organic semiconductors with relatively small amounts of conductive metals to boost conductivity. Organic molecular materials and conducting polymers offer a multi disciplinary challenge to Chemists, Physicists, Material Scientists and Electronic Engineers and have a greater potential for commercialization. The conductive polymers have aroused wide attention among Scientists, then developing the conductive polymers.

Most polymers do not possess natural intrinsic properties that will be enough for them to be used as semiconductors. In the world trend of industrial growth where polymers seem to be replacing all semiconductors because of their availability, durability, recyclability and reduced cost, attention is being strongly given to their improvement for this essential function and applications hence the need for this research.

Conductive polymers such as poly (o- phenylenediamine) continue to be the focus of active research in diverse fields including electronics. This discovery opened a new era of current research and device design.

1.3 Aim and Objectives of the study

The aim of this study is to determine the electrochromic performance of poly o-phenylenediamine thin films prepared by electropolymerization. The objectives include to:

1. synthesize the poly(o- phenylenediamine) by chemical oxidation method.
2. prepare the polymer thin film samples
3. characterize the prepared polymer samples with Uv – Vis, spectroscopy, SEM,TGA,BET methods, Raman spectroscopy, XRD, Profilometry and Four point probe to determine the existing parameters of the polymer

4. determine the electrochromic performance of the prepared thinfilms and other properties of poly (o- phenylenediamine)
5. deduce the possible electronic applications of the polymer from the obtained data.

1.4 Scope of study

The scope of this study covers the synthesis of the poly (o- phenylenediamine) using potassium dichromate, an oxidant (oxidizing agent) and electropolymerization using phosphate buffer, and determination of the electrochromic performances and other properties of the polymer.

1.5 Significance of the study

This study provides more information to the Scientists and Society at large on the electrochromic performances and other properties of poly (o- phenylendimine) and its possible applications in the field of electronics.

It also provides more interest and concern on the use advancement of conducting polymers placing them as good candidates for use in electronics.

Finally, it gives information to the future researchers who may wish to investigate or improve on this study for better results and more applications.

CHAPTER TWO

LITERATURE REVIEW

2.1 Conceptual Framework

2.1.1 Polymer

Polymer means many monomers. A monomer is a molecule that is able to bond in long chains. Monomers are small molecules which may be joined together in a repeating fashion to form more complex molecules called polymers. This linking up of monomers is called polymerization. Polymerization is therefore the process of covalently bonding the smaller monomers into the polymer (Majeed *et al*., 2013)

A polymer formed by one type of monomers is called a homopolymer while a polymer formed by more than one type of monomer is called heteropolymer / copolymer. Electroactive polymers (EAPs) are polymers that exhibit a change in size or shape when stimulated by an electric field. A polymer may be natural or synthetic. Examples of natural polymers are shellac, amber, wool, silk and natural rubber. A variety of other natural polymers exist such as cellulose which is the main constitutuent of wood and paper. Synthetic polymers are human made polymers which include synthetic rubber, phenol, formaldehyde resin (or Bakelite), neoprene, nylon, polyvinyln chloride, polyethene among others. Polymers have several advantages such as easy processing, low cost, flexibility, high strength and good mechanical properties.

Since its discovery, polymers have been extensively studied as new materials for electronic and optoelectronic application. The demands made on electronic components are constantly increasing..

Organic electronics is a field of material science concerning the design, synthesis, characterization and application of organic small molecules or polymers that show desirable electronic properties such as conductivity. Organic electronic materials are constructed from

organic (carbon - based) small molecules or polymers using synthetic strategies developed in the context of organic and polymer chemistry. One of the benefits of organic electronics is their low cost compared to traditional inorganic electronics

2.1.2 Conductive Polymers

The conductivity of certain organic polymers can be raised to metallic levels by chemical or electrochemical p–doping (oxidation) or n–doping (reduction). Synthesized conductive polymers exhibit very low conductivities.

Electrically conductive polymers can be divided into two groups depending on the type of charge transport by the carriers responsible for it ionically conductive and electronically conductive. An example of an ionically conductive polymer is poly (ethylene oxide) or PEO which contains lithium perchlorate ($LiClO_4$). It is used as a solid state electrolyte in batteries, the lithium – polymer system being the first true solid – state battery (Radoslav, 1996).

Electronically conductive polymers can be further divided into filled and intrinsically conductive polymers (ICPs). Filled systems are rendered electrically conductive by the incorporation (doping) of highly conductive metals into the polymer. Intrinsically conductive polymers do not incorporate any conductive additives. They gain their electrical conductivity through a property known as conjugation. Conjugation means that the polymer molecules have alternating double and single bonds and this provides a path way for free electron charge carriers. The most extensively studied conductive polymers include polyaniline, polythiophene, polypyrrole and polyacetylene (Chiang *et al*., 1977).

Conductivity can be defined simply by Ohm's law

$$V = IR \qquad 2.1$$

where R is the resistance, I is the current and V is the voltage present in the material.

Thus, from the relationship, conductivity depends on the number of charge carriers (number of electrons) in the material and their mobility. The versatility of polymer materials is expanding because of the introduction of electro – active behaviour into the characteristics of some of them. The most exciting development in this area is related to the discovery of intrinsically conductive polymers or conjugated polymers. Organic semiconductor is an organic material in the semiconductor properties. That is to say that the electrical conductivity is between insulator and metals.

Conducting polymers have been a popular area of investigation because of electrical and electrochemical properties and their potential applications in various areas. Among these are corrosion protection (Hosseini *et al*., 2011 and Hasanov *et al*., 2011), electronic devices such as diodes, capacitors or transistors (Nayak *et al*., 2010; Kim *et al*., 2011; Knoll and Thamer, 2011), electrochromic displays (Pages *et al*., 2001), rechargeable batteries and solid electrolytes (Chen *et al*., 2011; Wang *et al*., 2011; Erokhin *et al*., 2006), electrostatic materials (Yuan *et al*., 2007), electromechanical actuators (Yan *et al*., 2003) sensors or biosensors (Lange and Mirsky, 2011; Segut *et al*., 2007; Cosnier, 2007 and Lakard *et al*., 2011).

Intrinsically conductive polymers have become an efficient alternative to inorganic conductors in many practical applications in the recent decade (Hrehorova *et al*., 2007). Polyaniline, polytoluidine, polypyrrole, poly aminopyridine, polythiophene and polyphenylenediamine are examples of conductive polymers, showing high conductivity. Polyaniline is an important member of the intrinsically conductive polymers because of the ease of its preparation, an excellent environmental stability, interchangeable oxidation states, electrical and optical properties, economic cost (Guo *et al*., 2013; Jaymand, 2013) and because they can be used for chemical sensors (Zhao *et al*., 2013) and electromagnetic shielding, electrochemical and corrosion devices (Moon *et al*, 2013 and Guptal *et al*., 2013).

The derivatives of polyaniline are found applications in different fields like removal of heavy metals from the industrial effluents, anticorrosive agents (Suresh *et al*., 2012), for studies, microelectronics devices, electromagnetic shielding and in optics (Xiang *et al*., 2006; Kong *et al*., 2013; Saxens *et al*.; 2013, Shanthi and Rajendran, 2013; Archana and Jaya, 2014).

However, as the polymers are covalently bonded, the materials needs to be doped for electron flow to occur. The conductivity of polymers can be characterized by low – charge carrier mobility, dispersion ratio, aspect ratio, shape, orientation of conductive fillers insulating host materials and the particle size of the fillers (Jin *et al*., 2001)

Polymerization of a conducting polymer may be performed with chemical or electrochemical (Omar and Mariam 2017) methods. Different chemical oxidizing agents such as potassium dichromate (Sayyah *et al*., 2014; Melad, 2016), potassium iodate, (Hirase *et al*., 2004), hydrogen peroxide (GopalaKrishnan *et al*., 2012) Ferric chloride or ammonium persulphate (Molape *et al*., 2012) can be used. The application of polyaniline is limited because of its poor processability (Cao *et al*., 1992), which is true for most conducting polymers.

2.1.3 Doping in polymers

Doping is either the addition of electrons (reduction reaction) or the removal of electrons (oxidation reaction) from the polymer. Once doping has occurred, the electrons in the pi – bonds are able to jump around the polymer chain. As the electrons are moving along the molecule, an electric current occurs. However, the conductivity of the material is limited as the electrons have to jump across molecules for better conductivity and the molecules must be well ordered and closely packed to limit the distance jumped by the electrons. By doping, the conductivity of the polymer increases from 10^{-3} Sm^{-1} to 3000 Sm^{-1}.

Doping (p or n) generates charge carriers which move in an electric field. Positive charges (holes) and negative charges (electrons) move to opposite electrodes. This movement of charges

is what is actually responsible for electrical conductivity. Conductivity increases very rapidly as dopant is added. Doping is performed at much higher levels in conducting polymers than in semiconductors.

2.1.4 Poly (o- phenylenediamine) (PoPD)

Phenylenediamine is the simplest aromatic diamine. There are three isomers namely: o–phenylenediamine (orthphenylenediamine), m–phenylenediamine (methylphenylenediamine) and p–phenylenediamine (paraphenylenediamine). O–phenylenediamine has active chemical properties being able to have condensation reaction with acid, aldehydes, ketones and other compounds, generating heterocyclic compounds.

The main purpose and role of phenylenediamine is that it is used as fluorescent indicator and for chromatographic analysis reagent. O–phenylenediamine has moderate toxicity often due to inhalation of dust or skin absorption caused by poisoning. A phenylenediamine in which the two amino groups are ortho to each other is orthophenylenediamine (o – phenylenediamine). Phenylenediamine belongs to aniline derivatives and poly (o- phenylenediamine) shows different properties when compared to aniline (Salma *et al*., 2011).

Poly (o- phenylenediamine) is an aromatic amine base made from the polymerization of the monomer o–phenylendiamine ($C_6H_4(NH_2)_2$. The IUPAC name of o- phenylenediamine is benzene 1, 2 – diamine.This aromatic diamine is an important precursor to many heterocyclic compounds. It is isomeric with m – phenylenediamine and p –phenylenediamine and is commonly referred to as oPD. The chemical names for o – phenylenediamine are Benzene 1, 2 – diamine, 1, 2 – phenylenediamine, 1, 2-Benzene diamine, 1, 2 – Diaminobenzene. The molecular weight of o–phenylenediamine is 108.144g/mol. It is colourless monoclinic crystals if pure; technical grade brownish – yellow crystals or sandy brown solid. It can be used in manufacture of dyes, photograghy, organic synthesis among others. It turns dark on exposure to light.

O-phenylenediamine has a density of 1.031g/cm^3, melting point of 102 ^{o}C to 140 ^{o}C and boiling point of 252 ^{0}C (Robert, 2002). It is soluble in water, ethyl ether, benzene, chloroform; very soluble in ethanol (Haynes, 2011) when heated to decompose, it emits fumes of nitrogen oxides (Lewis, 1996).

Poly (o-phenylenediamine) homopolymer has attracted attention because it has been reported to be a high polymer containing a 2, 3 -diamino phenazine or quinoxaline repeat unit and exhibiting an unusually high thermostability. Electrochemical copolymerization of o–phenylendiamine with o/p toluidine using the chemical oxidative method has been reported (Omar and Mariam, 2017). So far, there has been no report on electrochromic performances of conductive poly (o-phenylenediamine) thin films prepared by electropolymerization (electrochemical). In this work, an electropolymerization of o – phenylenediamine at different pH will be synthesized and characterized using Raman spectroscopy, Brunauer-Emmett-Teller (BET) surface Area, Thermogravimetric analysis (TGA), X-Ray diffraction (XRD), Scanning Electron Microscopy (SEM), Ultraviolet (UV – VIS) spectroscopy, profilometer and four – point probe.

2.1.5 Electrochromism

Electrochromism is broadly defined as a reversible colour change induced in a material by an applied electric field or current (Sequeira and Santos, 2010). It is the reversible change in optical properties that can occur when a material is electrochemically oxidized, and is of great academic and commercial interest (Sequeira and Santos, 2010). Electrochromic displays are based on any material that changes colour depending on the applied potential (Grangvist, 2002). All conducting polymers are potentially electrochromic in thin – film form, redox switching giving rise to new optical absorption bands in accompaniment with transfer of electrons/ counter anions (Mortimer, 1999). Electrically conducting organic polymers are attracting considerable attention mainly because of their various electronic properties. In addition to their use as electrochromic

conducting polymers, advanced polymer materials can be used as thin film electrolytes in electrochromic devices for controlling the reversible optical absorption associated with the applied potential (Sequeira and Santos, 2010).

Electrochromism, a reversible and visible colour change is observed in a material as a result of electrochemical oxidation or reduction. The synthesis of electrochromic polymeric materials has been researched in many laboratories over the last few years (Hu *et al*., 2014). Electrochromic polymer (ECP) materials exhibit a change in transmittance and/or reflectance of electromagnetic radiation reaction called electrochromism (Rosseinsky and Mortimer, 2001). A certain set of properties such as, desired absorption profile, easily accessible redox process and ease of processing are of essential importance for materials to serve as effective electrochromes (Dyer *et al*., 2007).

Common magnitudes that defines the performance of an electrochromic device include optical contrast, colour change, colour uniformity, switching speed and the required voltage to power the device along with long–term switching and environmental stability (Huisheng *et al*., 2017)

Electrochromic materials can be used in display devices, reflective mirrors and smart windows since their optical absorption occurs in both the visible and near infra red regions of the spectrum (Reiter *et al*., 2009). The great interest of researchers during the last decade in the optical, electrical and mechanical properties of advanced solid polymers as reflected by the large number of studies developed worldwide is due to the fact that the most promising electrochromic devices use all solid state materials (Sequeira and Santos, 2010)

2.2 Empirical Literature Review

In recent years, intrinsically conducting polymers have been a popular topic of investigation because of their interesting electrical and electrochemical properties and their potential applications in various areas.

Pacios *et al*., (2007) studied combined electrochromic and plasmonic optical responses in conducting polymer/metal nanoparticles films. Poly (3, 4-ethylenedioxithiophene/poly(stylene suphonate) (PEDOT/PSS) aqueous dispersions were mixed with aqueous gold nanoparticles and aqueous silver nanoparticles colloids. PEDOT/gold nanoparticles (AuNP) and PEDOT/Silver nanoparticles (AgNP) films were obtained by solvent casting the corresponding aqueous solutions. The nanocomposites films showed the optical characteristic associated with both the surface plasmon absorption resonance of the metal nanoparticles and the excitation of the bipolaron band of the conducting polymer. As an interesting application they demonstrated the use of metal nanoparticles to tune the colour of PEDOT based electrochromic films from blue to violet in the case of AuNP or green in the case of AgNP.

Wang *et al*., (2007) studied electrochromic copolymers from o-phenylenediamine (oPD) with aniline (ANi). They were synthesized by a chemical oxidative polymerization. The synthesis, structure and properties of the copolymers were systematically studied by changing oPD content and polymerization temperature. The dependence of the polymerization yield at 70 ^{0}C on the oPD content is quite different from that at 17 ^{0}C indicating that the copolymerization between the oPD and ANi comonomers varies significantly with polymerization temperatures whereas the conductivity and solubility of the copolymers obtained at 17 ^{0}C and 70 ^{0}C demonstrate similar dependency of the oPD content. The reactivity ratios, Y_{oPD} and Y_{ANi} of oPD and ANi were found to be 9.70 and 2.74, respectively, implying a stronger formability and uniformity of the film, much higher electroactivity, and better tricolor electrochromism than oPD and ANi homopolymers. The copolymer film containing 50 mol% of oPD unit is red at – 0.5 to 0 V vs SCE, turns to green at 0 to ± 0.6 V vs SCE, and blue at ± 0.6 to + 1.35 V vs SCE.

Maiyalagan, (2008) studied electrochemical synthesis and the characterization of platinum nanoparticles dispersed by poly (o-phenylenediamine) nanotube electrodes, employing alumina

membrane. The morphology of the electrodes was characterized by SEM, AFM and TEM and catalytic activity and stability for the oxidation of methanol were studied by cyclic voltammetry and chronoamperometry. The results showed that poly (o-phenylenediamine) nanotubes electrodes significantly enhance the catalytic activity of platinum nanoparticles for oxidation of methanol. It also ahowed that the dispersion of the platinum particles is connected with catalytic response to a higher activity and stability of the nanotube based electrode compared to the commercial 20 wt% Pt/C (E-TEK) and template-free electrode. The nanotubular morphology of poly (o-phenylenediamine) helps in the effective dispersion of platinum particles facilitating the easier access of methanol to the catalytic sites. The poly (o-phenylenediamine) nanotubes modified with platinum nanoparticles cause a great increase in electroacitvity and the electro-catalytic oxidation of methanol.

Wang and Liao, (2012) reported the synthesis of fluffy poly (o– phenylenediamine) PoPD microsperes with chemical polymerization of oPD monomers by ammonium persulphate (APS) at room temperature. The SEM images showed that PoPD microsphere with an average diameter of 1.5 μm and their surfaces consist of highly oriented nanofibres. Also, PoPD microspheres were used as absorbent materials for the removal of Cr(VI) from aqueous solutions. The Cr(VI) absorption behaviour on the prepared PoPD microspheres was studied at different absorption contact times, solution pH values and amount of the absorbent. Experimental isotherms Cr(VI) ions were successfully fit to the Langmuir isotherm mode. The results indicates that the PoPD fluffy microsphere are an effective absorbent for the removal of Cr(VI) ions from aqueous solutions, and they could be useful in treatment of Cr(VI) polluted waste waters.

Li *et al*., (2013) studied synthesis of poly (o- phenylenediamine) submicropheres with an average diameter of about 400nm in glycine solution by mixing o phenylemediamine and ammonium persulphate at room temperature. XRD, FTIR and TGA characterizations of the prepared product

were done. Results showed that the doped PoPD is partly crystal and exhibits good thermal stability. The formation mechanism of the PoPD submicrospheres was investigated by monitoring the morphology development with the polymerization time, indicating that growth of the submicrospheres is a self assembly process.

Yadegari *et al*., (2013) studied poly (o-phenylenediamine)/graphite/Pt electrode by electrochemical method in a 2.0 M of H_2SO_4 solution by means of multiple potential cycling. The ortho phenylenediamine/graphite (PoPD/GR) nanocomposite showed greatly enhanced electrical properties and excellent capacitive behaviour due to the catalytic effect of polymerization of the nanocomposite. Electrochemical impedance spectroscopy, galvonostatic charge/discharge curves, and voltammetric investigations revealed good capacitive behaviour with a specific capacitance as high as 308.3Fg^{-1} at 0.1 Ag^{-1} which is almost three times higher than that of pure graphene (111.7 Fg^{-1}).The nanocomposite electrode retained more than 99% of the initial capacity after 1,500 cycles at a current density of 1 Ag^{-1}.

Wang *et al*., (2013) synthesized o- phenylenediamine bulk material using an electrochemical method. Sodium dodecyl sulphate (SDS) was added to o- phenylenediamine and the prepared materials are supercapacitors. The specific capacitance (SC) of the resultant PoPD electrode was determined to be 106.4 Fg^{-1} in one mol L^{-1} KNO_3 electrolyte from CV test. The electrochemical stability of PoPD electrode was investigated by charging and discharging the electrode for 1000 times in the potential range of -0.2 to 0.6 V versus SCE at the centre of density of 500 mAg^{-1}. The electrode exhibits a good cycling stability, retaining up to 82% of its initial specific capacitance at 1000^{th} cycle.

Wu *et al*., (2013) reported electrochromic devices by using polyaniline (PANI) doped with poly (styrene sulpfonic acid) (PSS) as colouring electrodes, poly(ethylenedioxythiophene) – poly(stylene sulfonic acid) (PEDOT – PSS) as complimentary electrodes and poly(methyl

methacrylate) (PMMA) – based electrolyte as gel electrolyte. Characterizations of the PANI-PSS were performed using FTIR spectroscopy, X-ray photoelectron spectroscopy (XPS), cyclic voltammetry (CV) and UV – VIS spectroscopy (UV). The spectroeletrochemical and electrochromic properties of electrochromic devices are investigated, electrochromic device based on PMMA-based gel electrolyte shows larger coloration efficiency, larger optical contrast and faster response time than that based on liquid electrolyte at long term cycles.

Siva *et al*., (2013) fabricated PoPD nanotubes of o- phenylenediamine in cetyl trimethyl ammonium bromide (CTAB) microemulsion polymerization using β- cyclodextrin (β- CD). Iron (III) chloride ($FeCl_3$) was used as a structure directing agent as well as an oxidant. The polymer nanotubes were characterized by FTIR, UV-Vis, NMR and XPS techniques. The surface morphology of nanotubes was analyzed using SEM and TEM. The coating containing PoPD nanotubes showed a higher coating resistance.

Aisha, (2014) studied anticorrosive properties of poly(o-phenylenediamine)/ZnO nanocomposites coated stainless steel. She prepared poly(o-phenylenediamine) and poly(o-phenylenediamine/ZnO) nanocomposites coating on type – 304 austenitic stainless steel using H_2SO_4 acid as electrolyte by potentiostatic methods. Fourier transforms infrared (FTIR) spectroscopy and SEM techniques were used to characterized the composition and structure of PoPD/ZnO nanocomposites. The corrosion protection of polymer coatings ability was studied by Eocp-time measurement, anodic and cathodic potentiodynamic polarization and impedance techniques in 3.5% NaCl as corrosive solution. She found that ZnO nanoparticles improve the barrier and electrochemical anticorrosive properties of poly(o-phenylenediamine).

Sayyah *et al*., (2014) studied polymerization of o- phenylenediamine in HCl solution with potassium dichromate as an oxidant at 5 ^{o}C using oxidative chemical method. The order of reaction with respect to potassium dichromate, hydrochloric acid, and monomer concentration

was found to be 1.011 M, 0.954 M and 1.045 M respectively. They also studied the effect of temperature on the polymerization rate and apparent activation energy of the reaction was found to be 63.658 KJ/mol. The TGA analysis confirmed the proposed structure and the number of water molecules in each polymeric chain unit. The surface morphology of the polymer was obtained by XRD and TEM. The a.c conductivity ($\sigma_{a.c)}$ of PoPD was determined as a function of frequency and temperature and was interpreted as a power law of frequency. The frequency exponent(s) was found to be less than unity and decreased with the increase in temperature which confirms that the correlated barrier hopping model was the dominant charge transport mechanism.

Yuan *et al*., (2015) studied nitrogen and oxygen doped hollow spheres (HCSs) prepared by pyrolysis of poly (o-phenylemediamine) submicrospheres, which were synthesized by a facile polymerization procedure with dopant glycine as the precursors. Effective heteroatom doping increases the supercapacitor performance of carbon materials as recognized. The prepared N- and O- doped HCS_s exhibit an enlarged specific surface area (~ 355 m^2g^{-1}) and pore volume (~0.14 cm^3g^{-1}), and they have superior performance in supercapacitors owing to the synergies gained from effective heterotom doping, their hollow structures, and their good mesoporosity.

Siddhartha *et al*., (2015) synthesized o- phenylenediamine with ammonium persulphate (APS) as an oxidant with varying pH values of the reaction medium by oxidative chemical polymerization method. The polymerization medium was prepared using disodium hydrogen phosphate and citric acid buffer and the pH (1, 2, 4, 6) was varied by adding aqueous dilute hydrochloric acid or sodium hydroxide solution. Characterization by Uv-Vis, HNMR and FTIR spectroscopy, TGA and elemental analysis of the polymers were done. Solubility tests for the synthesized polymers were performed in various solvents and it was found that the polymer synthesized in lower pH medium was insoluble. The difference in their solubility is due to their structural difference,

which can be supported by the proposed mechanisms of polymerization. The spectral results indicated that the ladder structure was formed in lower pH while open ring structure with some ladder unit or dimer was formed at higher pH. The average dc conductivity of the polymer doped with hydrochloric acid was found as 8.8 x 10^{-5} S/cm for synthesized open ring polymer and 1.7 x 10^{-7} S/cm for synthesized ladder polymer using four point probes.

Siddhartha *et al*., (2016) studied the structure and properties of conducting poly (o-phenylenediamine) synthesized in different inorganic acid medium by chemically synthesizing poly (o- phenylenediamine) from monomer o– phenylenediamine in HCl, H_2SO_4 and H_3PO_4. From the various characterizations, it was confirmed that the ladder type polymer with some open ring type amine derivative of polyaniline structure was obtained in H_2SO_4 medium and the ladder type dimer was formed in H_3PO_4 medium. The structural differences of the polymer were correlated with the polymerization mechanism in different acid medium. Thus, the polymer synthesized in H_2SO_4 was well soluble in polar organic solvent like dimethyl sufoxide (DMSO). N, N-dimethyl, formamide, tetrahydrofuran etc and casting of freestanding film was possible from DMSO solution. The highest average DC conductivity of doped polymer synthesized in H_2SO_4 medium was observed as 7.14 x 10^{-4} S/cm.

Rosanny *et al*., (2016) investigated electrochromic properties of polyaniline Based Hybrid Organic/Inorganic Materials. They obtained hybrid materials based on polyaniline by in situ polymerization of aniline with chitosan and /or originally modified clay (nanomer 1- 24) in HCl. The samples were characterized by FTIR spectroscopy, X-ray diffraction (XRD), SEM and direct current (DC) electricity conductivity. Thin films of PAni, PAni-clay, PAni-chitosan, and PAni-chitosan clay were prepared by casting a solution of each sample in N-methyl-2-pyrrolidone (NMP) onto indium tin oxide (ITO)/glass electrodes and their electrochromic properties were investigated. It was observed colour variation from transparent yellow in the

reduced state (E= -0.2 V vs Ag/AgCl) green in the intermediate state (E= 0.5 V) dark blue in the oxidized state (E= 0.8 V) for all samples. The colour change of each material as function of the applied potential were tracked using the commission internationale del'Eclairage (C/E). System of colorimetry, in which the colour change was much more significant for PAni-clay film

Omar and Mariam, (2017) synthesized Poly(o-phenylenediamine–co–o/p-Toluidine) by chemical oxidative co-polymerization at different molar ratios of monomer using potassium dichromate as an oxidant. The resulting copolymers were investigated using FTIR Spectroscopy and Uv-visible Spectroscopy. In the copolymer, the intensity of the band at 100 Scm^{-1} is substantially decrease due to the $-CH_3$ bending vibrations. A hyposochromic shift is observed in Uv-Visible spectroscopy. The electrical conductivity values obtained for the o-toluidine copolymers are higher than those for the P-toluidine copolymers.

Deepa and Shanthi, (2017) studied electrical conductivities of synthesized poly (o-phenylenediamine) and its nanocomposites with different concentrations of 5%, 10% and 15% of SiO_2 nanoparticles by chemical oxidative polymerization method using ammoniumpersulphate as an oxidant in the presence of HCl. The formation of poly(o-phenylenediamine) nanocomposites were confirmed by the change of polymer colour from red to brown and was found to exhibit band at 446 nm in Uv-Visible spectroscopy. The crystalline nature of the synthesized polymers and their nanocomposites were determined from the XRD studies. The SEM images of the polymers recorded at different magnification shows rod like structure and found to change to flake like structures in the polymer nanocomposites synthesized at different concentration of SiO_2 nanoparticles. The TEM recorded at different angles confirms the core shell structures. The stability of the synthesized polymer and its nanocomposite were sustained from thermal studies carried out using TGA, DTA and DSC. The comparative electrical conductivities of the polymer and its nanocomposites shows that the polymer nanocomposites

exhibit higher conductivities compared to the polymer and the electrical conductivity was found to be higher for the polymer nanocomposite synthesized with 15% of SiO_2. The polymer and its nanocomposites showed semiconducting nature.

Deepa and Shanthi, (2017) compared the electrical and photoluminescence properties of synthesized poly(o-plenylenediamine) and its SiO_2 nanocomposites by synthesizing poly orthophenylenediamine and their silicon dioxide nanocomposites with different concentration of SiO_2 nanoparticles of 5%, 10% and 15% by oxidative polymerization method using ammonium persulphate as an oxidant in the presence of HCl. The comparative electrical conductivities of the polymer and its nanocomposites shows semiconducting nature and the conductivities are found to be higher for the nanocomposites than the polymer and the electrical conductivity was found to be higher for the polymer nanocomposite synthesized with 15% of SiO_2. The photoluminescence (PL) spectrum of polymers and their nanocomposites were recorded with 5%, 10% and 15% SiO_2 nanoparticles and are found to fall under the green light emission region. Thus the synthesized polymer and its nanocomposites can be used as a green light emitter in different applications.

2.3 Characterization Techniques

Different characterization techniques have been practised for the analysis of various physicochemical properties of nanoparticles. These include techniques such as X-ray diffraction (XRD), Scanning electron microscopy (SEM), Brunauer – Emmett – Teller (BET) surface area, Ultraviolet-Visible (Uv-Vis) spectroscopy, Thermogravimetric analysis (TGA), Raman Spectroscopy, Four-point probe (FPP), profilometry among others.

2.4 Morphological characterizations

The morphological features of nanoparticles always attain great interest since morphology always influences most of the properties of the nanoparticles. There are different characterization

techniques for morphological studies, but microscopic techniques such as polarized optical microscopy (POM), SEM and TEM are the important ones though SEM is the most versatile one available for the examination analysis of the microstructure morphology and chemical composition characterizations.

2.4.1 Scanning electron microscopy (SEM)

The scanning electron microscopy (SEM) is one of the versatile instruments available for the examination and analysis of the microstructure morphology and chemical composition characterizations. SEM magnifications can go to more than 300,000x but most semiconductor manufacturing applications require magnifications of less than 3,000x only. When an electron beam strikes a sample, a large number of signals are generated. The scanning electron microscope is shown in Fig. 2.1

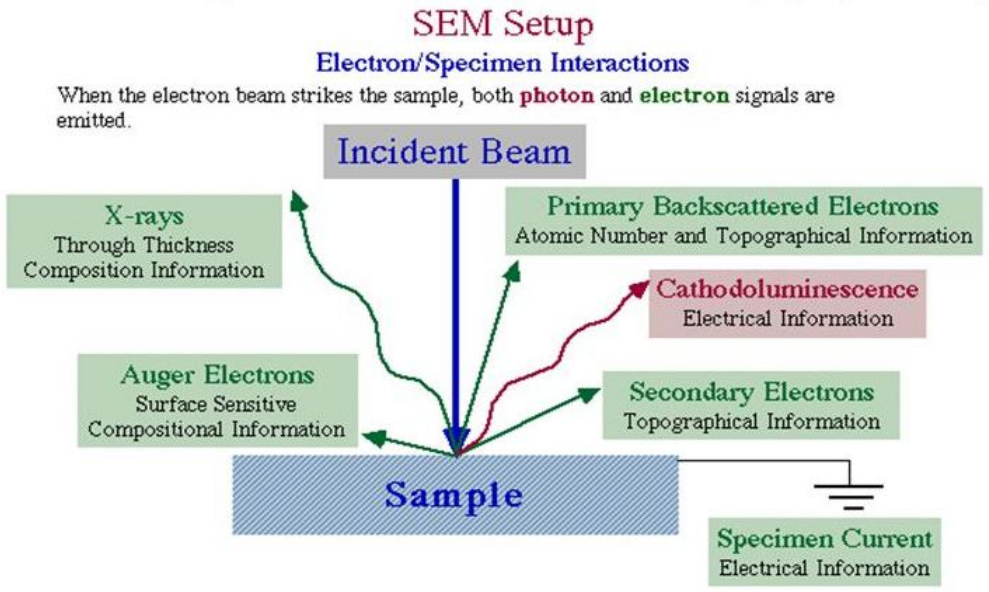

Fig. 2.1 Scanning Electron Microscopy (SEM) (Abdul, 2017)

Model: EFI Quanta 450 FEG-SEM

During SEM inspection, a beam of electrons is focused on a spot volume of the specimen, resulting in the transfer of energy to the spot. These bombarding electrons, also referred to as primary electrons, dislodge electrons from the specimen itself. The dislodged electrons also

known as secondary electrons are attracted and collected by a positively biased grid or detector and then translated into a signal.

To produce the SEM image, the electron beam is swept across the area being inspected, producing many such signals. These signals are then amplified, analyzed and translated into images of the topography being inspected. Finally, the image is shown on a CRT.

The energy of the primary electrons determines the quantity of secondary electrons collected during inspection. The emission of secondary electrons from the specimen increases as the energy of the primary electron beam increases until a certain limit is reached. Beyond this limit, the collected secondary electrons diminish as the energy of the primary beam is increased as the primary beam is already activating electrons deep below the surface of the specimen. Electrons coming from such depth usually recombine before reaching the surface for emission.

Apart from secondary electrons, the primary electron beam results in the emission of backscattered (or reflected) electrons from the specimen. Backscattered electrons possess more energy than secondary electrons and have a definite direction. As such, they cannot be collected by a secondary electron detector unless the detector is directly in their path of travel. All emissions above 50 eV are considered to be backscattered electrons.

Backscattered electron imagining is useful in distinguishing one material from another since the yield of the collected backscattered electrons increases monotonically with the specimen's atomic number. Backscatter imaging can distinguish elements with atomic numbers differences of at least 3 (materials with atomic number differences of at least 3) would appear with good contrast on the image.

A SEM may be equipped with an EDX analysis system to enable it to perform compositional analysis on specimens. EDX analysis is useful in identifying materials and contaminants as well as estimating their relative concentrations on the surface of the specimen.

The SEM has a large depth of field which allows a large amount of the sample to be in focus at one time and produces an image that is a good representation of the three dimensional sample. The combination of higher magnification, larger depth of field, greater resolution, compositional and crystallographic information makes the SEM one of the most heavily used instruments in academic/national laboratory research areas and industry.

2.5 Structural characterizations

The structural characteristics are of primary importance to study the composition and nature of bonding materials. It provides diverse information about the bulk properties of the subject material. XRD, energy dispersive X-ray (EDX), IR, Raman, BET among others are the common techniques used to study structural properties of nanopartciles.

2.5.1 X-Ray diffraction (XRD)

X-Ray diffraction is one of the most important characterization techniques to reveal the structural properties of nanoparticles. It gives enough information about the crystallinity and phase of nanoparticles. It also provides rough idea about the particles size through Debyer Scherer formula (Khan *et al*., 2017 and Ullah *et al*., 2017). Diffraction is a consequence of specific phase relationships established between two or more waves that have been scattered by the obstacles. It occurs when a wave encounters a series of regularly spaced obstacles that are capable of scattering the wave and have spacing that are comparable in magnitude to the wavelength (Josh *et al*., 2008). X-ray diffraction is one of the most important non-destructive tools to analyze all kinds of matter ranging from fluids to powders and crystals. XRD is an indispensable method for materials characterization and quality control. The properties and functions of materials largely depend on the crystal structures.

XRD relies on the fact that X-rays are in form of light, with wavelengths on the order of nanometers. When X-rays scatter from a substance with structure at that length scale, interference can take place resulting in a pattern of higher and lower intensities. The XRD produces a diffraction pattern which does not superficially resemble the underlying structure and provides information about the internal structure on length scales from 0.1 to 100 nm. Its most simplified form, a generic X-ray scattering measurement is shown in Fig. 2.2

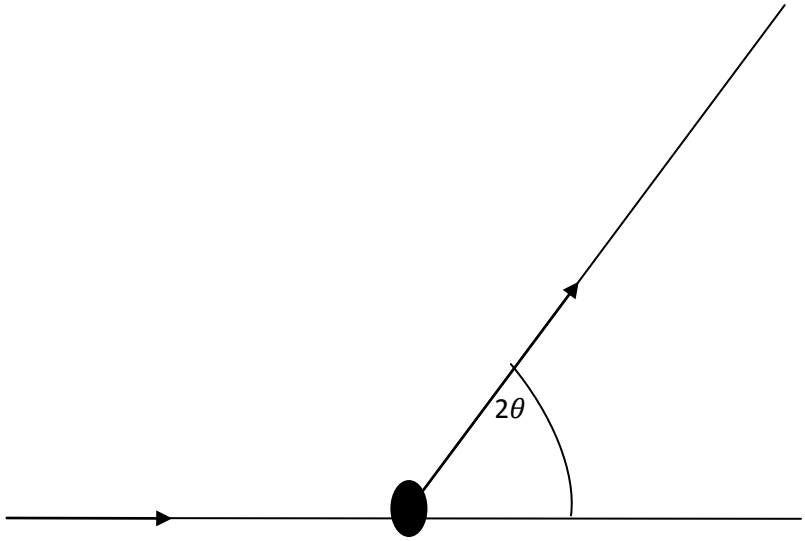

.

Fig. 2.2 X-Ray scattering measurement

A beam of X-rays is directed towards a sample, and the scattered intensity is measured as a function of outgoing direction. By convention, the angle between the incoming and outgoing beam directions is called 2θ. For the simplest possible sample, consisting of sheets of charge separated by a distance d, constructive interference (greater scattered intensity) is observed when Bragg's Law is satisfied:

$$n\lambda = 2d\sin\theta \qquad 2.2$$

where n is an integer (1, 2, 3 . . .), λ is the wavelength of the X-ray beam (incident wavelength), and θ is half the scattering angle 2θ shown in Fig. 2.2. Real materials are more complicated, of

course, but the general result holds that there is a relationship between interparticle distances within the sample and the angles at which the scattered intensity is the highest, with large distances d corresponding to smaller scattering angles 2θ.

When the entire sample has been picked, the information is recorded into the computer system as it results from the XRD machine. Results are commonly presented as peak positions at 2θ and X-ray counts (intensity) in the form of a table or an X-ray plot. Intensity is either reported as peak height intensity (that is intensity above background) or as integrated intensity (the area under the peak). The relative intensity is recorded as the ratio of the peak intensity to that of the most intense peak

The percentage crystallinity (X_C) is determined by dividing the total areas of crystalline peak by total area under the diffraction curve (Crystalline plus amorphous peaks)

XRD is a tool for identification of semi crystalline polymers and recognition of crystalline phases (polymorphism) of polymers, polymers are never 100% crystalline. XRD is a primary technique to determine the degree of crystallinity in polymers.

2.5.2 Brunauer-Emmett-Teller (BET) Surface Area

In 1938, Stephen Brunauer, Paul Hugh Emmett and Edward Teller published the first article about the BET Theory in the Journal of the American Chemical Society. BET is the initials of the three Researchers who developed the mathematics required for the measurement to work. Brunauer, Emmett, and Teller found a way to calculate the specific surface area of a sample including the pore size distribution from gas adsorption. The measurement of porosity and surface area by BET is a relatively simple measurement to carry out. However, the mathematics and physics behind BET is a little more complicated and so understanding the result can be difficult.

Two major methods used to determine the surface area analysis are;

(i) Multipoint Brunauer Emmett – Teller (BET) method

(ii) Langmuir method

Other methods such as single point Brunauer Emmett – Teller method, Barret, Joyner and Halenda (BJH) method, Dollimore and Heal (DH) method, t – method, Dubinin – Radashkevich (DR) method and Density Functional Theory (DFT) method.

BET measures surface area based on gas adsorption. More specifically, it allows determination of the overall specific external and internal surface areas of disperse (e.g nano powders) or porous solids by measuring the amount of physically adsorbed gas according to BET method. The BET Theory applies to systems of multilayer adsorption and usually utilizes probing gases that do not chemically react with material surfaces as adsorbates to quantify specific surface area. Nitrogen is the most commonly employed gaseous adsorbate used for surface probing by BET methods. For this reason, standard BET analysis is most often conducted at the boiling temperature of -196 ^{0}C. The concept of the theory is a theory of monolayer molecular adsorption to multilayer adsorption.

The volume of gas (usually nitrogen) adsorbed to the surface of the particles is measured at the boiling point of nitrogen (-196 ^{0}C). At this temperature, the nitrogen gas is below the critical temperature and so condenses on the surface of the particles. It is assumed that the gas condenses onto the surface in a monolayer and so, because the size of the gas atom/molecule is known, the amount of adsorbed (condensed) gas is correlated to the total surface area of the particles including pores at the surface (inaccessible pores are not detected). It is this correlation calculation, volume adsorbed to surface area that BET theory gives.

Adsorption is the adhesion of atoms, ions or molecules from a gas, liquid or dissolved solid to a surface. There are generally accepted six adsorption Isotherms shown in Fig. 2.3. The BET method is applicable only to adsorption isotherms of type II (disperse, nanoporous or

macroporous solids) and type IV (mesoporous solids, pore diameter 2 nm and 50 nm). The BET method cannot reliably be applied to solids which absorb (as opposed to absorb) the measuring gas. As the gas (adsorbative) is pumped into the sample tube the gas covers the external and the accessible internal pore surfaces of a solid.

The amount of gas used in creating the monolayer can be calculated from the adsorption isotherm using the BET equation (equation 2.3). Any gas may be used provided it is physically adsorbed by weak bonds at the surface of the solid (Van Da Wall Forces) and can be desorbed by a decrease in pressure at the same temperature.

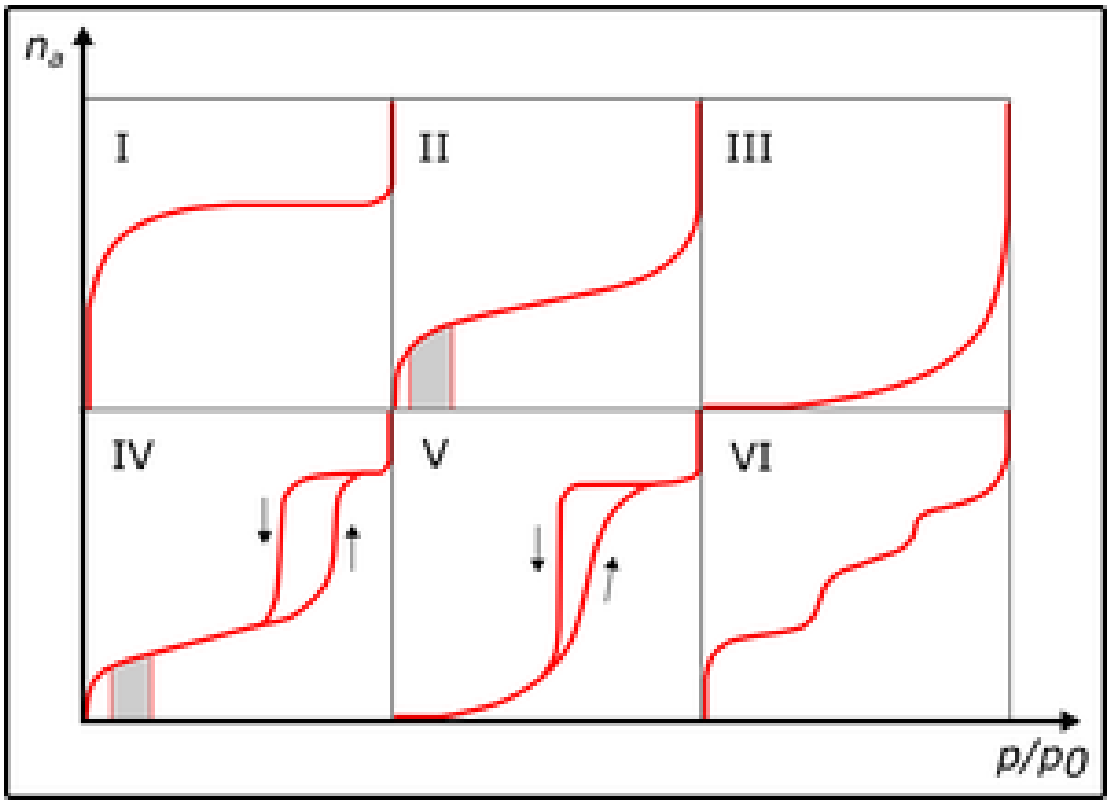

Fig. 2.3 — IUPAC classification of adsorption isotherms (typical BET range is indicated in Types II and IV by the shaded areas), n_a=quantity of absorbed gas, p/p_0 is the relative pressure (Brunauer *et al*., 1938)

The BET equation can be used to calculate the surface area of a sample. Other equations are available to calculate surface area from gas adsorption. It is sufficient to show that the measured inputs to this equation include the equilibrium (p) and the saturation (p0) pressure of adsorbates at the temperature of adsorption.

The adsorbed gas quantity (n_a) (for example, in volume units) is given by

$$\frac{p}{n_a(p_0-p)}\ S_{total} = \frac{\mathbf{1}}{\boldsymbol{n_m C}} + \frac{(\boldsymbol{C}-\mathbf{1})}{\boldsymbol{n_m C}}\ \frac{\boldsymbol{P}}{\boldsymbol{P_0}} \qquad 2.3$$

The calculated quantities are:

The n_m, is the monolayer capacity:

$$n_m = \frac{\mathbf{1}}{\boldsymbol{gradient - intercept}} \qquad 2.4$$

The BET constant, C

$$C = 1 + \frac{gradient}{intercept} \qquad 2.5$$

$$S_{total} = \frac{\boldsymbol{n_m N s}}{\boldsymbol{v}} \qquad 2.6$$

where S_{total} is total surface area, N is Avogadro's number, S the absorption cross section of the absorbing species, and V the molar volume of the absorbate gas.

The exact form of this equation will vary depending on the units being used.

To calculate these values the BET equation is plotted as an absorption isotherm typically at a relative pressure (P/P0) between 0.05-0.35. In this range, BET Theory suggests it should form a straight line, Fig. 2.4. The value n_m can then be found from the gradient and from that the surface area can be calculated using the molecular cross-sectional area.

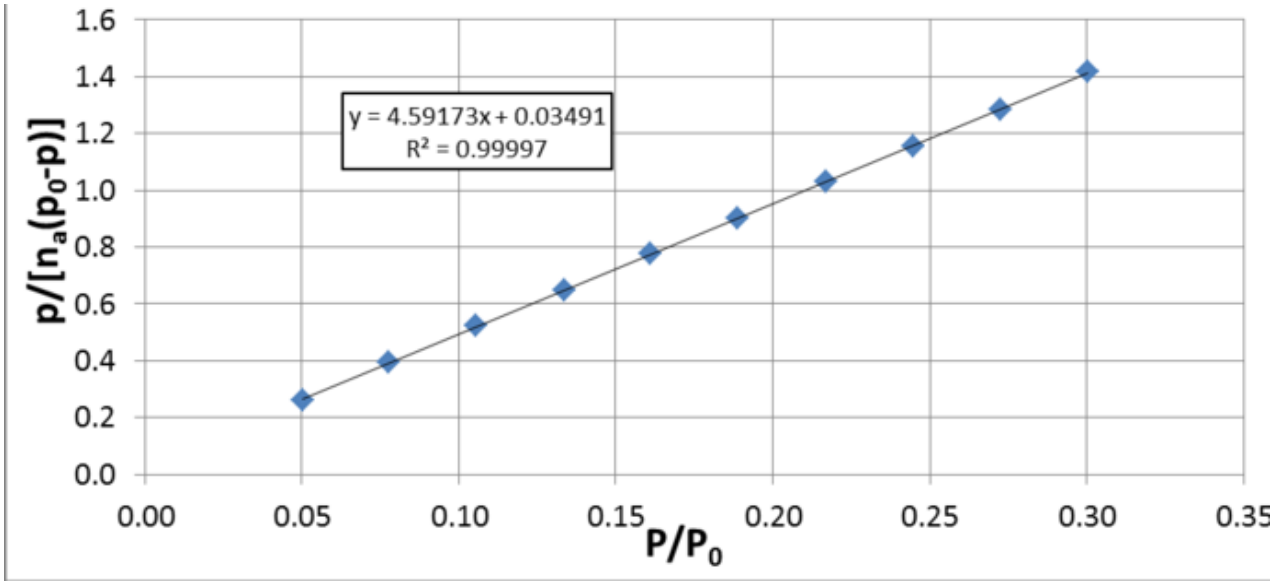

Fig. 2.4 BET plot of $P/[n_a (P_o-P)]$ and Relative pressure P/P_o (Brunauer *et al.*, 1938)

The BET constant C is also calculated from the intercept and gradient and is related to the energy of absorption in the first adsorbed layer. Consequently the value of C is an indication of the magnitude of the adsorbent/adsorbate interactions. C is normally between 100–200. If it is lower than around 20 there is significant adsorbent/adsorbate and the BET method is invalid. Greater than 200 and the sample may contain significant porosity (Brunauer *et al.*, 1938). Various measurements available in BET is shown in Table 2.1

Table 2.1: Various measurements available on BET instruments ((Brunauer *et al*., 1938)

Measurement	Calculation methods	Notes
Surface area	BET, Langmuir, Temkin, Freundlich	Can be calculated from section of isotherm (generally P/P_0 = 0.05-0.35)
Total Pore Volume	Kelvin equation	Generally carried out at P/P_0 = 0.09-0.998 although theoretically all pores should be full at P/P_0 = 0.995
Mesopore volume, area, and distribution	BJH, Dollimore-Heal	Requires full absorption and desorption isotherm
Micropore distribution	Dubinin- Radushkevich and Astakhov, Horvath-Kawazoe, Saito-Foley, Cheng Yang, MP method	Requires full absorption isotherm
Pore size modeling	Density Functional Theory	Requires full absorption isotherm
Surface energy	Density Functional Theory	Requires full absorption isotherm

The specific surface area is then calculated using the mass of sample.

$$S_{BET} = \frac{S_{BET}}{Sample\ \ mass} \qquad 2.7$$

2.5.3 Raman spectroscopy

Raman Spectroscopy (named after Indian physicist, Sir C.V. Raman) is a spectroscopic technique used to observe vibrational, rotational and other low – frequency modes in a system (Gardiner, 1989). It relies on inelastic scattering, or Raman Scattering of monochromatic light usually from a laser in the visible, near infrared, or near ultraviolet range. The laser light interacts with molecular vibrations phonons or other excitations in the system, resulting in the energy of the laser photons being shifted up or down. The shift in energy gives information about the vibrational modes in the system.

Typically, a sample is illuminated with a laser beam. Electromagnetic radiation from the illuminated spot is collected with a lens and sent through a monochromator. Elastic scattered radiation at the wavelength corresponding to the laser line (Rayleigh scattering) is filtered out by either a notch filter, edge pass filter, or a band pass filter, while the rest of the collected light is dispersed onto a detector.

The magnitude of the Raman effect correlates with polarizability of the electrons in a molecule. It is a form of inelastic light scattering where a photon excites the sample. This excitation puts the molecule into a virtual energy state for a short time before the photon is emitted. Inelastic scattering means that the energy of the emitted photon is of either lower or higher energy than the incident photon. After the scattering event, the sample is in a different rotational or vibrational state. For the total energy of the system to remain constant after the molecule moves to a new rovibronic state, the scattered photon shifts to a different energy and therefore a different frequency. This energy difference is equal to that between the initial and final rovibronic states of the molecule. If the final state is higher in energy than the initial state, the scattered photon will be shifted to a lower frequency (lower energy) so that the total energy remains the same. This shift in frequency is called a stoke shift or downshift. If the final state is lower in energy, the scattered photon will be shifted to a higher frequency which is called an anti – stokes shift or upshift (Krishnan and Raman, 1928)

For a molecule to exhibit a Raman effect there must be a change in its electric dipole polarizability with respect to the vibrational coordinate corresponding to the rovibronic state. The intensity of the Raman scattering is proportional to this polarizability change. Therefore, the Raman spectrum, scattering intensity as a function of the frequency shifts depends on the rovibronic states of the molecule.

Raman shifts are typically reported in wave numbers which have units of inverse wavelength as this value is directly related to energy. In order to convert between spectral wavelength and wave numbers of shift in the Raman spectrum, the corresponding equation is from Gardiner, 1989,

$\Delta w = 1/\lambda_0 - 1/\lambda_1$ (Gardiner, 1989) 2.8

where Δw = the Raman shift expressed in wave number

λ_0 = the excitation wavelength and

λ_1 = the Raman spectrum wavelength

Mostly, the unit chosen for expressing wave number in Raman Spectra is inverse centimeters (cm^{-1}). Since wavelength is often expressed in units of nanometers (nm), equation 2.8 can scale for this unit conversion explicitly giving

$$\Delta w\ (cm^{-1}) = \left(\frac{1}{\lambda_0}\ (\text{nm}) - \frac{1}{\lambda_1}(\text{nm})\right) \times \frac{1}{10^7}(\text{nm})\text{cm}) \quad 2.9$$

Raman spectroscopy is one of the vibrational spectroscopic techniques used to provide information on molecular vibrations and crystal structures. This technique uses a laser light source to irradiate a sample and generates an infinitesimal amount of Raman scattered light which is detected as a Raman spectrum using a CCD camera. The characteristic fingerprinting pattern in a Raman spectrum makes it possible to identify substances including polymorphs and evaluate local crystallinity, orientation and stress.

Raman spectroscopy has some unique advantages such as

1. Non- contact and non- destructive analysis
2. High spatial resolution up to sub- micron scale
3. In depth analysis of transparent
4. No sample preparation needed
5. Both organic and inorganic substances can be measured.

6. Sample in various state such as gas, liquid, solution, solid, crystal, emulsion can be measured.
7. Samples in a chamber can be measured through a glass window
8. Typically, only 10 millisec to 1 sec exposure to get a Raman spectrum.
9. Imaging analysis is possible by scanning the motorized stage or laser beam.

As a result of these advantages, Raman spectroscopy plays an important role in academic fields such as semiconductors, polymer, pharmaceuticals, batteries, life sciences among others.

Raman scattered light is too weak to be seen by the naked eye.

The Raman spectrum is expressed in a form of intensity of scattered light verses wave number (the reciprocal of wavelength, called Raman shift).

Light is often characterized by wavelength. However, in Raman spectroscopy, wavenumber is commonly used because it is linearly related with energy and makes the form of the Raman spectrum independent of excitation wavelength.

A peak appearing in the Raman spectrum will be derived from a specific molecular vibration or lattice vibration. Peak position shows the specific vibrational mode of each molecular functional group included in the material. The same vibrational modes for each functional group will show a shift in peak position due to the nearby environment surrounding the functional group, thus it is said the Raman spectrum shows the “molecular fingerprint” of the target.

Crystal polymorphism of a material occurs when the chemical formula is the same but the crystal structure of the material is different. Raman Spectroscopy allows for analysis of crystal polymorphism, with similar but slight differences in position and intensity ratios of particular peaks between polymorphs, sufficient for identification.

Both polymerization and damage to the molecular structure are accelerated via irradiation by ultraviolet rays. By recording the Raman spectrum over time, one can follow changes in the

molecular structure of the sample. For example, in a polymer the C=C bond be formed by the irradiation of ultraviolet rays, thus changes can be tracked by focusing on the change in the corresponding peak intensity. Related energy level in Raman scattering is shown in Fig. 2.5

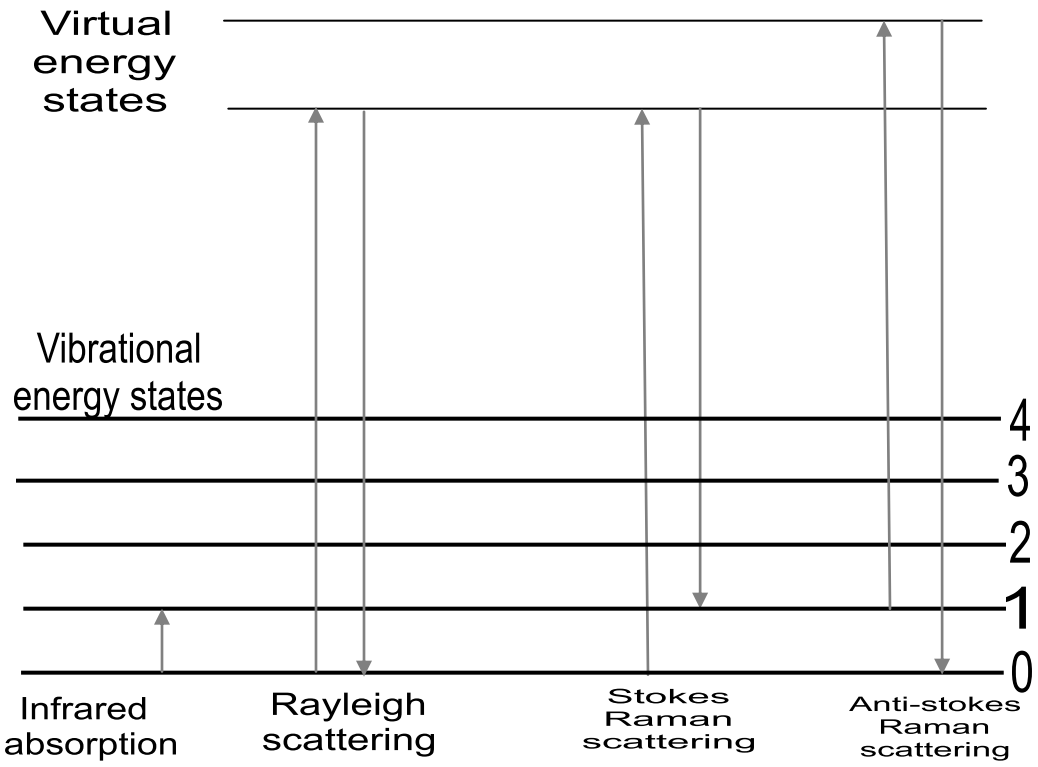

Fig. 2.5Energy levels in Raman scattering (Gardiner, 1989)

Therefore, Raman Spectroscopy provides information about molecular vibrations that can be used for sample identification and quantitation. The technique involves shining a monochromatic light source (i.e laser) on a sample and detecting the scattered light. The majority of the scattered light is of the same frequency as the excitation source. This is known as Rayleigh or elastic scattering. A very small amount of the scattered light is shifted in energy from the laser frequency due to interactions between the incident electromagnetic waves and the vibrational energy levels of the molecules in the sample. Plotting the intensity of this "shifted" light versus frequency results in a Raman Spectrum of the sample. Generally, Raman Spectra are plotted with respect to the laser frequency such that the Rayleigh band lies at 0 cm^{-1}. On this scale, the band

positions will lie at frequencies that correspond to the energy levels of different functional group vibrations. The Raman Spectrum can thus be interpreted similar to the infrared absorption spectrum.

2.6 Optical characterization

Optical properties are of great concerned in electronic applications and can be performed using UV – Vis spectroscopy.

2.6.1 Ultraviolent-visible spectroscopy (Uv-Vis)

This spectroscopy refers to absorption spectroscopy or reflectance spectroscopy in the ultraviolent-visible spectral region. It uses light in the visible and adjacent ranges. The absorption or reflectance in the visible range directly affects the perceived colours of the chemicals involved. In this region of the electromagnetic spectrum, atoms and molecules undergo electronic transitions. Absorption spectroscopy is complementary to fluorescence spectroscopy, in that fluorescence deals with transitions from the excited state to the ground state while absorption measure transitions from the ground state to the excited state (Skoog *et al*., 2007).

2.6.1.1 Principles of Uv-Vis absorption

Molecules containing π-electrons or non-bonding electrons (n-electrons) can absorb energy in the form of ultraviolet or visible light to excite these electrons to higher anti-bonding molecular orbitals (Alias *et al*., 2013). The more easily excited the electrons (i.e. lower energy gap between the HOMO and the LUMO), the longer the wavelength of light it can absorb. There are four light possible types of transitions (π - π *, n - π *, σ-σ*, and n-σ*), and they can be ordered as follows: σ - σ * > n - σ * >π - π * >n – π *.

Organic compounds especially those with a high degree of conjugation, also absorb light in the UV or visible regions of the electromagnetic spectrum. The solvents for these determinations are often water for water-soluble compounds, or ethanol for organic-soluble compounds. (Organic solvents may have significant UV absorption; not all solvents are suitable for use in UV spectroscopy. Ethanol absorbs very weakly at most wavelengths). Solvent polarity and pH can affect the absorption spectrum of an organic compound. While charge transfer complexes also give rise to colours, the colours are often two intense to be used for quantitative measurement.

The Beer-Lambert law states that the absorbance of a solution is directly proportional to the concentration of the absorbing species in the solution and the path length, (Alias *et al*., 2013).

The nature of the solvent, the pH of the solution, temperature, high electrolyte concentrations and the presence of interfering substances can influence the absorption spectrum.

Uv-Vis Spectroscopy is also used in the semiconductor industry to measure the thickness and optical properties of thin films on a wafer. It is used to measure the reflectance of light and can be analyzed via the Forouhi-Bloomer dispersion equations to determine the index of Refraction (n) and the extinction coefficient (k) of a given film across the measured spectral range. For convenience of reference, definitions of the various spectral regions have been set by the Joint Committee on Nomenclature in Applied Spectroscopy as shown in Table 2.2

Table 2.2 UV-Vis Regions and Equivalent wavelengths

Region	**Wavelength (nm)**
Far ultraviolet	10 – 200
Near ultraviolet	200 – 380
Visible	380 – 780

The human eye is only sensitive to a tiny proportion of the total electromagnetic spectrum between approximately 380 and 780 nm and within this area we perceive the colours of the rainbow from violet through to red. Fig 2.6 shows the EM spectrum.

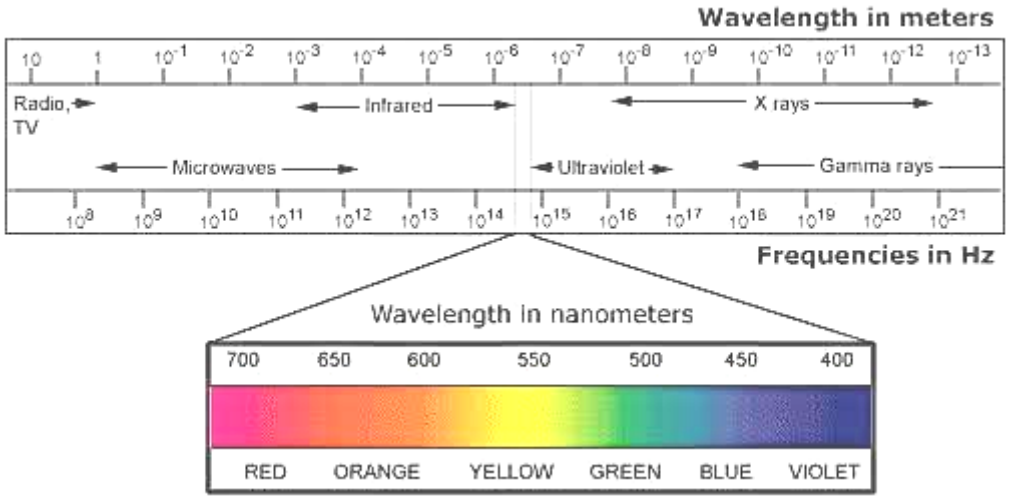

Fig. 2.6 The electromagnetic spectrum (Young and Freedman, 2008)

Besides the sun, the most conveniently available source of visible radiation which is familiar is the tungsten lamp. If the current in the circuit supplying such a lamp is gradually increased from zero, the lamp filament at first can be felt to be emitting warmth, then glows dull red and the gradually brightens until it is emitting an intense white light and a considerable amount of heat. Table 2.3 shows the relationship between light absorption and colour.

Table 2.3 Wavelengths for colours in the visible spectrum (Young and Freedman, 2008)

Wavelength (nm)	Colour
400 - 440	Violet
440 - 480	Blue
480-560	Green
560-590	Yellow
590-630	Orange
630-700	Red

A close relationship exists between the colour of a substance and its electronic structure. A molecule or ion will exhibit absorption in the visible or ultraviolet region when radiation causes an electronic transition within its structure. Thus, the absorption of light by a sample in the ultraviolet or visible region is accompanied by a change in the electronic state of the molecules in the sample. The energy supplied by the light will promote electrons from their ground state orbitals to higher energy, excited state orbitals or anti bonding orbitals.

The instrument used in ultraviolent-visible Spectroscopy is called a Uv-Vis Spectrophotometer which measures the intensity of light (I_T) passing through a sample (intensity of the transmitted radiation) and compares to the intensity of light (I_0) before it passes through the sample (intensity of the incident radiation). The ratio I_T/I_0 is called the transmittance (T) and is usually expressed as a percentage (%T). The absorbance, A is based on the transmittance A= -log(%T/100), the percentage transmission is $\%T=I_T/I_0 \times 100$.

The Uv–Visible spectrophotometer can also be configured to measure reflectance. In this case, the spectrophotometer measures the intensity of light reflected from a sample (I_R), and compares

it to the intensity of light reflected from reference material (I_o) such as a white tile. The ratio I_R/I_o is called the reflectance, and is usually expressed as a percentage (%R).

Absorption spectroscopy is a technique where the absorption of electromagnetic wave is measured as a function of the frequency or wavelength. The absorption process induces an interaction between electromagnetism and the sample, which can be interpreted through variations in the absorption spectra (Alias *et al*., 2013). An absorption spectrum is a fingerprint of a molecule or polymer material. Uv–Vis absorption is a commonly used analytical tool for studying the interaction between electrons and radiation. There are four basic components, namely the light source, monochromator, sample holder and optical detector. In general optical absorption spectrophotometer uses either a single or double beam (Tkacheno, 2006).

Fig. 2.7 (a) shows the simplest single beam which is easy to utilize and is compatible. A double beam, as shown in Fig. 2.7 (b), consists of two beams from the same source divided into two optical paths.

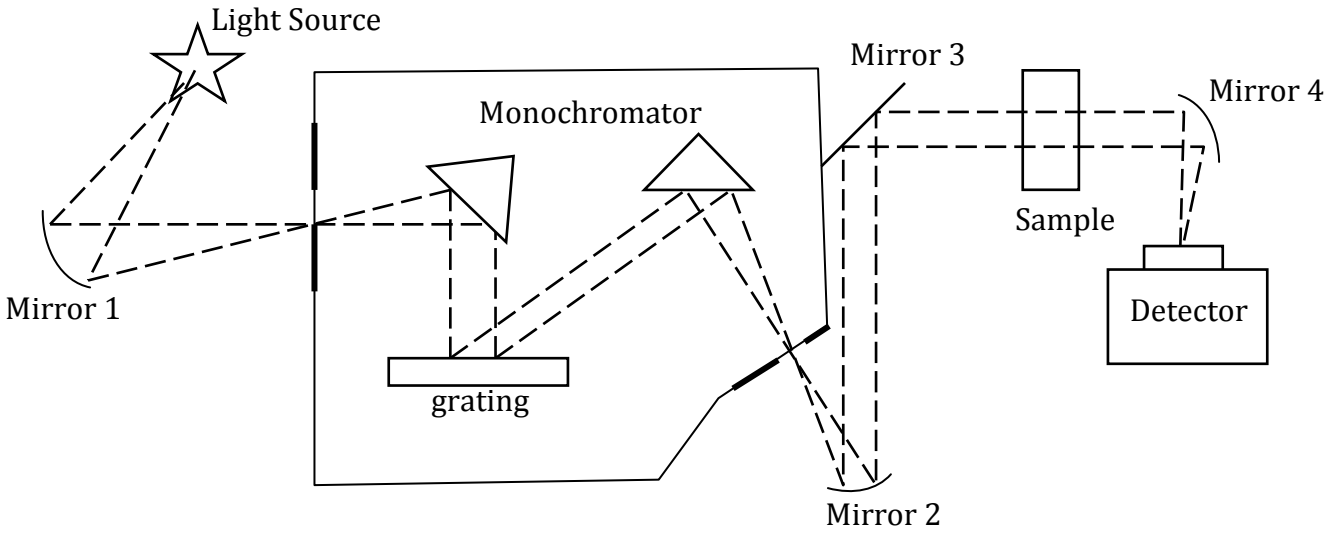

(a)

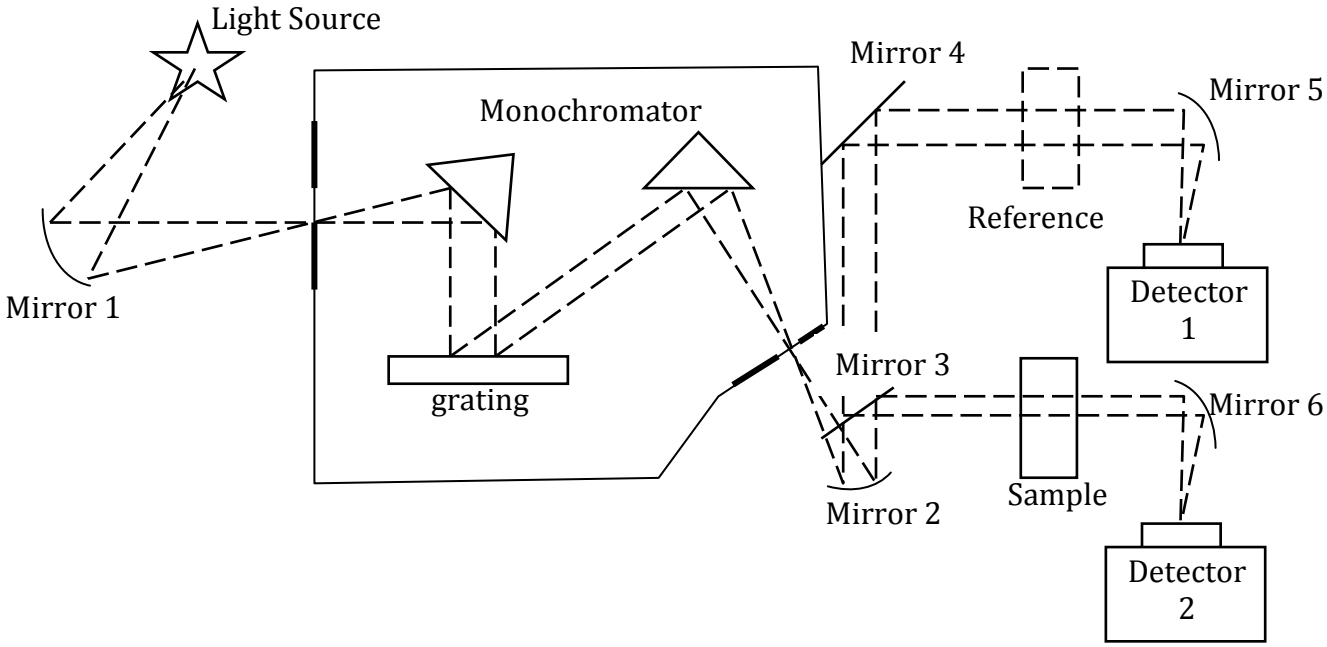

Fig. 2.7 (a) Single and 2.7 (b) Double-channel UV-vis spectrophotometers.

(Alias *et al*., 2013)

The first beam passes through the reference and second beam passes through the sample. The main advantage of the double beam channel is the reference material that makes measurement more stable, precise and accurate compared to the single beam channel (Porro and Terhaar,

1976). However, one of drawbacks of the double beam channel is the low ratio signal - to – noise which affected the sensitivity of the system.

In absorption spectroscopy, normally two types of interference can occur namely; spectra interference and interference from the absorption species (Skoog *et al.*, 2007). Spectra interference appears from the overlapping line in the monochromator. Interference filter are needed to limit the number of wavelength. Interference from the absorption species involves thick or opaque thin film. In thick thin film, the absorbance depends on the optical length path in the sample. To avoid this circumstance, diffuse reflectance measurement with integrated sphere can be used (Bosch and Sanchez, 2004).

In the absorption process, the intensity of light decreases when propagates in the medium as shown in Fig 2.8(a) and Fig 2.8(b) shows the light absorption process in the film.

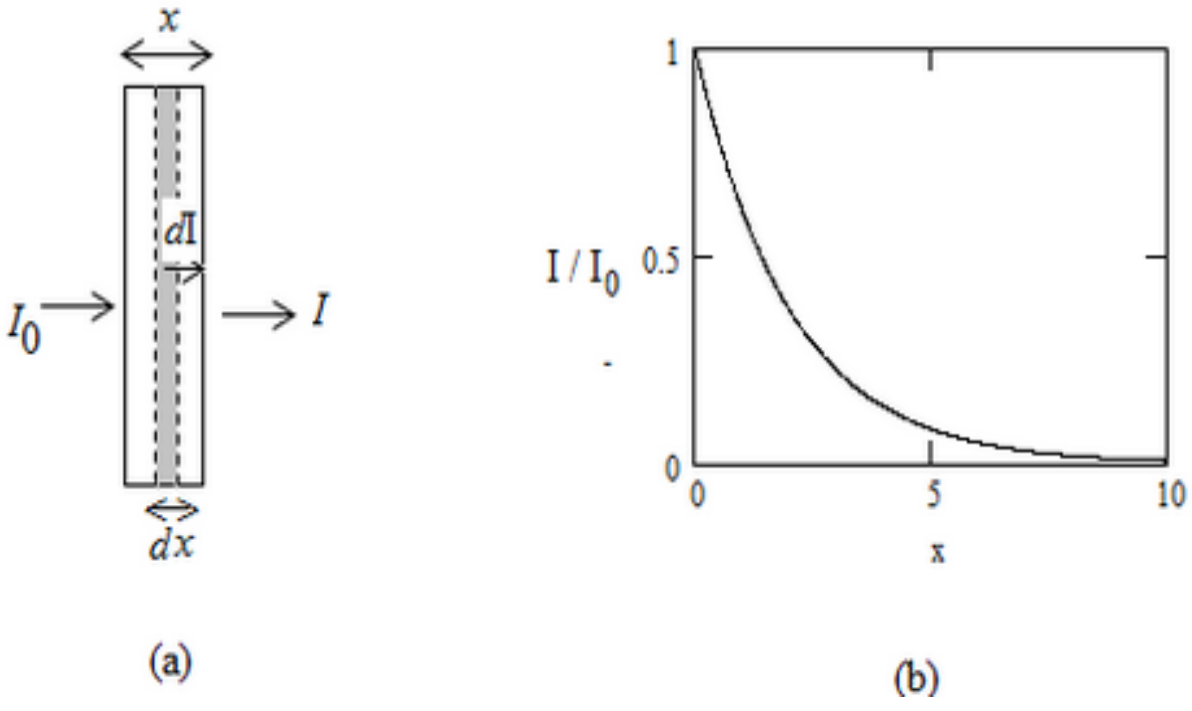

Fig. 2.8 (a) The light absorption process in thin film 2.8 (b) The normalized light intensity absorbed in the thin film as the function of sample thickness *x* with α = 0.5 m $^{-1}$

(Alias *et al.*, 2013)

where *di* = small change in the intensity and I = absorbed intensity.

The ratio intensity loss (*di* /I) is proportional with small changes in the sample thickness *dx.* This relation can be given by equation 2.10 (Alias *et al*., 2013)

$$\frac{dI}{I} = -\alpha dx \qquad 2.10$$

If I_o is the initial or incident light intensity before entering the medium, I is the transmitted light and *x* is the sample thickness. The intensity absorbed by the sample can be calculated by integrating equation 2.10 of both side as

$$\int_{I_0}^{I} \frac{dI}{I} = -\alpha \int_0^x dx \qquad 2.11$$

$$I = I_0 \, exp\,(-\propto x) \qquad 2.12$$

This equation is known as Lambert-Beer Laws. According to this law, the light intensity exponentially decays with the sample thickness. The coefficient of proportionality in equations 2.11 and 2.12 is known as absorbance coefficient and it measures how strong the sample absorbs light at a specific wavelength (Alias *et al*, 2013).

2.6.2 Profilometry

A profilometer is a device used to measure the roughness of a surface. It gives difference between the high and low point of a surface in nanometers. There are contact profilometers and non-contact profilometers.

A diamond stylus is moved vertically in contact with a sample and then moved laterally across the sample for a specified distance and specified contact force. A profilometer can measure small surface variations in vertical stylus displacement as a function of position. A typical profilometer

can measure small vertical features ranging in height from 10 nanometers to 1 millimeter. The height position of the diamond stylus generates an analog signal which is converted into a digital signal, stored, controlled by the scan speed and data signal sampling rate. The stylus tracking force can range from less than 1 to 50 milligrams.

2.6.2.1 The principles of profilometer

All profilometers consist of at least two parts – a detector and a sample stage. The detector is what determines where the points on the sample are and the sample stage is what holds the sample. In some systems, the sample stage moves to allow for measurement, in others the detector moves and in some both move. There are two overarching types of profilometers: contact (stylus) and optical. Stylus profilometers use a probe to detect, or physically 'feel' the surface. Physically moving a probe along the surface in conjunction with a feedback loop to maintain a constant force allows for the acquisition of surface height and roughness information along the scan line. A stylus profilometer is shown in Fig. 2.9

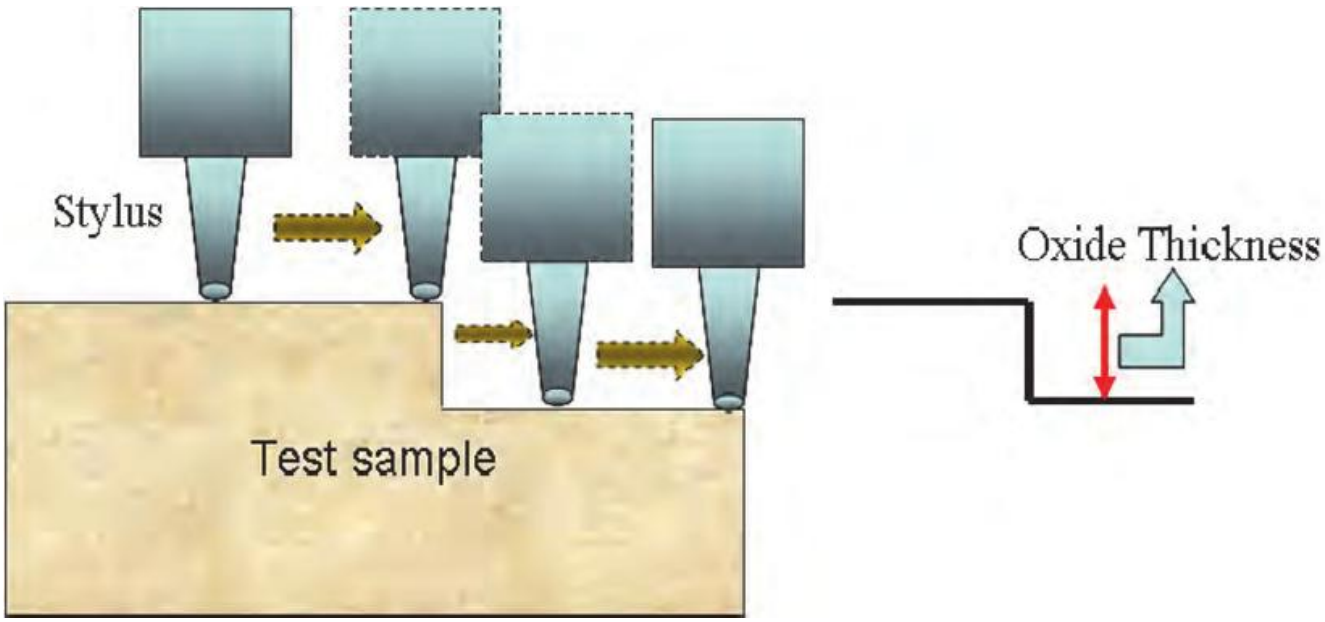

Fig. 2.9 A stylus profilometer (Sanjeev and Jamil, 2011)

Optical profilometer utilize the wavelike properties of light while scanning the sample (or objective) in the z-dimension to obtain 3D data through various techniques. Examples of optical profilometry include white light interferometry, scanning confocal microscopy, and grid confocal. Since optical profilometers use a camera as the detector they obtain data over a 2D area. Stylus profilometers use a probe as the detector so they obtained data along the length of an ID line. Since all profilometers obtain height (z) information this means that optical profilometers are 3D (x, y, z) techniques while stylus profilometry is a 2D (x, z) technique.

The advantages include: acceptance, surface, independence, resolution and direct technique.

The disadvantages include:

1. It is not suitable for very soft (or even liquid) and easily damageable surface.
2. It is very hard and damage surface can damage the stylus.
3. It is a 2D (x, z) technique.

2.6.2.2 Non-contact Profilometers

An optical profilometers is non-contact method for providing much of the same information as a stylus based profilometers. There are many different techniques which are currently being employed, such as laser triangulation (triangulation sensor), confocal microscopy (used for profiling of very small objects), low coherence interferometry and digital holography.

Stylus Proficometry is the technique recommended because it can easily measure thickness parameters as well as stress and surface roughness.

2.7 Electrical characterization

This determines the conductivity of nanoparticles and can be performed using four point probes or two point probes.

2.7.1 Four - point probe resistivity measurement techniques

Four-point probe method is an electrical resistance measuring technique that uses separate pairs of current carrying and voltage – sensing electrodes to make more accurate measurements than the simpler and more usual two-terminal sensing. Separation of current and voltage electrodes eliminates the lead and contact resistance from the measurement. This is an advantage for precise measurement of low resistance values.

For high resistivity samples, the current is reduced so as not to have an excessively larger voltage at the contacts. It is recommended that voltage on the inner probes should be less than 100 mV/mm.

Low resistivity samples are usually much easier to measure as the contacts to the silicon are ohmic. For very low resistivity, the current has to be increased to 45.3 mA and set the voltmeter to a lower scale. For very low resistivity samples, the current passing through the sample causes resistive heating that will in turn increase the measured resistivity. Four terminal sensing is used in some ohmmeters and impedance analyzers, and in wiring for strain gauges and resistance thermometer. Four – point probes are also used to measure sheet resistance of thin film (Chandra *et al*., 2017). The sketch of Four-point probe is shown in Fig. 2.10.

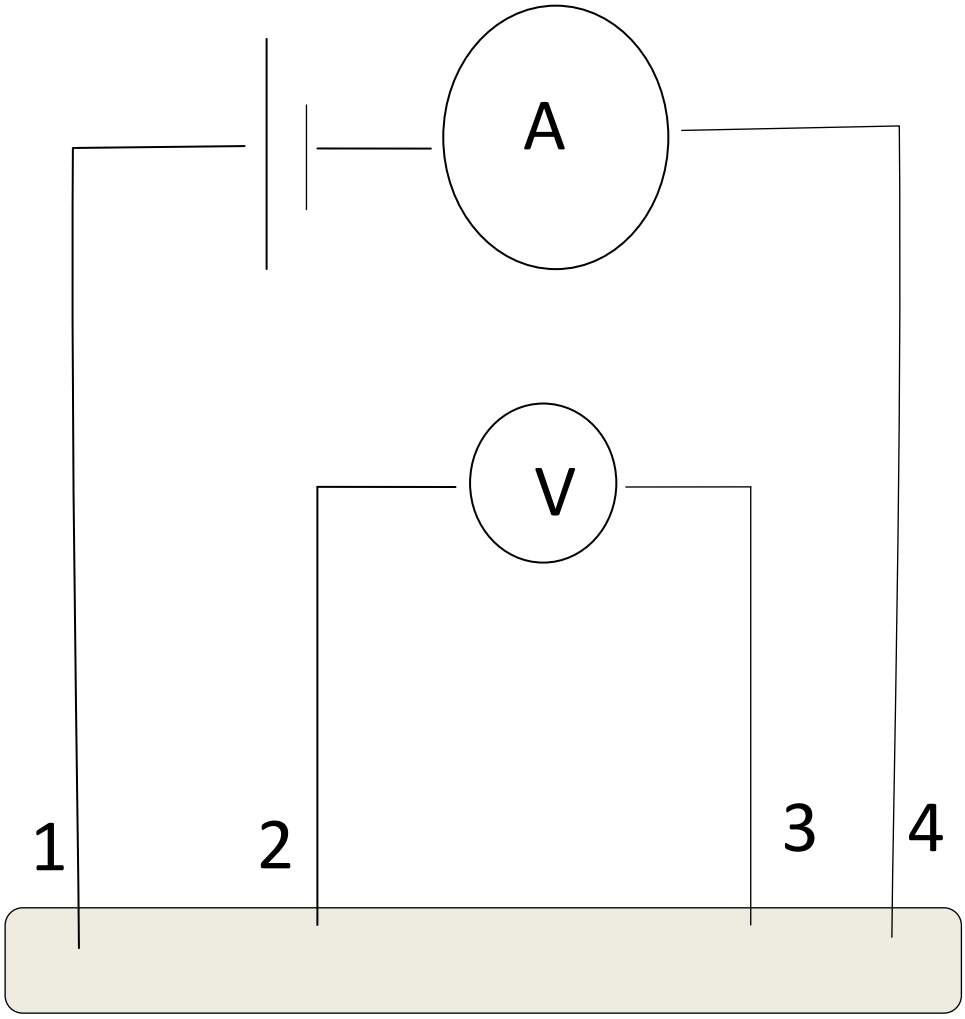

Fig. 2.10 Four point probe measurement. (Chandra *et al*., 2017)

Four- point measurement of resistance between voltage sense connections 2 and 3. Current is supplied via force connections 1 and 4.

Four-terminal technique is also known as Kelvin sensing, after William Thomson (Lord-Kelvin) who invented the Kelvin bridge in 1861 to measure very low resistances using four-terminal sensing. Each two-wire connection can be called a Kelvin connection. A pair of contacts that is designed to connect a force – and – sense pair to a single terminal or lead simultaneously is called a Kelvin contact. A clip, often a crocodile clip that connects a force and sense pair is called a Kevin clip.

Four-point probe offers 4 point probe equipment for measuring the sheet resistance and bulk (volume) resistivity of materials used in the semiconductor industry, universities, and in materials science including thin films, wafers, ingots, and other materials and conductive coatings.

2.7.1.1 Principles of the four point probe

In derivations for this, we assume that the metal tip is infinitesimal and samples are semi-infinite in lateral dimension. For bulk samples where the sample thickness t>>s, the probe spacing assuming a spherical protrusion of current emanating from the outer probe tips, the differential resistance is given by the equation 2.13 (Smits,1958; Chandra*etal.*,, 2017)

$$\Delta R = \rho\left(\frac{dx}{A}\right) \quad (\rho = \frac{RA}{l} => R = \frac{\rho l}{A} \quad (l = x) \qquad 2.13$$

Carrying out the integration between the inner probe tips (where the voltage is measured):

$$R = \int_{x_1}^{x_2} \rho \frac{dx}{2\pi x^2} = \frac{\rho}{2\pi}\left(-\frac{1}{x}\right)|_{x_1}^{x_2} = \frac{1}{2s}\frac{\rho}{2\pi}(A = 2\pi x^2) \qquad 2.14$$

where probe spacing is uniformly s. Due to the superposition of current at the outer tips, R =V/2I. Thus, we arrive at the expression for bulk resistivity:

$$\rho = 2\pi S\left(\frac{V}{I}\right) \qquad 2.15$$

$$\left([R2S2\pi] = \rho, \qquad if R = {}^{V}/_{2I} => \frac{V}{I}S2\pi = \rho => \rho = 2\pi S\frac{V}{I}\right)$$

Thin sheet for a very thin layer (thickness t << s), there are current rings instead of spheres. Therefore, the expression for the area

$$A = 2\pi xt \qquad 2.16$$

the derivation is as follows:

$$R = \int_{x_1}^{x_2} \rho \frac{dx}{2\pi xt} = \int \frac{\rho}{2\pi t}\frac{dx}{x} = \frac{\rho}{2\pi t} lnx, |_s^{2s} = \frac{\rho}{2\pi t} ln2 \qquad 2.17$$

Consequently, for R =$V/2I$, the sheet resistivity for a thin sheet (Lamouri et al., 2014) is:

$$\rho = \frac{\pi t}{ln2}\left(\frac{V}{I}\right) \qquad 2.18$$

$$\left(R = \frac{\rho}{2\pi t} ln2, \qquad if R = \frac{V}{2I} \Rightarrow \frac{V}{2I} = \frac{\rho}{2\pi t} ln2 \Rightarrow \rho = \frac{2\pi t}{2ln2}\left(\frac{V}{I}\right)\right)$$

$$\rho = 4.53t\left(\frac{V}{I}\right) \qquad \left(\frac{\pi}{ln2} = 4.53\right) \qquad 2.19$$

Note that this expression is independent of the probe spacings. Furthermore, this latter expression is frequently used for characterization semiconductor layers, such as diffused N+ region in a p-type substrate. In general, the sheet resistivity:

$R_s = \rho/t$ can be expressed as:

$$R_s = k\left(\frac{V}{I}\right) \qquad 2.20$$

where the factor k is geometric factor, in the case of a semi-infinite thin sheet, k=4.53, which is just $\pi/In2$ from the derivation. The factor will be different for non-ideal samples.

Therefore, the conductivity (σ) of a material is given as

$$\sigma = \frac{1}{\rho} = \frac{1}{4.53t(\frac{V}{I})} \quad 2.21$$

Resistivity, Rho (ρ), is a particularly important semiconductor parameter because it can be related directly to the impurity content of a sample. The four point probe is the apparatus typically used to determine bulk resistivity. The mobility of the carriers depends upon temperature, crystal defect density, and all impurities present. Hall Effect measurements can determine the mobility of the carriers in a given sample to allow for more accurate dopant concentration measurements, but hall measurements are usually destructive to the sample.

Conductivities of different samples of poly (o-phenylenediamine) are measured using four point probe set-up instrument (Chandra et al., 2017).

Current I is passed through the outer probes (1 and 4) and the floating potential "V" is measured across the inner pair of probes (2 and 3).

The sample pellet was put on the base plate of the four probe arrangement and the four probe was gently paced on the pellet and a very gentle pressure was applied and tightens the pipe. By adjusting the milliammeter reading current was kept constant. The millivoltage was then measured. Do the same with the other side of the pellet and also repeat the same experiment using another pellet of the same polymeric sample.

2.8 The Thermogravimetric characterization

Thermogravimetric analysis (TGA) is conducted on an instrument referred to as a thermogravimetric analyzer. A thermogravimetric analyzer continuously measures mass while the temperature of a sample is changed over time. Mass, temperature, and time in thermogravimetric analysis are considered base measurements while many additional measures may be derived from these three base measurements.

A typical thermogravimetric analyzer consists of a precision balance with a sample pan located inside a furnace with a programmable control temperature. The temperature is generally increased at constant rate (or for some applications, the temperature is controlled for a constant mass loss) to incur a thermal reaction.

The thermal reaction may occur under a variety of atmospheres including: ambient air, vacuum, inert gas, oxidizing/reducing gases, corrosive gases, carburizing gases, vapors of liquids or "self-generated atmosphere"; as well as a variety of pressures including: a high vacuum, high pressure constant pressure, or a controlled pressure.

The thermogravimetric data collected from a thermal reaction is compiled into a plot of mass or percentage of initial mass on the y axis versus either temperature or time on the x-axis. This plot, which is often smoothed, is referred to as a TGA curve. The first derivative of the TGA curve (DTG curve) may be plotted to determine inflection points useful for in-depth interpretations as well as differential thermal analysis (DTA).

A TGA can be used for materials characterization through analysis of characteristic decomposition patterns. It is an especially useful technique for the study of polymeric materials including thermoplastics, thermosets, elastomers, composites, plastic films, fibers, coatings, paints, and fuels.

2.8.1 Applications of TGA

Thermal stability

TGA can be used to evaluate the thermal stability of a material. In a desired temperature range, if a species is thermally stable, there will be no observed mass change. Negligible mass loss corresponds to little or no slope in the TGA trace. TGA also gives the upper use temperature of a material. Beyond this temperature the material will begin to degrade.

TGA is used in the analysis of ceramics and thermally stable polymers. Ceramics usually melt before they decompose as they are thermally stable over a large temperature range, thus TGA is mainly used to investigate the thermal stability of polymers. Most polymers melt or degrade before 200 °C. However, there is a class of thermally stable polymers that are able to withstand temperatures of at least 300 °C in air and 500 °C in inert gases without structural changes or strength loss, which can be analyzed by TGA (Liu and Yu, 2006; Tao *et al*., 2009).

2.9 Preparation of conducting polymer films

Various techniques have been developed to prepare conducting polymer films. They include; electrochemical deposition, dip-coating, spin- coating, langmuir- blodgett (lb) technique, layer-by-layer (lbl) self-assembly technique, thermal evaporation. vapour deposition polymerization and drop –coating.

2.9.1 Electrochemical deposition

Electrochemical deposition is the most convenient method to deposit conducting films. The thickness of the film can be deposited on patterned microelectrodes (Lu *et al*., 2005). The deposition must be carried out on a conducting substrate. If the insulating gap between the neighbouring electrodes is close enough (~several tens of micrometer), the growing film can cover the insulated gap and connect electrodes (Reemts *et al*., 2004).

2.9.2 Dip-coating

When dipping a substrate into a chemical polymerization solution, part of the polymer will be deposited onto its surface (McGovern *et al*., 2005; Cho *et al*., 2005). This process occurs on different substrates and the thickness of the film is usually controlled by dipping time. Another similar process involves alternatively immersing a substrate into the monomer and oxidant

solutions. The absorbed monomer will be polymerized on the surface of substrate (Brady *et al*., 2005; Silverstein *et al*., 2005).

2.9.3 Spin- Coating

Spin coating is a simple method for preparing films from soluble conducting polymers. In this process, the conducting polymer solution is spread on a rotating substrate (Prasad *et al*., 2005; Tongpool and Yoriya, 2005) After evaporation of solvent, a thin film was formed. Repeating above process is feasible, which can control the thickness of the film. Concentration of the solution and rotating rate of the substrate also play important roles in adjusting the thickness of the formed film. This method can coat conducting polymers on both conducting and insulating substrates.

2.9.4 Langmuir- Blodgett (LB) technique

LB technique is a famous method to produce a thin film of polymer and surfactant. Two different ways are reported to deposit a conducting polymer film by LB technique: directly depositing polymer and depositing monomer followed by polymerization on the substrate. A LB film is ultrathin (mono-molecular, layer), and a thick film can be obtained by repeating the procedure of LB deposition.

2.9.5 Layer-by-Layer (LBL) self-assembly technique

By alternative immersing the substrate into a polymeric anion solution and a polymeric cation solution, an alternative composite film (Layer by Layer) consists of the two polymeric electrolytes is fabricated (Ram *et al*., 2005;). Doped conducting polymers, such as PAni, bring positive charge on their backbone, which allow it or make it possible to deposit with a polymeric anion. The thickness of LBL film depends on the number of repeating times.

2.9.6 Thermal Evaporation

This technology can be realized by heating conducting polymer under vacuum, and the evaporated conducting polymer deposits on the target substrate. The thickness of the film is determined by the evaporation duration (Agbor *et al*., 1995).

2.9.7 Vapour deposition polymerization

This technology consist of two steps: prepare an oxidant film and then place the film into monomer vapour. (Stussi *et al*., 1996). The monomer diffuses into the film and polymerized on it. This technique is useful not only in preparing a pure conducting polymer film but also in coating composite films of different conducting polymers.

2.9.8 Drop –Coating

A polymer solution is drop dried (Ruangchuang *et al*., 2004; Sandberg *et al*., 2005), or some drops of the monomer and oxidant solutions are dropped and reacted on a substrate. This technology is rather simple. However, the resulting film is usually not in uniform.

Other methods: An electric field induced electrochemical polymerization can fabricate patterned conducting polymer film. For example colloidal suspension of PAni is controlled to directionally deposited on microelectrodes at controlled voltages (Li *et al*., 2005). For soluble conducting polymers, inkjet-print also is a convenient method for producing thin films (Mabrook *et al*., 2006).

2.10 Synthesis of conducting polymers

Conducting polymer films with a high conductivity and a high stability can be synthesized either by a chemical oxidation from a monomer solution in the presence of a strong oxidant or by electrochemical oxidation from a monomer solution in the presence of a supporting salt. Electrochemical polymerization is limited to metallic or semi conducting substrates but offers

many advantages including its easiness, rapidity of the reaction, and possibility to accurately control the experimental conditions. Another attractive advantage of electrochemical deposition method for synthesizing conducting polymers is that the desired product may be anchored onto substrate materials at the desired quantity, shape and size for the final application in one single step. Hence, electrochemical methods to produce conducting polymer films have been extensively studied. (Liang *et al*., 2002; Dinh and Birss, 2000; Zhou*et al*., 2004; Guo and Zhou, 2007; Carquing *et al*., 2008; Patois *et al*., 2011).

2.11 Electrochromic material

Numerous chemical materials exhibit redox states with distinct electronic (Uv-visible) absorption spectra. Where the switching of redox states generates new or different visible region bands, the material is said to be electrochromic (Barnfield, 2001; Monk *et al*., 1995; Granquist, 1995; Green, 1996).

Colour changes in an object give visual signals that can be used to convey useful information to an observer (Barnfield, 2001).Where a chemical or physical external stimulus causes a reversible colour change or variation in light transmission, the possible applications are considerable. For such systems, colour change phenomena are classified (Mortimer *et al*., 2006), after stimulus that causes the change such as electrochromism, photochromism, themochromism and gasochromism. An electrochromic material is one where a reversible colour change takes place upon reduction (gain of electrons) or oxidation (loss of electrons), on passage of electrical current after the application of an appropriate electrode potential (Monk*et al*., 1995; Leventis, 2002; Mortimer 1999; Rowley and Mortimer 2002; Mortimer and Rowley, 2004; Rosseinsky and Mortimer, 2001).

While materials are considered to be electrochromic when marked visible colour changes are shown under illumination. Recent interest in electrochromic devices (ECD's) for multispectral energy modulation by reflectance and absorbance has extended the definition (Mortimer *et al*., 2006). Chemical species are now being studied for modulation of radiation in the near infra-red (NIR), (Mortimer and Rowley, 2004; Ward and McCleverty, 2002), thermal infra-red, (Wu *et al*., 2004) and microwave regions and colour can mean response of detectors to these electromagnetic regions not just the human eye (Mortimer *et al*., 2006).

2.11.1 Types of electrochromic materials

Electrochromic materials are of three basic types, (Mortimer *et al*, 2006). In a given electrolyte solution, type I materials are soluble in both the reduced and oxidized (redox) states. An example is methyl viologen. Type II materials are soluble in one redox state, but form a solid film on the surface of an electrode following electron transfer. An example is heptyl viologen. In type III materials such as conductive polymers, both redox states are solids and such systems are generally studies as thin films on electrode surfaces. For types II and III, once the redox state has been switched, no further charge injection is needed to retain the new electrochromic state and such system are said to have optical memory. For type I elcectrochromic materials, diffusion of the soluble electrochemically generated product material away from the electrode occurs and it is necessary to keep current flowing until the whole solution has been electrolyzed. Where more than two redox states are electrochemically accessible in a given electrolyte solution, the electrochromic material may exhibit several colours and be termed poly-electrochromic, a frequent property of electrochromic polymers (Monk *et al*., 1995).

2.11.2 Applications of Electrochromic Materials

Commercial applications of electrochromic materials in devices include anti-glare car, rear-view mirrors, (Green, 1996; Rosseinsky and Mortimer, 2001), electrochromic strips as battery state-of –charge indicators and electrochromic sunglasses. Proposed applications include smart windows (based on modulation of either the transmitted or reflected solar radiation) for use in cars and buildings (Mortimer *et al*., 2006), re-usable price labels, protective eyewear, controllable aircraft canopies, glare-reduction systems for offices, devices for frozen –food monitoring (Colley *et al*., 2000) camouflage materials, spacecraft thermal control, and controllable light-reflective or light transmissive display devices for optical information and storage.

2.12 Gap in Literature

Though different researchers have used chemical oxidation and electrochemical methods for the synthesis of poly (o- phenylenediamine) with different oxidizing agents and different acid media, but in this work, poly (o- phenylenediamine) thin films are prepared by electropolymerization at different pH values using fluorine doped thin oxide (FTO) substrate and phosphate buffer.

Also different researchers have studied the electrochromism of some metals, conducting polymer/metal nanoparticles films and few copolymers. But this research aimed at determining electrochromic performance of the thin films of homopolymer of o- phenylenediamine.

The point of inflection (peak degradation temperature) of the PoPD by thermogravimetric analysis is also determined in this work which has not been reported in previous literatures.

CHAPTER THREE

MATERIALS AND METHODS

3.1 Materials and Equipment

The o-phenylenediamine (oPD) used in this work was procured from Quallkems. The potassium dichromate ($K_2Cr_2O_7$) was procured from Kermel. The concentrated Hydrochloric (HCl) acid was procured from Sigma Aldrich, Oceanic chemicals Nig. Ltd. The conducting substrates used were fluorine doped Tin Oxide (FTO)TCO22-15 5X5cm SOLARONIX. Graphite was procured from MERCH, sodium hydroxide from AVONDALE Laboratories LTD, phosphoric acid (H_3PO_4), dihydrogen sodium phosphate i.e sodium phosphate monobasic monohydrate (NaH_2PO_4) and disodium hydrogen phosphate i.e sodium phosphate dibasic heptahydrates anhydrous (Na_2HPO_4) from Sigma Aldrich, Oceanic chemicals Nig. Ltd.

The equipment used are electronic balance (Metlar MT-200), magnetic stirrer hot plate (Pec Medicals USA 78-1), digital thermometer (Benetech GM 320), thermostat oven (DHG - 9023A) measuring cylinder, hand gloves, nose mask, stirring bar, beakers, distilled water, aluminium foil, centrifuge (Meheco 800), ice block, burette with tripod stand, multimeter, D.C Power supply (Koocu 150200), pH-meter(Techmel & Techmel USA, PHS-25), volumetric flask, glass funnel, wash glass, spatula, glass rod, Scanning Electron Microscope (PRO: X: Phenonm World. Serial number: MVEO1570775; Model number:800-07334), X-ray Diffractometer (Thermo Scientific model: ARL'XTRA X-ray with Serial Number: 197492086), Raman Spectroscope (Model No. Pro Raman-L-785-B1S with Serial Number: 196166), Thermogravimetric Analysis (MSE-TGA, Perkin Elmer, TGA 4000, made in Netherlands), Brunauer Emmett Teller (Quantachrome Novawin-Data Acquisition and reduction for NOVA Instruments © 1994-2013, Quantachrome Instruments Version 11.03), Ultra Violet spectroscope (Axiom medical Ltd. UK,

UV 752), surface profilometer (Veeco, ektat 150, Vintage: 2010 software:ektat) and four –point probe number: 0104636, Software: Quadpro 3.7.0.

3.2 Experimental procedures

For the dry sample preparation

The experiment was performed at Namiroch Laboratory Nig. Ltd., Plot 62B Oversea Quarter Extension, Kwali,Abuja.

The measuring cylinders (50 ml and 10 ml) and 250 ml beaker were first rinsed with distilled water. 1.622 g of o-phenylenediamine (oPD) was weighed using electronic balance and was added to 50 ml of 0.1 M of HCl.

For the HCl,

Molar mass = 36.4611 g/mol, Density = 1.189 g/cm^3 and % Concentration = 37.5%

$$\text{Reacting mass of HCl} = \frac{0.1\ X\ 36.4611\ X\ 1000}{1000} = 3.6411\ g \qquad 3.1$$

$$\text{Volume required} = \frac{3.6411\ g}{0.375\ X\ 1.189} = 8.166\ ml \qquad 3.2$$

$$\text{Reacting mass of oPD} = \frac{108.1\ X\ 0.3\ M\ X\ 50\ ml}{1000} = 1.622\ g \qquad 3.3$$

The solution was covered with aluminum foil, placed on the magnetic stirrer hotplate for heating and stirring for about 5minutes. While still leaving the cover foil on top of the beaker, the covered beaker was placed inside a 500 ml beaker with ice block to bring the temperature of the solution down to 20 ^{o}C.

50 ml of potassium dichromate ($K_2Cr_2O_7$) as the oxidizing agent was prepared by dissolving 4.413 g of $K_2Cr_2O_7$ in 50 ml of 0.1 M of HCl.

Reacting mass of $K_2Cr_2O_7 = \frac{294.185\ X\ 0.3\ MX\ 50\ ml}{1000} = 4.413\ g$ 3.4

The solution of $K_2Cr_2O_7$ and HCl was placed on the magnetic stirrer hot plate for stirring only. It does not need heating because it dissolves easily.

The temperature probe was removed from the dissolved o-phenylenediamine and was inserted inside the 500 ml beaker with ice block to avoid reaction with $K_2Cr_2O_7$ and HCl solution and still maintained the temperature below 20 ^{o}C.The burette (50 ml) was rinsed with distilled water and was set up with tripod stand. The dissolved $K_2Cr_2O_7$ and HCl was poured inside the burette with the help of a glass funnel and was set to drop bit by bit (dropwise) to slow the reaction for good result and made sure nothing blocked the flow.

The first drop turned the solution into black (very dark brown). The magnetic stirrer was still on while these were taking place. The flow rate was maintained.

The time between the first drop and last drop when the $K_2Cr_2O_7$ solution finished was noted, was 35 minutes and was used to calculate the flow rate.

Therefore

Flow rate = $\frac{\text{50 ml of } K_2Cr_2O_7}{\text{35 minutes}}$ = 1.43 ml/mins 3.5

The magnetic stirrer was switched off and the solution was brought down on the table and left for 24 hrs.Then, the poly (o-phenylenediamine)(insoluble) was separated from the soluble material with the aid of centrifuge (3000 RPM). The poly-o-phenylenediamine was collected after filteration and repeated washing with distilled water and allowed to dry at a temperature of 50 ^{0}C.

For the electropolymerization

The solution (electrolyte) of 0.15 M of o-phenylenediamine and 0.1 M of phosphate buffer was prepared, and Fluorine doped Tin Oxide (FTO) was used as substrates.

The phosphate buffer was prepared with 11.36 g of 0.08 M of Na_2HPO_4 and 2.40 g of 0.02 M of NaH_2PO_4 using 1000 ml of volumetric flask by dissolving the two components with 800 ml of distilled water and making up to 1litre with distilled water. 24.50 g of 1.0 M of phosphoric acid (H_3PO_4) in 250 $cm^3$and 10.0 g of 1.0 M of sodium hydroxide (NaOH) in 250 cm^3 were also prepared for varying the pH of the electrolyte.

From Henderson-Hasselbalch equation; the pH of a solution is related to its pKa, by

$$pH = pKa + \log \frac{[\underline{HPO_4}^{2-}]}{[H_2PO_4^-]} \quad 3.6$$

If pH =7.4, pKa = 6.8,

$$\text{Then } 7.4 = 6.8 + \log \frac{[\underline{HPO_4}^{2-}]}{[H_2PO_4^-]} \quad 3.7$$

$$0.6 = \log \frac{[\underline{HPO_4}^{2-}]}{[H_2PO_4^-]} \quad 3.8$$

$$\frac{[\underline{HPO_4}^{2-}]}{[H_2PO_4^-]} = \text{antilog } 0.6 = 3.98 \approx 4 \quad 3.9$$

4/5 mole or 80% = HPO_4^{2-}conjugate base 3.10

1/5 mole or 20% = $H_2PO_4^-$acid component 3.11

Therefore, 0.8 x 0.1 M = 0.08 mole of conjugate base 3.12

0.08 x 141.96 = 11.36 g of disodium hydrogen phosphate 3.13

0.02 x 119.98 = 2.38 g of dihydrogen sodium phosphate 3.14

For 0.15 M of oPD,

$$\text{Reacting mass of oPD} = \frac{0.15 \times 108.14 \times 250\ cm^3}{1000\ cm^3} = 4.06\ g \quad (3.15)$$

For 1.0 M of H_3PO_4,

$$\text{Reacting mass of } H_3PO_4 = \frac{1.0 \times 97.99 \times 250\ cm^3}{1000\ cm^3} = 24.50\ g \quad (3.16)$$

For 1.0 M of NaOH,

$$\text{Reacting mass of NaOH} = \frac{1.0 \times 39.997 \times 250\ cm^3}{1000\ cm^3} = 10.0\ g \quad (3.17)$$

5 g of Sodium Lauryl Sulphate dissolved in 100 ml of distilled water was used for washing the FTO substrates, rinsed with distilled water and dried before being used. The conducting side of FTO was detected using multimeter and was dropped vertically into the electrolyte for the deposition process using hand gloves with the d.c power supply of 1.2 V. The FTO was connected to the positive terminal and graphite used as negative electrode (connected to the negative terminal). The pH probe was used as reference electrode. Four electropolymerizations were done at different pH values (1.0, 1.5, 2.0 and 9.0) at the deposition time of 5 minutes each. The pH was varied with drop-wise addition of phosphoric acid to the electrolyte to make it acidic or drop-wise addition of sodium hydroxide to reduce the pH to alkaline while stirring, with pH meter probe meter inserted in the prepared electrolyte. The substrates (FTO) were removed at the end of the various pH depositions and were allowed to dry in open air. Figure 3.1 shows the circuit diagram for the electropolymerization.

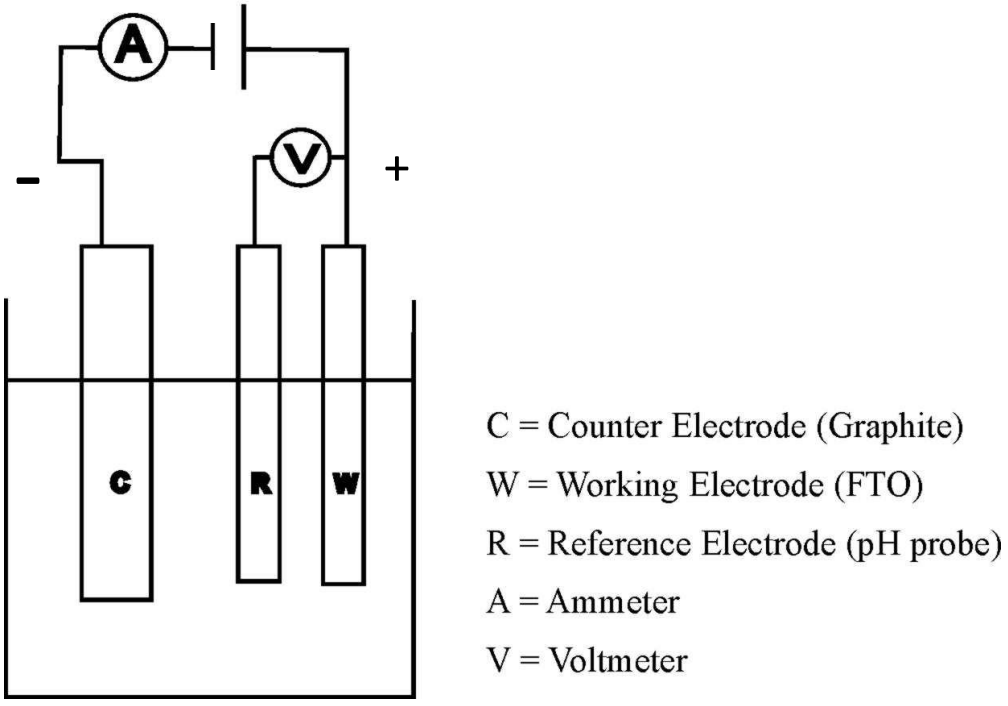

Figure 3.1 The circuit diagram of the electropolymerization of the PoPD thin films

3.3 Characterization of the samples

The samples were characterized using XRD, Raman, SEM, BET, TGA, UV, Four point probe and profilometry. The Raman, TGA , and BET were done at the Federal University, Minna.The SEM and XRD were done in the central Research Laboratory of the Umaru Musa Yar'adua University, Katsina State, The four point probe and profilometry were done at SHEDA Science and Technology Complex Abuja. UV spectroscopy was done at Namiroch Laboratory Nig. Ltd., Kwali Abuja.

3.3.1. Electrical Characterization

The resistivity measurement of the thin films was done using four point probe (Signatone 393 –J Tomkins CT, Model Quadpro 6,220 V, Serial number: 0104636, Software: Quadpro 3.7.0)

The resistivity (ρ) of the sample was calculated using the relation

$\rho = \ 4.53t\left(\frac{V}{I}\right)$ $(\frac{\pi}{ln2} = 4.53)$ and the conductivity (σ) using $\sigma = \frac{1}{\rho} = \frac{1}{4.53t(\frac{V}{I})}$

The sheet resistance was got by multiplying the value of V/I by 4.53, some text use 4.44.

Sheet resistance was used to measure the conductive properties of the conductive layer of FTO coated glass.

3.3.2. The profilometry

The thickness of the thin films was determined using profilometer. The profilometry tool was based on contact measurement of the sample.

The thickness of the deposited material on the substrate is represented by steeps, valleys and hills.

3.3.3. Structural Characterization

Raman spectroscopy used was Mod. No Pro Raman-L-785-B1S with serial number: 196166. Raman has been extremely useful in the structural analysis of a sample. The prepared sample was placed on slide and the slide on the sample chamber so that the distance between the slide and the lens should be about 7 mm apart. The machine was instructed to scan the sample to obtain a suitable peak.

3.3.4. Scanning electron microscopy (SEM)

The microstructure (surface) morphology characterization of the samples was done using SEM (PRO:X: Phenonm world. Serial Number: MVE01570775, Model Number: 800-07334). The sample to be analyzed was placed on a double adhesive sticker placed in a sputter coater machine for 5 seconds. Sample stub was fixed on a charge reduction sample holder and then was injected

into the machine column after which the door of the SEM was closed. The charge reduction sample holder is designed to reduce sample charging by coating and eliminate extra samples such as paper and polymers fast. The SEM machine was allowed to stabilize for ten seconds before setting up parameters to be used. Accelerating voltage of the 15 KV was used in imaging the sample set at different magnifications. The image of the sample was focused using a rotary knob until a clear and proper image was produced in NavCam mode before being transferred to an electron imaging mode.

3.3.5. X-ray diffraction

The XRD of the sample was done using X-ray diffractometer (Thermo scientific model: ARL'X TRA X-ray and serial number: 197492086 Cuk$\propto$ radiation (k$\propto$=1.54056 Å). The diffraction angle 2θ was scanned from 5.000^0 to 70.000^0 step size of 0.030^0 and rate of 12.000^0/min. The XRD determines the type of crystal lattice and intensities of the diffraction peaks. The diffraction pattern was annealed at 25^0C for 0.150 sec.

3.3.6. Thermal Stability

Thermal stability of poly (o-phenylenediamine) was investigated by TGA (Perkin Elmer TGA 4000, made in Netherland). This was done with sample weight of 11.352 mg and heat from 45.00^0C to 950.00^0C at 10.00^0C/minute. The maximum operating temperature is 1200^0C, maximum heat up rate is 20^0C.

3.3.7. Brunauer-Emmett-Teller (BET)

BET (Quantachrome NovaWin – Data Acquisition and Reduction for NOVA instruments © 1994 – 2013, Quantachrome instruments version 11.03) was used to measure surface area of the sample including the pore size distribution from gas absorption.

The analysis gas used was Nitrogen with pressure tolerance of 0.100/0.100 (ads/des), analysis time was 77.4 mins, outgas time of 3.0 hrs with samples weight of 0.14 g, sample volume was 1cc,outgas temperature of 298.0 K and bath temperature of 273.0 K. Equilibrium time was 60/60 sec (ads/des) and equilibrium timeout was 240/240 sec(ads/des). The nitrogen molecular weight was 28.013, temperature of 77.350 K with cross section of 16.200 A^2 and liquid density of 0.808 g/cc. The absorbent used is carbon with DR: Exp(n) :2.000. The critical temperature was 126.200 K, critical pressure was 33.500 atm super critic k was 1.000

3.3.8. Optical Properties

The optical properties of the prepared PoPD thin films were obtained using Ultra Violet spectroscope (Axiom medical Ltd. UK, UV 752) with absorbance in arbitrary units.

Transmittance was calculated using

$$T\% = 10^{-A} \times 100\% \qquad 3.21$$

where T is the transmittance and A is the absorbance.

Reflectance(R) was determined using R = 1 - A + T.

The photon energy (E) in joule = $h\upsilon = \frac{hc}{\lambda}$ 3.22

h = Plank's constant = 6.626 x 10^{-34} Js

$$\upsilon = \frac{c}{\lambda} \qquad 3.23$$

where c = velocity of light = 3 x 10^8 m/s

λ = wavelength

The photon energy in joule was converted into electron volt by dividing by 1.6 x 10^{-19} J/eV

The photon energy in electron volt was also multiplied by the absorption coefficient (α) and was squared = $(\alpha hv)^2$

The absorption coefficient (α) is given as

$$\alpha = \frac{2.303\ x\ A}{t} \qquad 3.24$$

A = absorbance and t = thickness of the thin film

CHAPTER FOUR

RESULTS AND DISCUSSION

2.1 Optical Analysis

The optical characterization was carried out using UV-VIS spectroscope where the absorbance in arbitrary units were obtained. Parameters which include transmittance, reflection, photon energy and absorption coefficient were calculated using the formula listed in chapter three.

Figure 4.1 shows the graph of absorbance plotted against wavelength for thin film samples of poly – o phenylenediamine (PoPD). The absorbance of the PoPD films increases as pH of the films increases toward alkaline region of the pH scale. The wavelengths of electromagnetic radiation used were between 290 nm to 1100 nm. PoPD deposited at a pH of 1.0 shows absorption band peaks at 336 nm and 428 nm. PoPD deposited at pH of 1.5 shows an absorption band peaks at 342 nm and 439 nm. PoPD deposited at pH value of 2.0 shows absorption band peaks at 344 nm, and 445 nm. PoPD deposited at pH value of 9.0 shows absorption band peaks at 358 nm and 452 nm. These band peaks at 336 nm, 342 nm, 344 nm and 358 nm are attributed to $\pi - \pi^*$transitions of the benzenoid and quinoid rings while the band peaks at 428 nm, 439 nm, 445 and 452 nm are due to $\pi - \pi^*$ transition associated with the phenazine ring conjugated to the lone pair of electrons present in the nitrogen of the amine group. From the spectroscopic analysis, it could be suggested that the synthesized PoPD film has a head to tail type arrangement with the benzenoid and quinoid structures in the phenazine – like backbone which is in line with what was obtained by Muthirulan *et al.*, (2013). Comparative study of the absorbance spectra of the films presented in Figure 4.1 shows that the absorption bands of deposited PoPD slightly shifted to longer wavelength (lower energy) commonly known as red shift or Bathochromic shift.

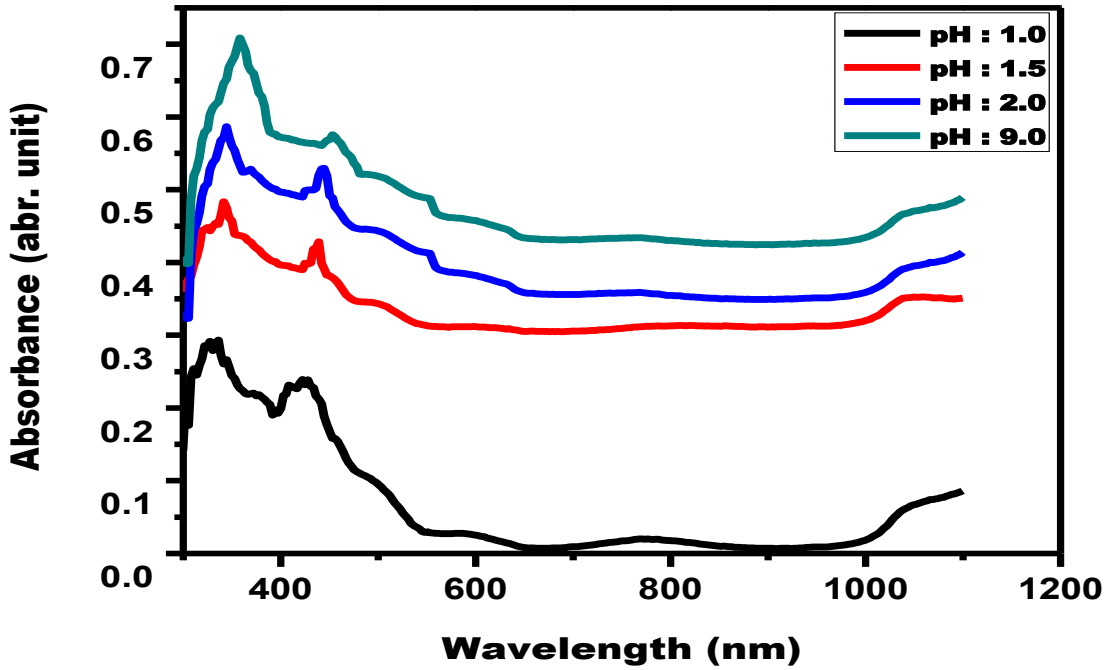

Figure 4.1: Absorbance against Wavelength for the PoPD Samples

Figure 4.2 shows the graph of transmittance plotted against wavelength.

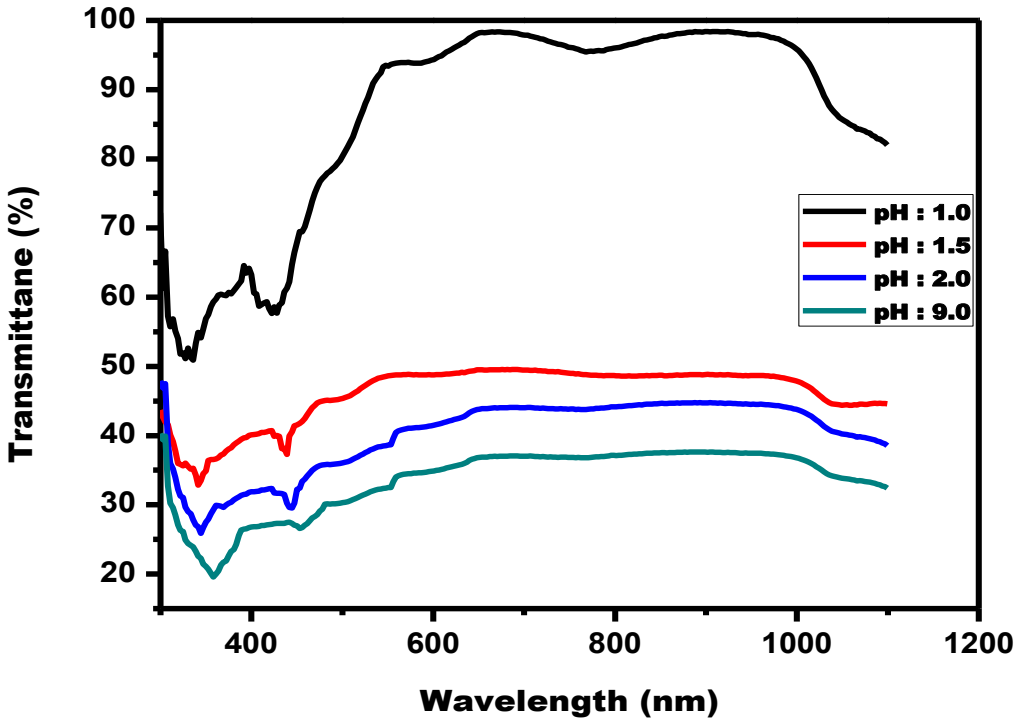

Figure 4.2: Transmittance against Wavelength for the PoPD Samples

The transmittance of the films is found to decrease as pH of the medium tends towards the alkaline region. The transmittance of the polymer films increases slightly as the wavelength increases. Film deposited at a pH of 1.0 has the highest value of transmittance within all regions of the spectrum while film deposited at pH of 9.0 has the least value of transmittance. This suggests that PoPD films with higher transmittive power could best be produced under acidic condition while PoPD films with lower transmittive power could best be produced under alkaline condition.

The graph of reflectance plotted against wavelength is shown in Figure 4.3.

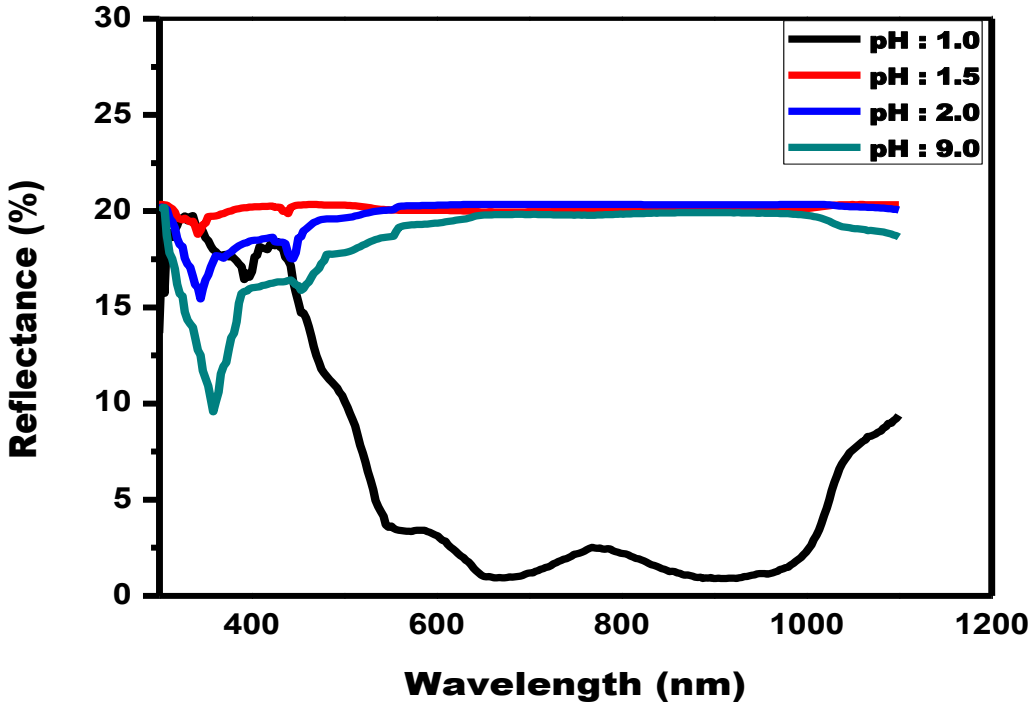

Figure 4.3: Reflectance against Wavelength for the PoPD Samples

The reflectance of the polymer film is generally low. The values for the films fall between 0.93 % and 20.5 %. The patterns of the reflectance spectra for films deposited at pH values of 1.5, 2.0 and 9.0 are similar. This shows that pH values of the reaction medium affect reflective power of

the film produced in such medium. Film deposited at strong acidic condition of pH of 1.0 has the least reflective power.

The graphs of $(\alpha hv)^2$against photon energy are presented in Figure 4.4.

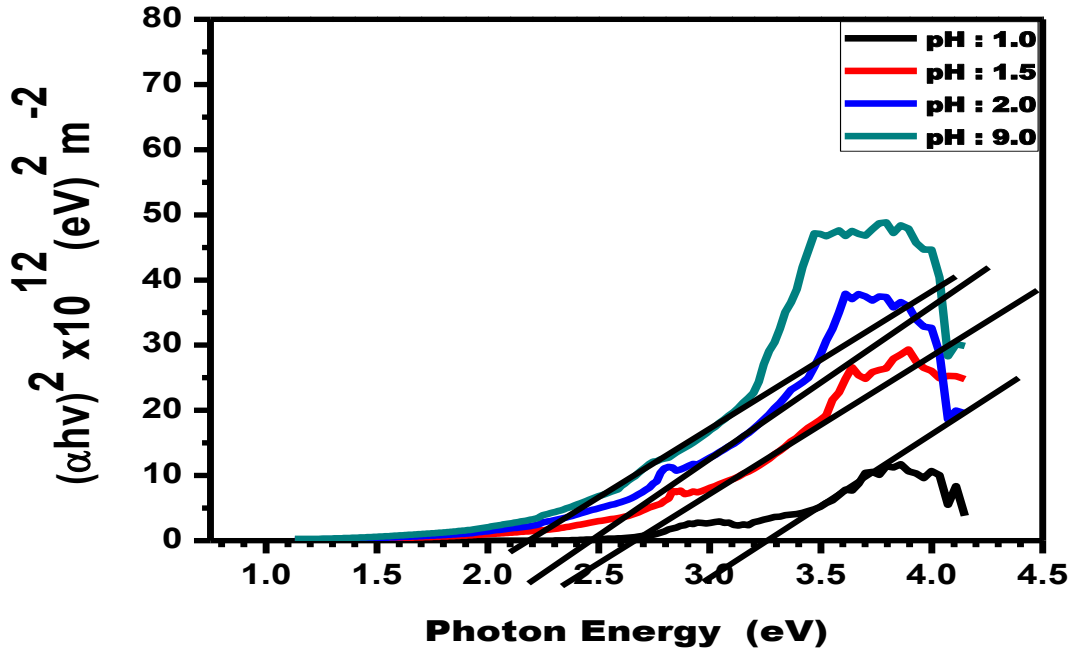

Figure 4.4: $(\alpha hv)^2$ against Photon Energy (eV) for the PoPD Samples

The optical energy band gaps (E_g) of the films were estimated from the plot of $(\alpha hv)^2$ versus photon energy (hv) curves shown in Figure 4.4 for samples deposited at pH of 1.0, 1.5, 2.0 and 9.0 respectively. The straight nature of the plots indicates the existence of direct transition. The direct band gap energies of grown films were determined by extrapolating the straight portion of the graph to the photon energy (hv) axis at $(\alpha hv)^2 = 0$. It was found to be 3.25 eV for film deposited at pH of 1.0, 2.65 eV for film deposited at pH of 1.5, 2.5 eV for film deposited at pH of 2.0 and 2.20 eV for film deposited at pH of 9.0. These results show that the energy band gaps of deposited PoPD films decreases as the pH of the reaction increases.

Figure 4.5 shows the graph of transmittance plotted against wavelength for films deposited at pH of 1.5 and its reverse voltage values.

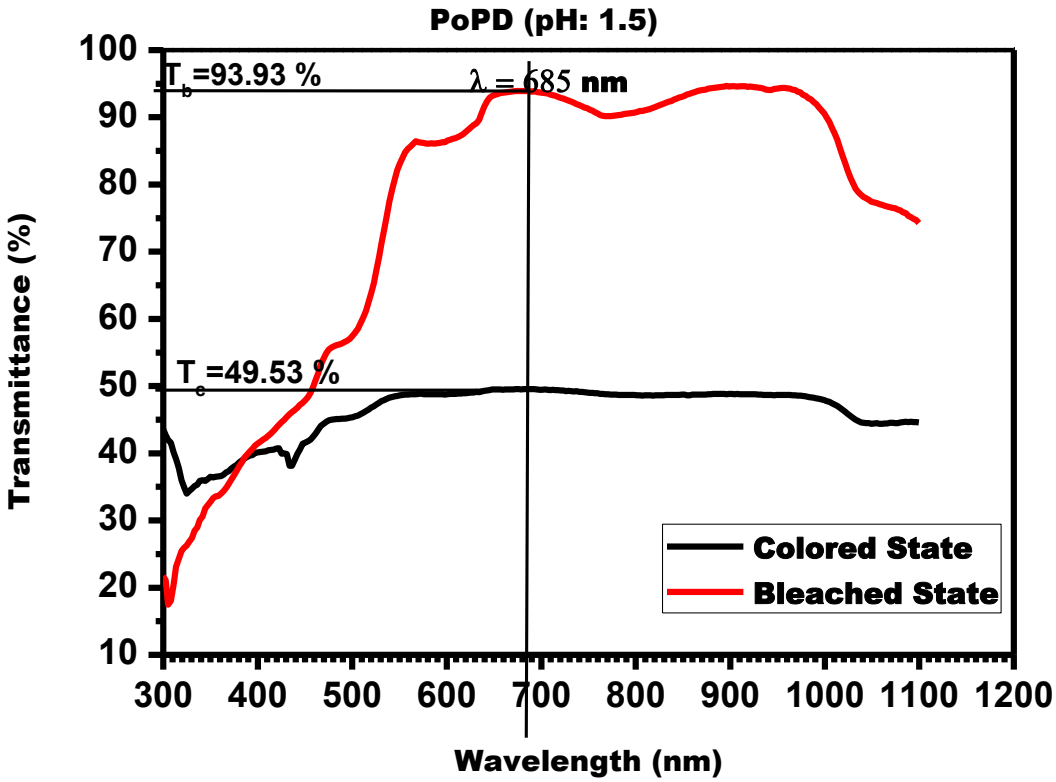

Figure 4.5: Transmittance against Wavelength for pH 1.5 PoPD Samples

A reverse voltage of $(-0.7\,V)$ was applied. The graph of figure 4.5 was used to determine electrochromic behaviour of the film. The optical transmittance spectra showed the coloured and bleached state of the PoPD thin film with pH of 1.5 in the wavelength range from 300 nm to 1100 nm. The optical transmittance of the coloured and bleached ($T_c$and T_b) state at the wavelength of 685 nm (the wavelength at which both states have their highest transmittance) are $T_c = 49.53$ % and $T_b = 93.93$ % respectively. The optical transmittance difference

$$\Delta T = T_b - T_c = 44.40\ \%. \qquad 4.1$$

The optical density (ΔOD) was calculated using the equation (Kraft 2019; Cai *et al.*, 2016)

$$\Delta OD = \ln\left(\frac{T_b}{T_c}\right)_{\lambda=685\ nm} = \ln\left(\frac{93.93}{49.53}\right) = 0.64 \qquad 4.2$$

The contrast ratio (CR) defined as the ratio of the optical transmittance at the bleached state to the optical transmittance at the coloured state at a particular wavelength (685 nm) was calculated using equation provided by (Kraft, 2019).

$$CR = \left(\frac{T_b}{T_c}\right)_{\lambda=685\ nm} = \left(\frac{93.93}{49.53}\right) = 1.896 \approx 1.9 \qquad 4.3$$

The values of the ΔT, ΔOD and CR make the sample a potential material for use in electrochromic devices. According to Stafstrom *et al.*, (1987), an optical density (ΔOD) above 0.3 is suitable for monitors and smart glasses / windows and display applications.

4.2 Scanning Electron Microscopy

The accelerating voltage of 15 KV and backscatter detector (BSD) were used in determining the SEM image. ImageJ for Microscopy Image Analysis software was used to determine the average grain size of the films from the micrograph images (Abramoff *et al.*, 2004). Figures 4.6 to 4.10 give the micrograph images of the powdered and thin film poly (o – phenylenediamine) samples.

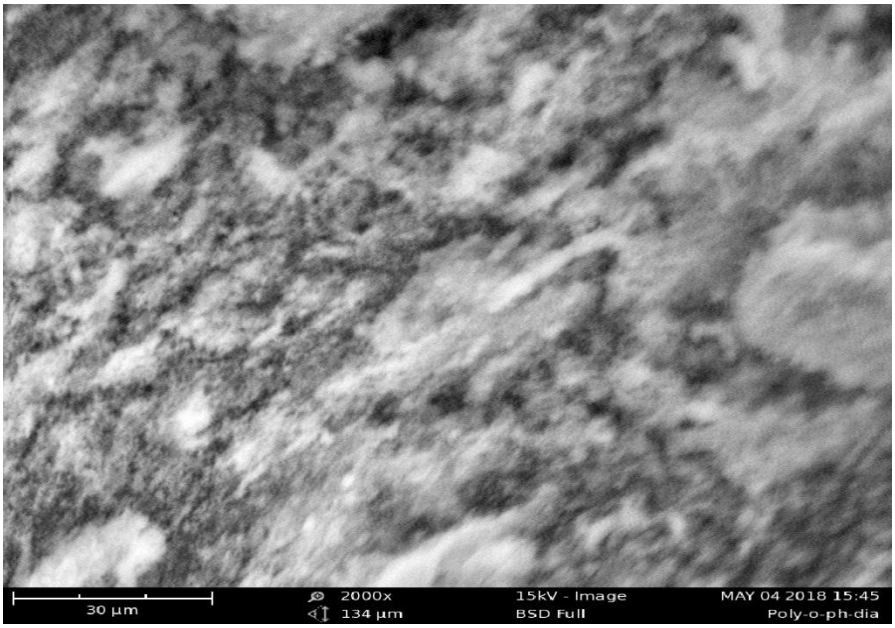

Figure 4.6: Powdered PoPD sample

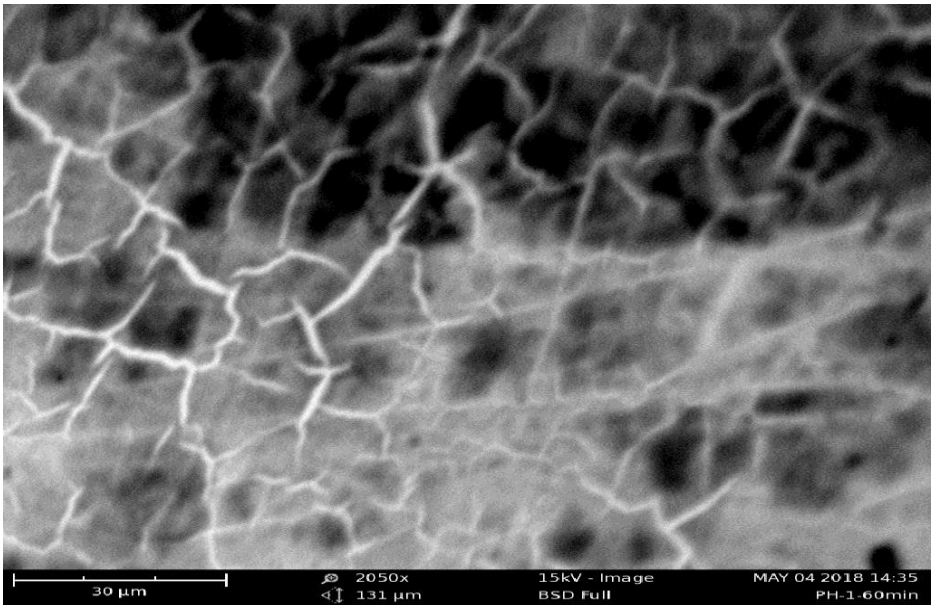

Figure 4.7: PoPD film sampleelectropolymerized at pH : 1.0

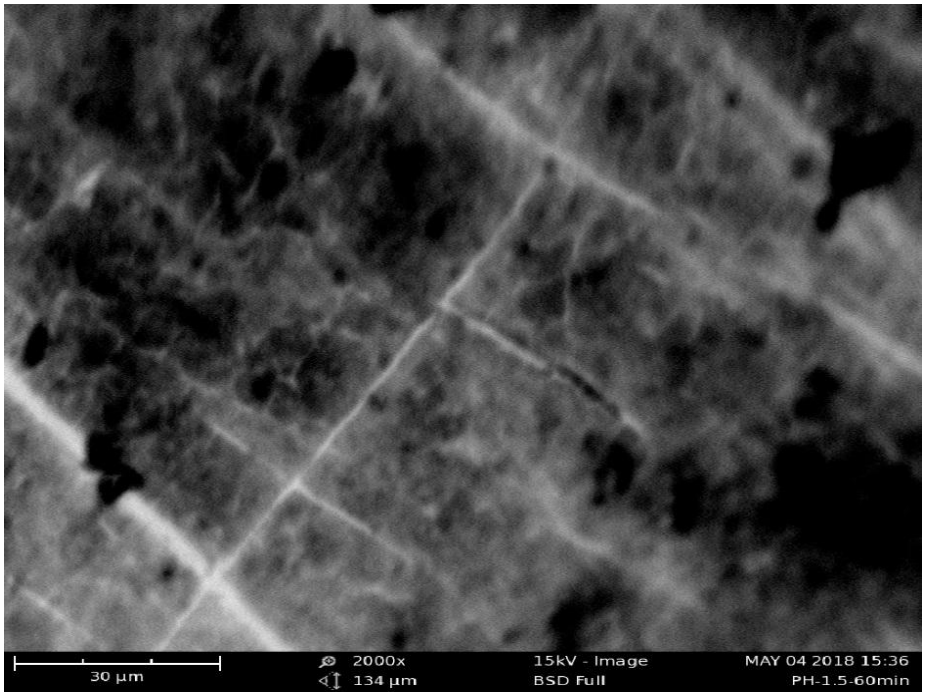

Figure 4.8: PoPD film sampleelectropolymerized at pH : 1.5

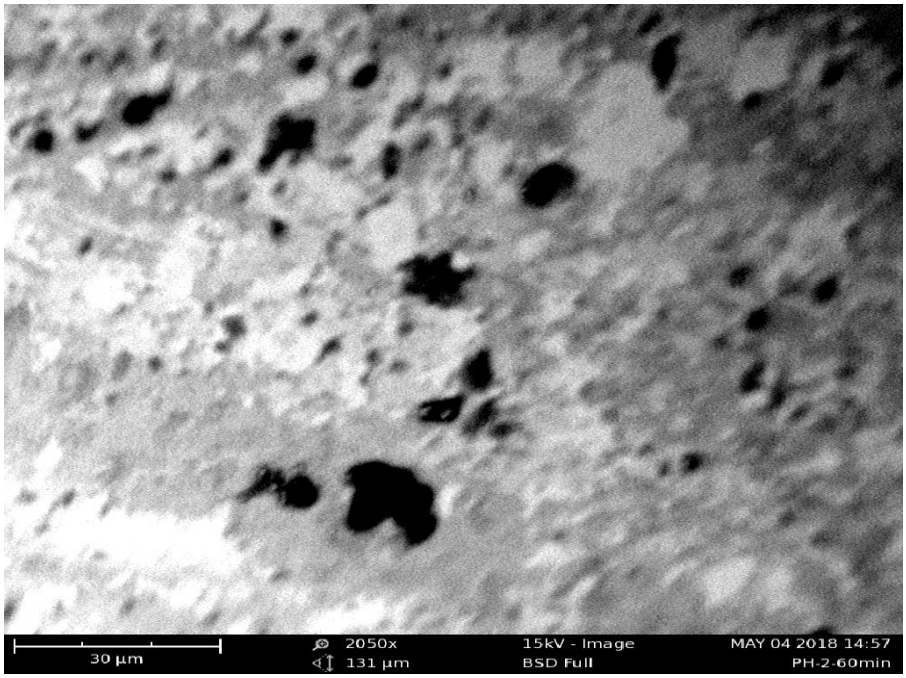

Figure 4.9: PoPD film sampleelectropolymerized at pH : 2.0

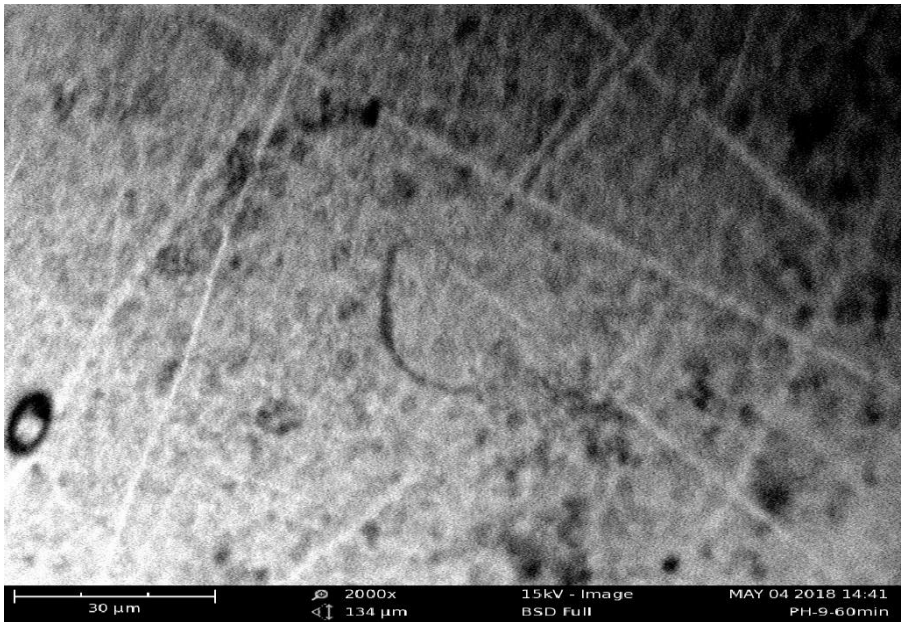

Figure 4.10: PoPD film sampleelectropolymerized at pH : 9.0

The surfaces of the samples look rough and show few spaces that were not properly coated in the case of thin film polymers coated on the FTO conducting glasses. More unevenly dispersed particles of the Poly (o - phenylenediamine) polymer were observed. Figure 4.6 shows the micrograph of the powdered PoPD sample taken at 2000 magnification. The SEM analysis of the image showed that the sample has grain sizes ranging from $200\ \mu m - 50\ \mu m$. The sample is made of uneven grain sizes which are in granular form. Figure 4.7 show the micrograph image of PoPD deposited at pH value of 1.0 taken at 2050 magnification. SEM analysis of the image showed that the material has grain sizes that range from $100\ \mu m - 25\ \mu m$. Figure 4.8 shows micrograph image of PoPD film deposited at pH value of 1.5 taken at 2000 magnification. SEM analysis of the image showed that the grain sizes of deposited polymer film is between $200\mu m - 50\mu m$. Figure 4.9 shows micrograph image of PoPD film deposited at pH value of 2.0 taken at 2050 magnification. SEM analysis of the image showed that the grain sizes range between $50\mu m - 10\mu m$. Figure 4.10 shows the micrograph image of PoPD film deposited at pH

value of 9.0 taken at 2000 magnification. SEM analysis of image showed that the particle sizes of deposited poly (o – phenylenediamine) range between $20\ \mu m$ – $1\ \mu m$. From the results of the SEM analysis, grain sizes of the polymer samples increases as pH value moves towards low acid region from 1.0 to 1.5, reaching an optimal particle size ranging from $200\mu m\ -\ 50\mu m$ at pH of 1.5, then it decreases to grain size range of $20\ \mu m$ – $1\ \mu m$ as the pH of the reaction medium moves towards weak alkaline medium of pH value of 9.0.

4.3 X – ray Diffraction Analysis

The x – ray pattern of the fabricated films of poly (o – phenylenediamine) (PoPD) at 25.0℃ with 2 theta angles step of 0.030° and scanning rate of 12.0 $°/min$ is shown in Figure 4.11.

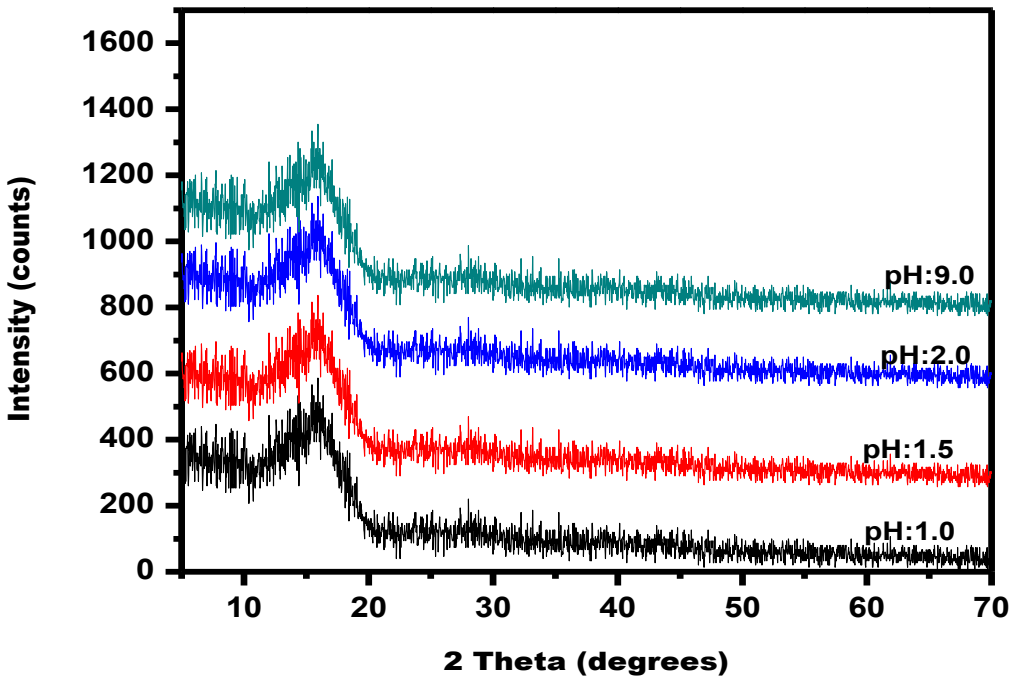

Figure 4.11: XRD pattern of PoPD films

The angle ranged from 5.0 ° - 70.0 ° at Cu-$k_{\alpha 1}$ wavelength of 1.5405Å. The result revealed that the samples are amorphous in nature due to its broad features which is not defined by crystalline model and amorphous materials do not produce sharp diffraction peaks. The pattern is as a result

of the incoherent scatter of the x – ray radiation by the molecules of the polymer samples. Several minor peaks centered between 2θ =15 ° and 2θ = 17 °. The shift in the pH values from highly acidic to weakly basic caused an increase in the intensity of the X– ray radiation. Figure 4.12 shows the XRD plot of powdered PoPD sample.

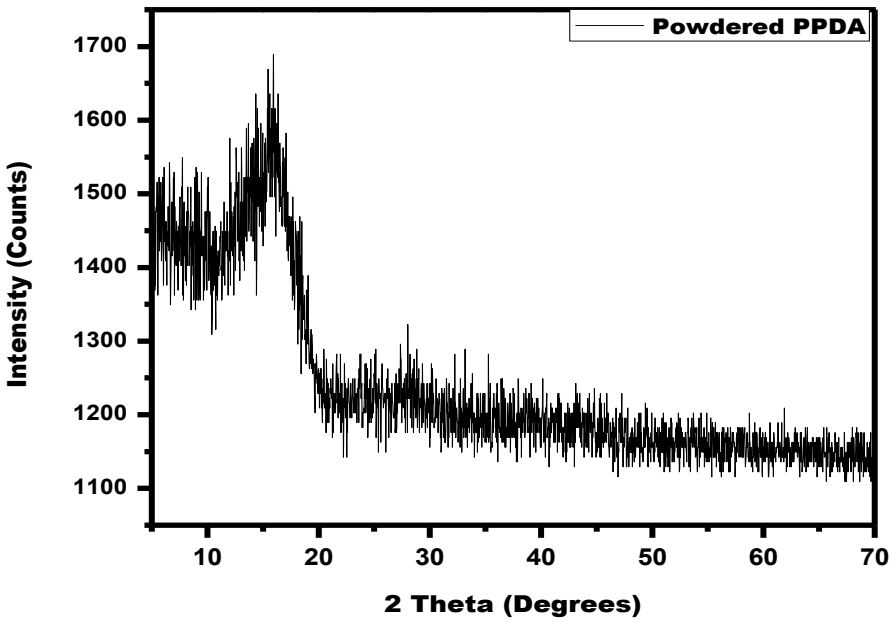

Figure 4.12: XRD pattern of powdered PoPD sample

The powdered polymer sample has similar XRD pattern with that of the thin films shown in Figure 4.11 with difference only in the intensity of the XRD pattern. X – ray intensity of the powdered polymer is higher than that of the thin film samples. This confirms the formation of PoPD particles with good structural arrangement compare to the thin films of the same polymer.

4.4 Thermogravimetric analysis (TGA) and Derivative Thermogravimetric analysis

Thermogravimetric analysis (TGA) measures the amount of weight change of a material, either as a function of increasing temperature or isothermally as a function of time, in an atmosphere of

Nitrogen, Helium, air, other gas or in vacuum. It is a method for thermal analysis in which the mass of a sample is measured over time as the temperature changes. TGA can also be used to evaluate the thermal stability of a material, in a desired temperature range, if a specie is thermally stable, there will be no observed mass change. Negligible lost in the mass corresponds to little or no slope in the thermogram. TGA also gives the upper use temperature of a material, beyond this temperature the material will begin to degrade. Mostly it is used to investigate the thermal stability of polymers since most polymers degrade at < 200 ℃.

Figure 4.13 shows the thermogram of the powdered poly (o – phenylenediamine) with sample weight of 11.352 mg.

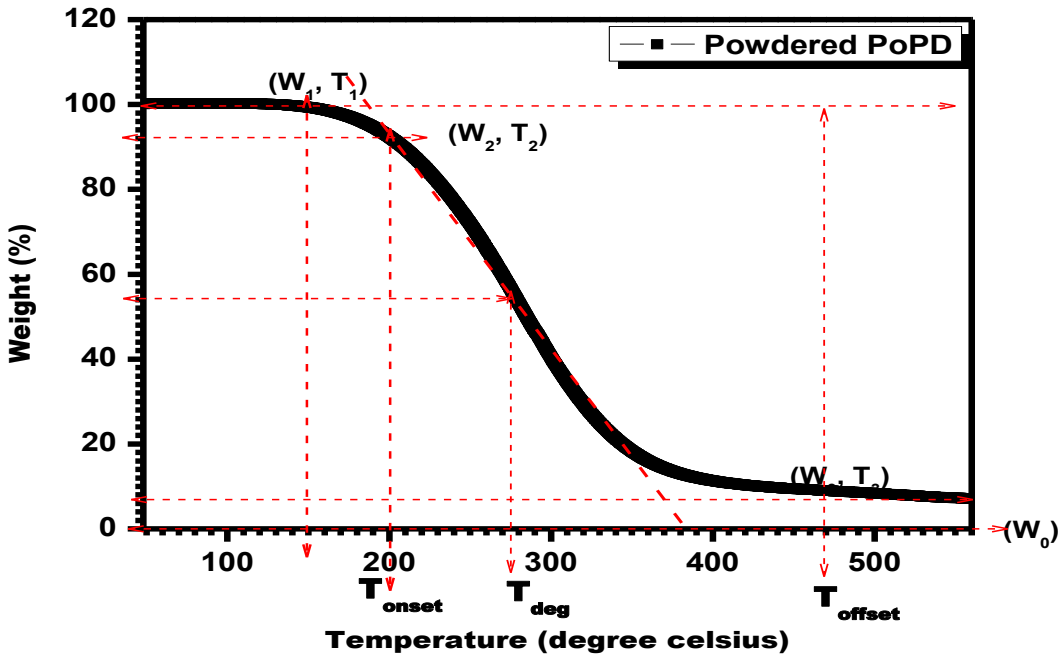

Figure 4.13: Thermogram (TGA) of powdered PoPD sample

The descending TGA thermal curve shown in Figure 4.13 indicates that weight loss occurred due to application of heat to the powder polymer sample. The temperature of the heat applied ranged from 45.00 ℃ to 950.00 ℃ at 10.00 ℃/min with Nitrogen as atmospheric condition. Beyond

572 ℃ the sample shows no further degradation. The thermogram in Figure 4.13 gives the various stages that lead to the thermal degradation of the synthesized polymer. The thermogram provide quantitative information such as loss of water (%), loss of solvents (%), pyrolysis (thermal decomposition), oxidation, and weight of ash or residual (%). The summary of the thermal degradation process is shown in Table 4.1.

Table 4.1: Analysis of the stages on weight loss in the thermogram of PoPD powder

Stages	**Change in weight (%)**	**Loss of mass (mg)**	**Temperature change** $= \boldsymbol{T_{offset} - T_{onset}}$ (℃)
1st (loss of water)	$W_1 - W_2$ $= 100 - 92$ $= 8.0$	$\frac{8.0}{100} \times 11.352$ $= 0.908$	$200 - 150 = 50$
2nd(Pyrolysis or Thermal decomposition)	$W_2 - W_3 = 92 - 7$ $= 85.0$	$\frac{85}{100} \times 11.352$ $= 9.649$	$470.0 - 200.0$ $= 270$
3rd (Residual)	$W_3 - W_0$ $7 - 0$ $= 7$	$\frac{7}{100} \times 11.352$ $= 0.795$	$572 - 470$ $= 102$

From Table 4.1, the weight percentage of moisture content (water and other solvent) removed from the actual weight of the synthesized poly (o phenylenediamine) within the onset temperature (T_{onset}) of 150 ℃ and offset temperature of 200 ℃ is given in the first stage. 8.0 % which is equivalent to 0.908 mg of the actual sample used for the TGA analysis was lost. The second stage involves thermal decomposition (pyrolysis) of the sample with an onset temperature of 200 ℃ and offset temperature of 470 ℃. The percentage weight loss in this stage is 85.0 % which is equal to 9.649 mg of the original sample. The third stage which contain residual in form of charcoals has an onset temperature of 470 ℃ and offset temperature of 572 ℃. Percentage weight of the residual remaining is 7.0 % which represents 0.795 mg.

Therefore, the weight loss as a result of the thermal energy applied to the polymer sample is 9.649 mg which represents about 85 % of the original polymer sample. The temperature of the onset of thermal degradation was observed at 200 ℃ while the offset temperature of thermal degradation is found to be 470 ℃. The derivative thermogram (DTA) of the powdered PoPD sample is shown in Figure 4.14.

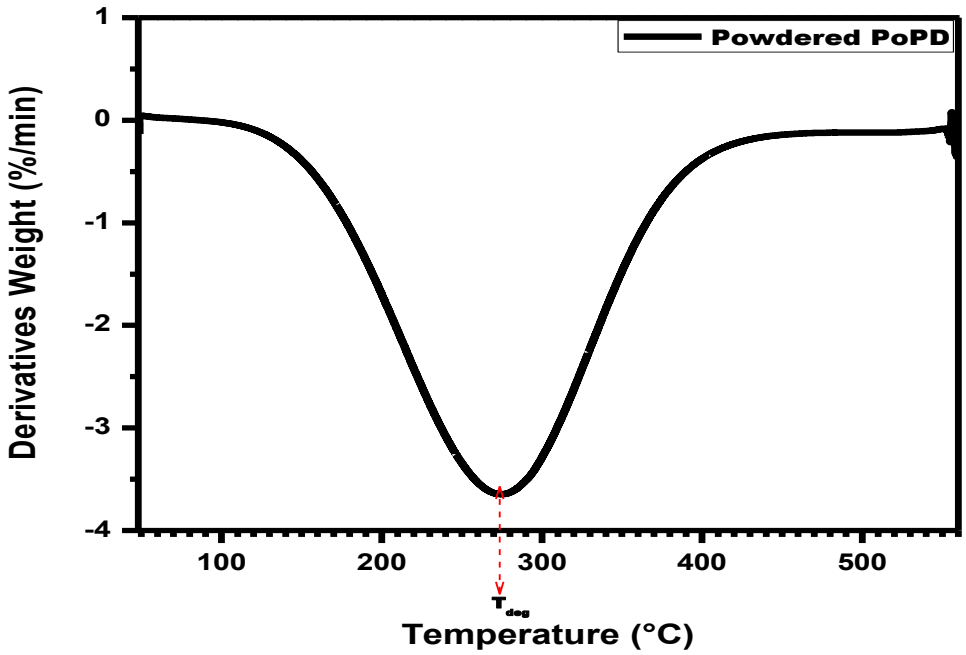

Figure 4.14: Derivative Thermogram (DTA) of Powdered PoPD sample

Figure 4.14 shows the time derivatives of the weight loss against temperature. At any given temperature in Figure 4.14, the rate of weight loss is a function of the amount of original material remaining, the nature and relative amount of degradation product (residue) present. The peak temperature of the derivative indicates the point of greatest rate of change on the weight loss curve shown in figure 4.13. This is known as point of inflection and is the most sensitive point at the temperature axis. This corresponds to the point at which the curve is changing direction at the greatest rate which can also be regarded as the peak degradation temperature. The peak temperature of degradation of the PoPD is found to be 275 ℃.

Figure 4.15 shows both the thermogram and the derivative of the thermogram.

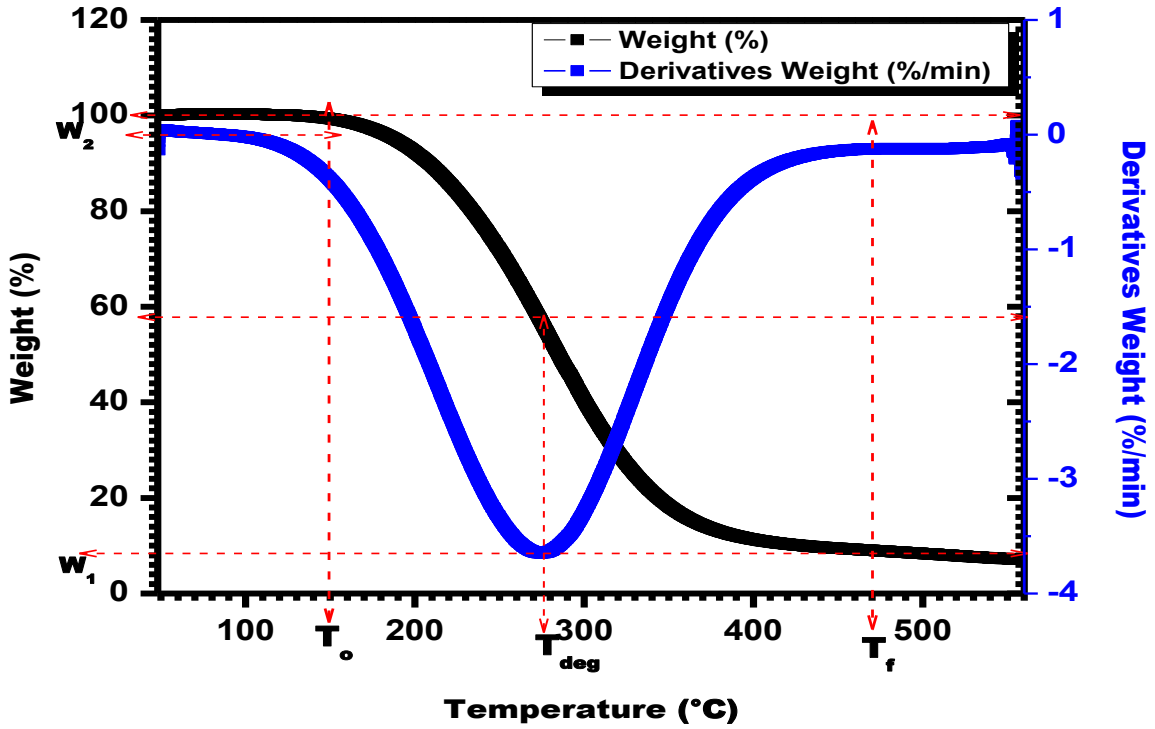

Figure 4.15: Thermogram (TGA) and Derivative Thermogram (DTA) of Powdered PoPD sample

The derivative of weight loss is measured in percentage of weight loss per minute.

4.5 Raman Spectroscopy Analysis

The bond structures of the synthesized polymers were analyzed by Raman spectroscopy analysis. The characteristic vibrational bands obtained from the Raman spectra of the polymers are shown in Figure 4.16 to 4.20 respectively. In general, all the samples have sharp band.

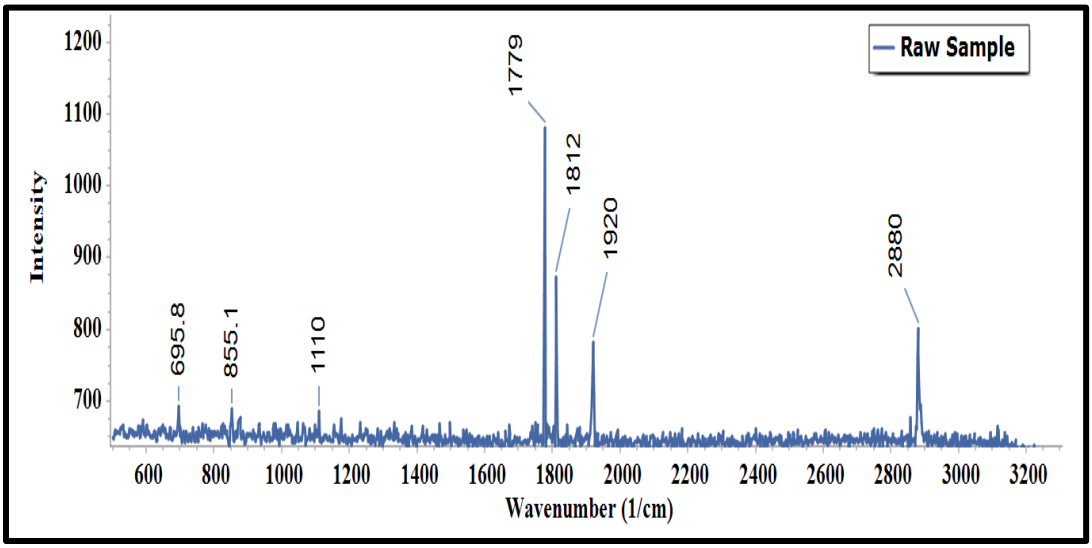

Figure 4.16: Raman Spectra of the powdered PoPD sample

Figure 4.16 shows the Raman spectra of the powered PoPD (raw sample). A total of seven bands were observed for the powdered sample. The characteristic vibrational band appeared at 2880 cm^{-1} is due to stretching of aromatic $C-H$ bond, hydrogen bonded amine ($-NH_2$) and ($-NH-$) groups. This confirms the presence of primary and secondary amine functional groups in the synthesized polymer. The pairs of bands at 1920 cm^{-1}, 1812 cm^{-1} and 1779 cm^{-1} are due to stretching vibrations of $C=C$ bond in quinoid and benzenoid rings, and bending vibrations of $C-H$ in quinoid and benzenoid rings respectively. The band at 1110 cm^{-1} is due to $C-N$ stretching frequency of quinoid units and quinoxaline rings. The weak band at 855.1 cm^{-1} is due to out of plane bending deformations of $C-H$ bond present in 1, 2 disubstituted benzene derivatives. The band at 695.8 cm^{-1} is attributed to bending deformation of $N-H$ functional group attached to benzene ring in primary aromatic amines.

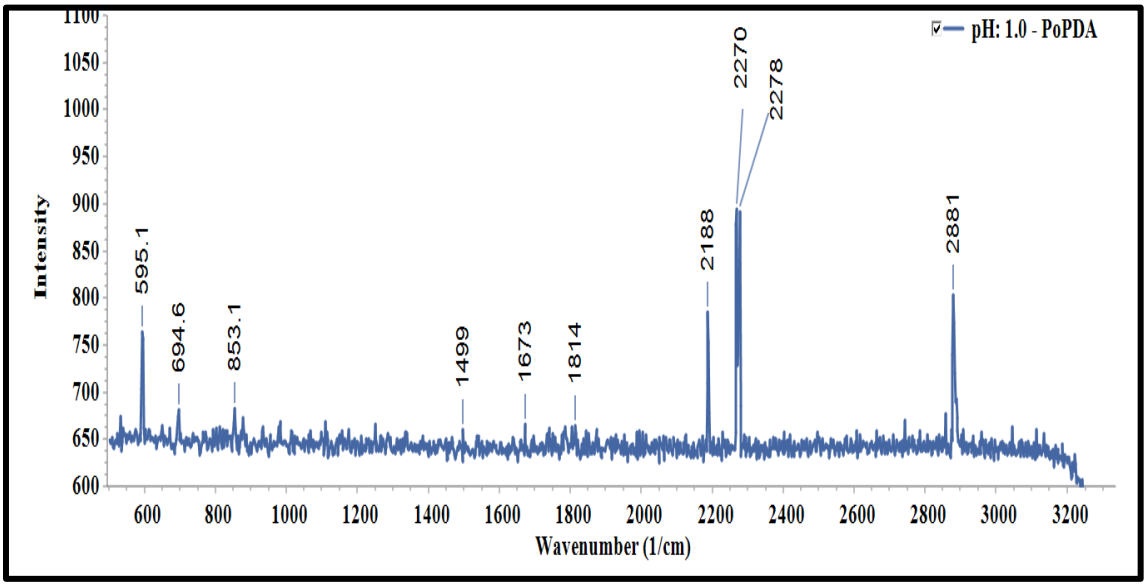

Figure 4.17: Raman Spectra of PoPD sample at pH value of 1.0.

Figure 4.17 shows the Raman spectra of PoPD films deposited at a pH of 1.0. A total of nine sharp bands were observed. The strong vibrational bands appearing at 2881 cm^{-1}, 2278 cm^{-1}, 2270 $cm^{-1}$and 2188 cm^{-1} are attributed to the stretching of aromatic $C-H$ bond, primary amine $(-NH_2)$ and secondary amine $(-NH-)$ benzene derivatives.The weak band at 1814 cm^{-1} is due to stretching vibrations of $C=C$ bonds in the quinoid and benzenoids rings. The band could also be attributed to bending vibrations of $C-H$ bonds in the quinoid and benzenoid rings. Weak band at 1673 cm^{-1} could be due to stretching vibrations of $C=C$ in quinoid and benzenoid rings, bending vibrations of $C-H$ bonds in quinoid and benzenoid rings inside the phenazine ring ladder structured polymers and bending vibrations of amine $(-NH-)$ bonds. Band at 1499 cm^{-1} is attributed to both stretching vibrations of $C=C$ bond in the benzene derivative rings and $C-N$ bond attributed to aromatic amine. The characteristic vibrational frequency at 853.1 cm^{-1} is attributed to out of plane bending deformation of $C-H$ bonds in 1, 2 disubstituted benzene derivatives. The bands at 694.6 cm^{-1} and 595.1 cm^{-1} are due to bending deformation of $N-H$ functional group attached to benzene ring in primary aromatic amines.

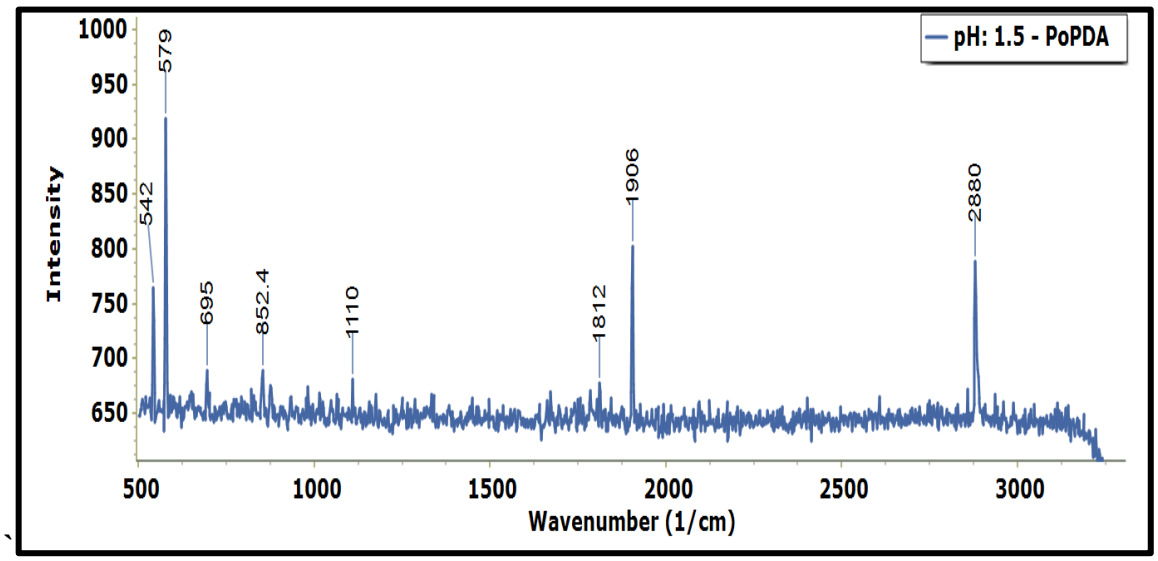

Figure 4.18: Raman Spectra of PoPD sample at pH value of 1.5.

Figure 4.18 shows the Raman Spectra of PoPD film fabricated at a pH value of 1.5. A total of eight sharp bands were observed. Weak bands occurred at 1812 cm^{-1}, 1110 cm^{-1}, 852.4 cm^{-1} and 695 cm^{-1} while relatively strong bands were observed at 2880 cm^{-1}, 1906 cm^{-1}, 579 cm^{-1} and 542 cm^{-1}. Characteristic vibrational frequency observed at 2880 cm^{-1} is attributed to stretching vibrations of $C-H$ bond in aromatic ring, primary amine $(-NH_2)$ and secondary amine $(-NH-)$ functional group. The band at 1906 cm^{-1} and 1812 cm^{-1} are due to stretching vibrations of $C=C$ bonds in quinoid and benzenoid rings which could also be attributed to bending vibration of $C-H$ bonds in the same quinoid and benzenoid rings. The band at 1110 cm^{-1} is due to $C-N$ stretching frequency of quinoid and quinoxaline. The bands at 852.4 cm^{-1} and 695 cm^{-1} are attributed to out of plane bending deformation of $C-H$ bond in 1, 2 disubstituted benzene derivatives. The bands at 579 cm^{-1} and 542 cm^{-1} are due to bending deformation of $N-H$ functional group attached to benzene ring in primary aromatic amines.

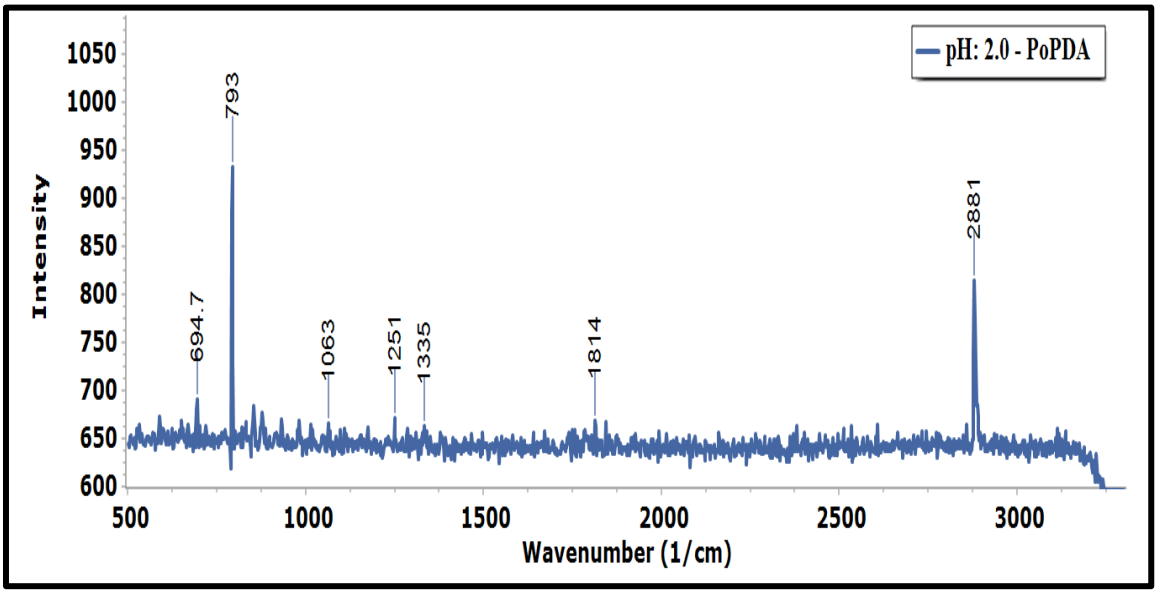

Figure 4.19: Raman Spectra of PoPD sample at pH value of 2.0.

Figure 4.19 shows the Raman spectra of PoPD film fabricated at a pH value of 2.0. The Raman spectra obtained has two sharp strong bands at 2881 cm^{-1} and 793 cm^{-1} while five weak bands occurred at 1814 cm^{-1}, 1335 cm^{-1}, 1251 cm^{-1}, 1063 cm^{-1} and 694.7 cm^{-1}. Characteristic vibrational frequency observed at 2881 cm^{-1} is attributed to stretching vibrations of $C-H$ bond in aromatic ring, primary amine $(-NH_2)$ and secondary amine $(-NH-)$ functional group. The band at 1814 $cm^{-1}$is due to stretching vibrations of $C=C$ bonds in quinoid and benzenoid rings which could also be attributed to bending vibration of $C-H$ bonds in the same quinoid and benzenoid rings. The bands at 1335 cm^{-1}, 1251 cm^{-1} and 1063 $cm^{-1}$are due to $C-N$ stretching frequency of aromatic amine derivatives (quinoid and quinoxaline). They are also attributed to the stretching vibrations of $C-N$ bond present in amine functional group. The bands at 793 cm^{-1} and 694 cm^{-1} are attributed to out of plane bending deformation of $C-H$ bond in 1, 2 disubstituted benzene derivatives.

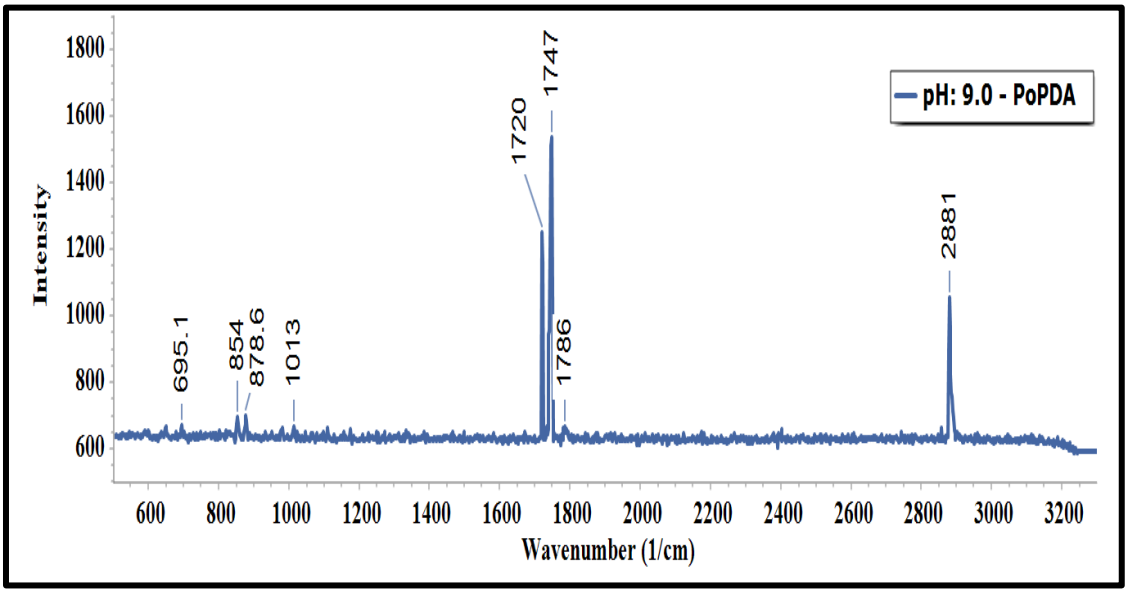

Figure 4.20: Raman Spectra of PoPDsample at pH value of 9.0.

Figure 4.20 shows the Raman Spectra of PoPD film fabricated at a pH value of 9.0. A total of eight sharp bands were observed. Weak bands occurred at $1786\,cm^{-1}$, $1013\,cm^{-1}$, $878.6\,cm^{-1}$, $854\,cm^{-1}$ and $695.1\,cm^{-1}$ while relatively strong bands were observed at $2881\,cm^{-1}$, $1747\,cm^{-1}$and $1720\,cm^{-1}$. Characteristic vibrational frequency observed at $2881\,cm^{-1}$ is attributed to stretching vibrations of $C-H$ bond in aromatic ring, primary amine $(-NH_2)$ and secondary amine $(-NH-)$ functional group. The bands at $1786\,cm^{-1}$, $1747\,cm^{-1}$ and $1720\,cm^{-1}$ are due to stretching vibrations of $C=C$ bonds in quinoid and benzenoid rings which could also be attributed to bending vibration of $C-H$ bonds in the same quinoid and benzenoid rings. The band at $1013\,cm^{-1}$ is due to $C-N$ stretching frequency of quinoid and quinoxaline. The bands at $878.6\,cm^{-1}$, $854\,cm^{-1}$and $695.1\,cm^{-1}$ are attributed to out of plane bending deformation of $C-H$ bond in 1, 2 disubstituted benzene derivatives.

From the Raman spectra obtained, it was confirmed that the PoPD powdered and thin film polymer samples consist of predominantly quinoid, benzenoid rings, and primary and secondary diamine functional group which confirmed that the polymer fabricated contained phenazine ring

ladder – structure made of quinoids and benzenoids imine units. The results are in line with spectra obtained by Paulraj *et al.*, (2018); Samanta *et al*., (2015); Li *et al.*, (2015); Baibarac *et al.*, (2011); Mallick *et al.*, (2006,).

4.6 Thickness Measurement

The stylus profilometry tool is based on contact measurement of the sample. The profiler plot of the sample deposited at pH of 1.0 is shown in Figure 4.21. The measured thickness is 1100 Å. Profiler plot of film fabricated at pH of 1.5 is shown in Figure 4.22. Its thickness is 5500 Å. Figure 4.23 shows the profiler plot of film deposited at pH of 2.0. From Figure 4.23, the thickness is 3800 Å. Figure 4.24 shows the profiler plot of film deposited at pH of 9.0 with the thickness of the sample 1000 Å measured.

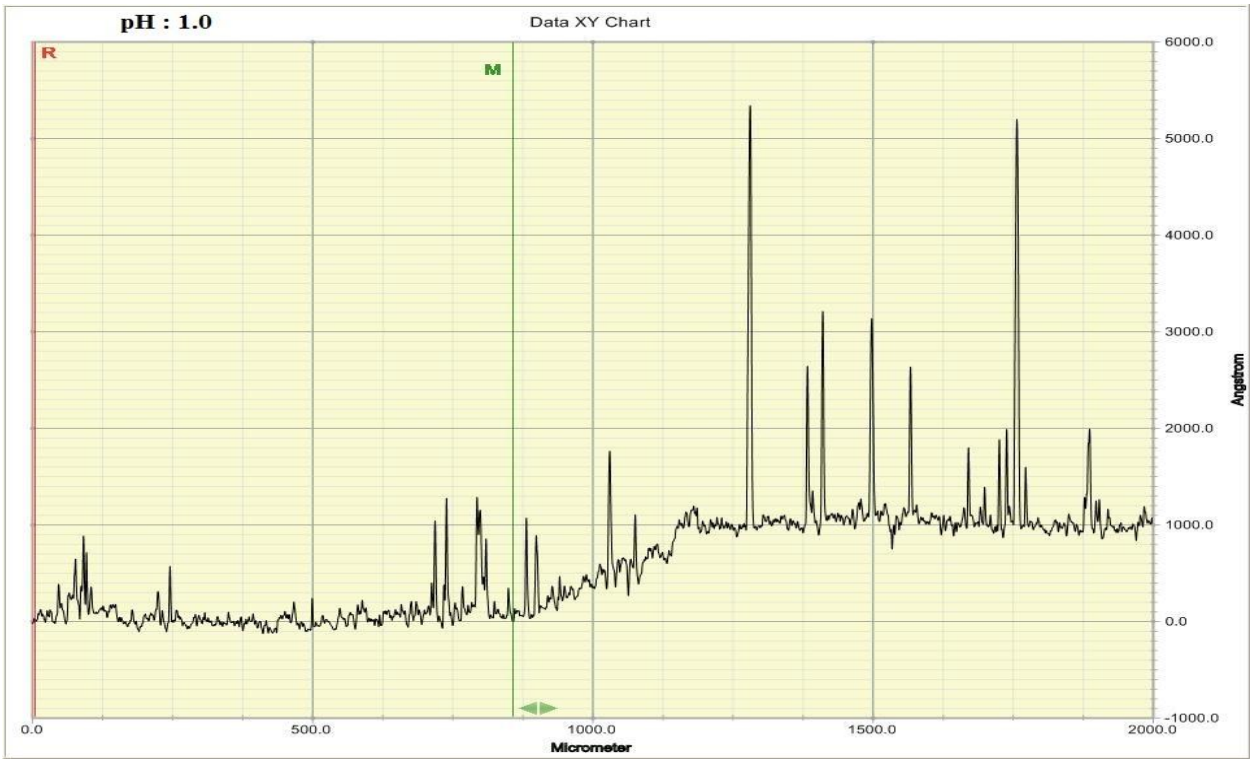

Figure 4.21: Surface Profiler of Poly (o – Phenylenediamine) (PoPD) sample at pH value of 1.0.

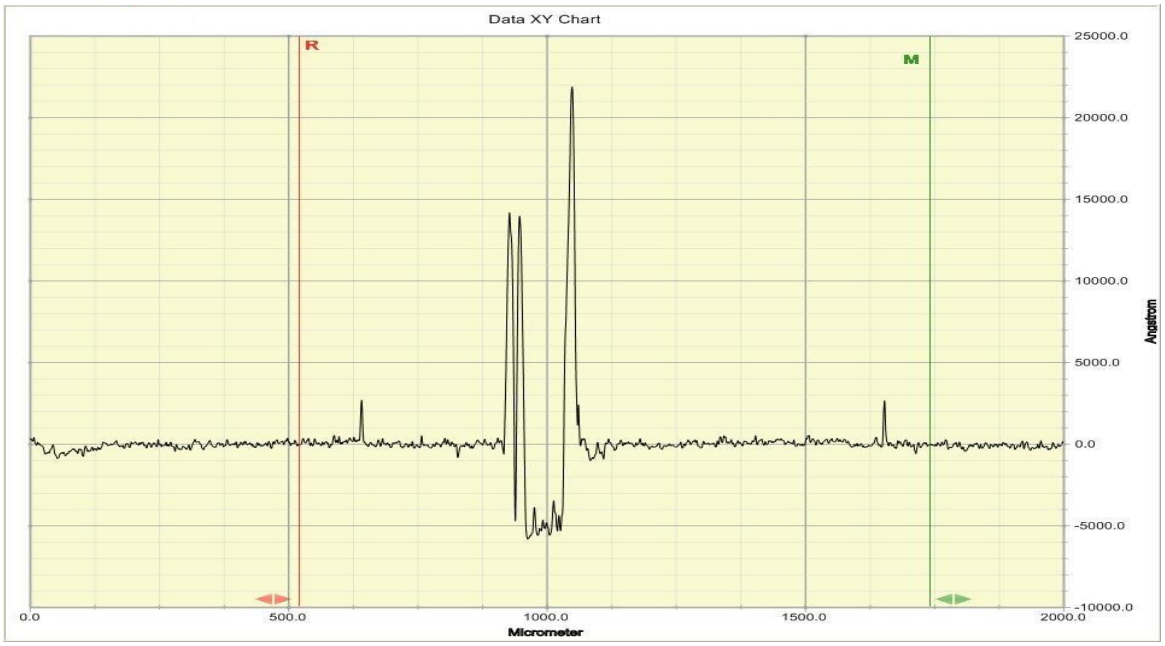

Figure 4.22: Surface Profiler of Poly (o – Phenylenediamine) (PoPD) sample at pH value of 1.5.

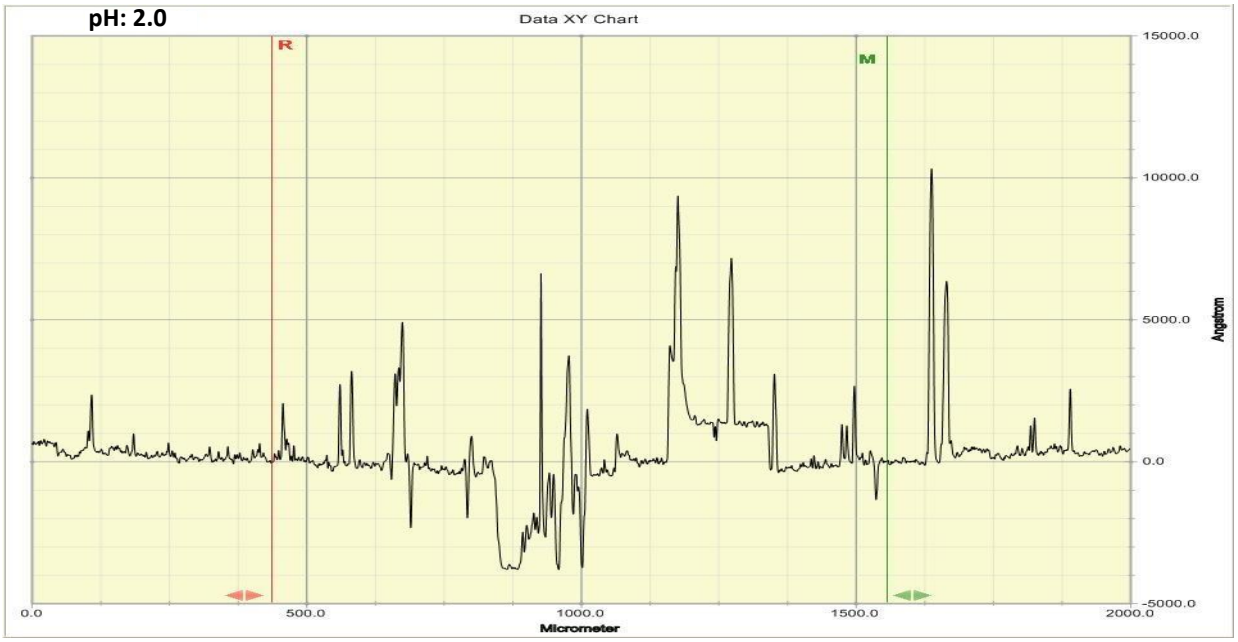

Figure 4.23: Surface Profiler of Poly (o – Phenylenediamine) (PoPD) sample at pH value of 2.0.

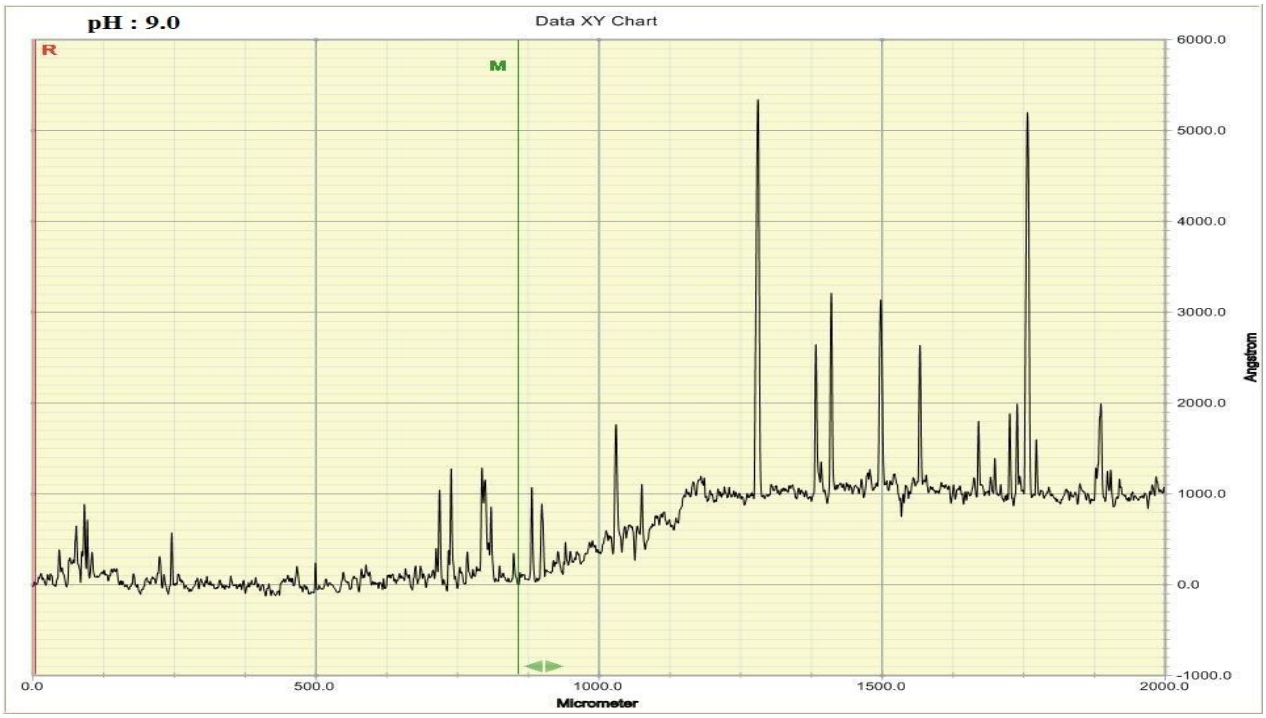

Figure 4.24: Surface Profiler of Poly(o – Phenylenediamine) (PoPD) sample at pH value of 9.0.

4.7 Electrical Properties of PoPD

The electrical properties of the doped polymers were measured with the four – point probe machine (SignatoneQuadpro Resistance Wafer Mapping V. 3.7.0) using a Keithley 2400 source meter. The four – point probe apparatus has four probes in a straight line with an equal inter – probing spacing of 1.60 mm and a probe needle radius of 125 µm. A constant current passes through the two outer probes and an output voltage is measured across the two inner probes. This signatoneQuadpro resistance wafer mapping machine gives the values of the resistance (V/I), constant current, resistivity, sheet resistance and thickness of the film. The thicknesses of the films were obtained using stylus profilometry as given in section 4.6. Table 4.2 shows average electrical properties of the fabricated polymer samples.

Table 4.2: Electrical Properties of Fabricated Poly (o – Phenylenediamine) samples

Samples	$V\ (mV)$	$I\ (\mu A)$	$t \times 10^{-5}(cm)$	$R \times 10^{6}$ (Ω)	$\rho \times 10^{2}$ $(\Omega\ -\ cm)$	$\sigma \times 10^{-3}$ (S/cm)
pH-1.0	529.3	0.05	1.10	10.59	5.27	1.90
pH-1.5	119.8	0.05	5.50	2.40	5.96	1.68
pH-2.0	165.5	0.04	3.80	4.14	7.11	1.41
pH-9.0	294.9	0.04	1.00	7.38	3.34	3.00

The values of the electrical conductivity suggest that the PoPD samples fabricated are conducting polymers. Electrical conductivity of the PoPD films increases towards strong acid medium and as the pH moves towards weak alkaline medium. The resistivity of the film decreases towards strong acid medium and as the pH moves towards weak alkaline medium. The range of electrical conductivity obtained in this work is close to values obtained by (Lakouraj *et al.*, 2014).

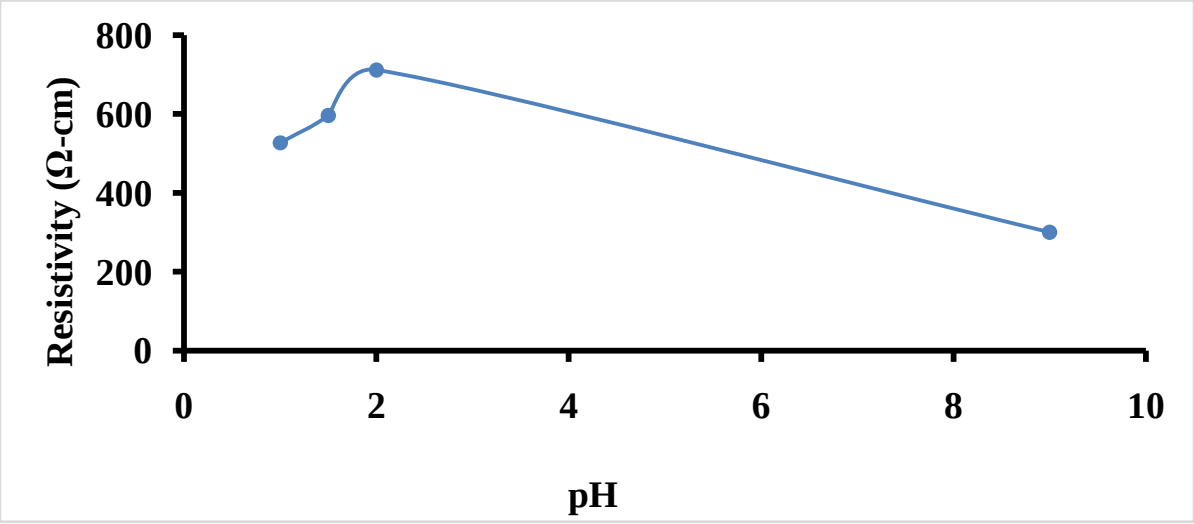

Figure 4.25: Plot of Resistivity against pH values for Poly (o – Phenylenediamine) (PoPD) samples.

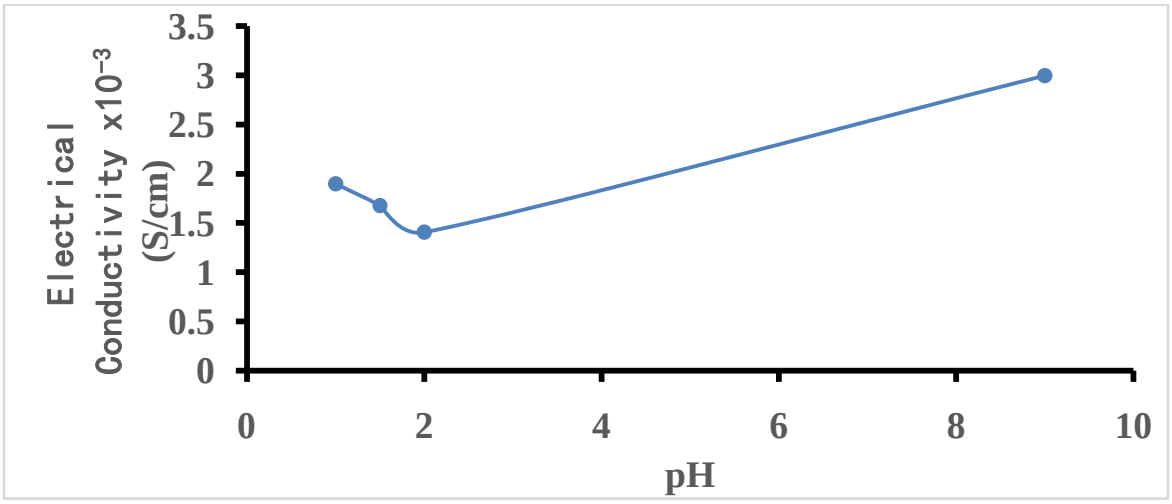

Figure 4.26: Plot of Conductivity against pH values for Poly (o – Phenylenediamine) (PoPD) samples.

4.8 Surface Area, Porosity and Micropore volume analyses

The produced Poly(o – Phenylenediamine) (PoPD) powder was subjected to surface area, porosity and micropore volume analyses using several approaches discussed in chapter two of this work.

4.8.1 Surface Area Analysis

The surface area analysis of the powdered PoPD polymer was done using Nitrogen as an adsorbate at a temperature of $\approx 77\,K$. $0.14\,g$ of the sample was subjected to an outgas temperature of 25.0 ℃ for 3.0 $hours$ with a bath temperature of 273.0 K.

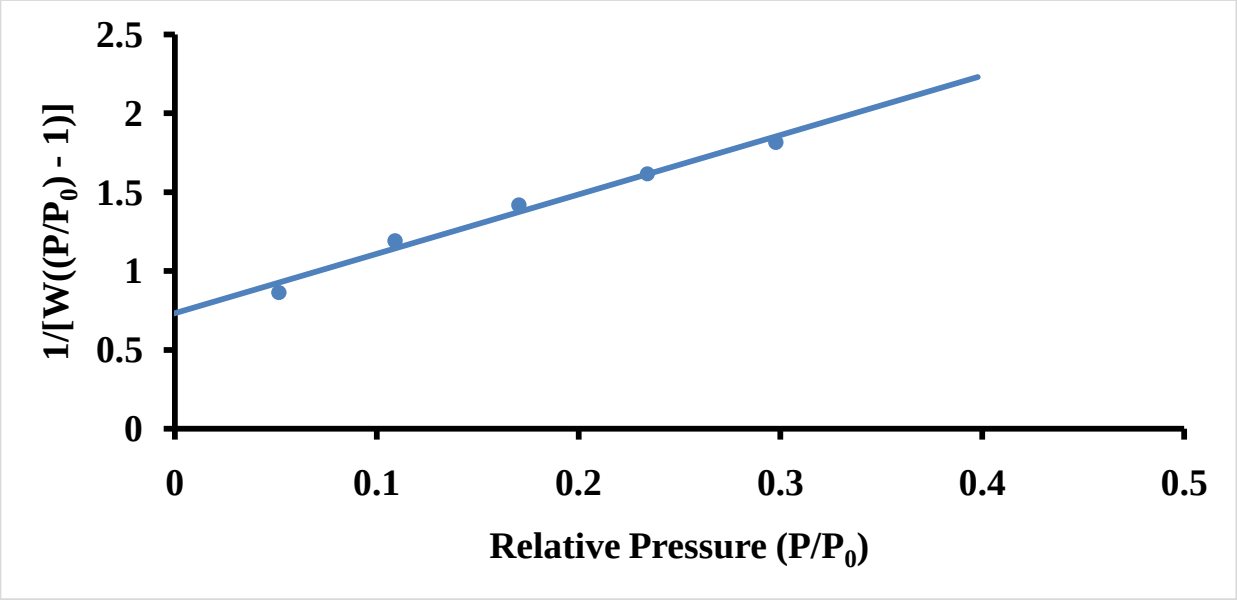

Figure 4.27: Multipoint BET plot of the powdered Poly (o – Phenylenediamine) (PoPD) sample.

Figure 4.27 shows the multipoint BET plot of the powdered PoPD polymer sample. In the figure, $\frac{1}{\left(W\left\{\left(\frac{P_o}{P}\right)-1\right\}\right)}$ is plotted against $\frac{P}{P_0}$ with the slope and intercept determined. The slope and intercept were used to determine the weight of adsorbate constituting a monolayer of the surface coverage (W_m), the total surface area of the sample (S_t) and the specific surface area of the solid polymer sample (S). The slope (s) of the plot is 3.764 while the intercept (i) is 7.318×10^{-1}, the correlation coefficient (R) is 0.991 and the constant C in the BET's equation is 6.143. The total surface area of the sample is $774.66\ m^2/g$.

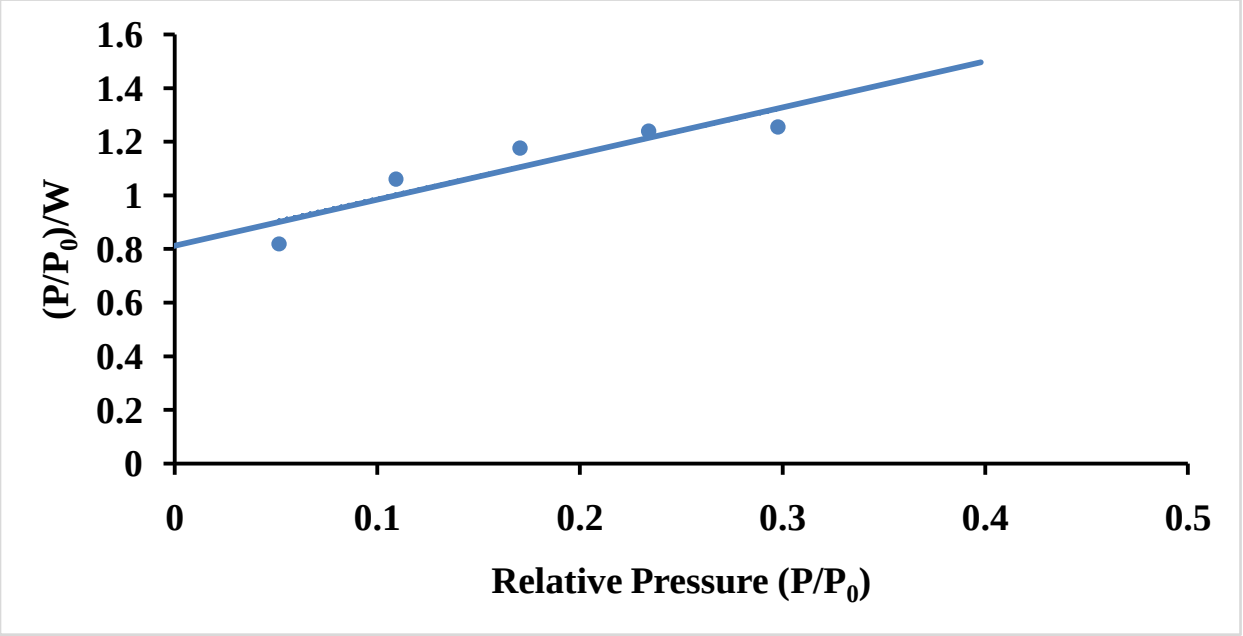

Figure 4.28: Langmuir plot of the powdered Poly (o – Phenylenediamine) (PoPD) sample.

Figure 4.28shows the Langmuir plot of the powdered PoPDA polymer sample. Langmuir as well as the multipoint BET plot is a linear plot. In the Langmuir plot, $(P/P_0)/W$ is plotted against (P/P_0). The slope, intercept and correlation coefficient were determined. The slope was found to be 1.7497, intercept was 0.8123 and correlation coefficient was 0.930. The surface area according to Langmuir approach is given as 1990.33 m^2/g. The Langmuir surface area depends on adsorptions capacity of the adsorbent and is inversely proportional to the molecular mass of the adsorbate only. The Langmuir adsorption model considers that only a monolayer of adsorbate can be formed on top of the sample. Other approaches used in the estimation of the surface area of the sample and their results are presented in Table 4.3

Table 4.3: Surface Area Data for the Powdered PoPD

Analysis	Surface Area per unit mass (m^2/g)
Singlepoint BET	571.1
Multipoint BET	774.7
Langmuir Surface Area	1990.0
BJH method (cumulative adsorption surface area)	987.6
DH method (cumulative adsorption surface area)	1050.0
t – method (external surface area)	774.7
DR method (Micropore area)	939.0
DFT method (cumulative adsorption surface area)	235.0

4.8.2 Porosity Analysis

Porosity analysis is basically to determine the volume of micropore and pore size created due to the adsorption of the adsorbate by the polymer sample. Porosity or void fraction is a measure of the void or spaces in a material and is a fraction of volume of void over the total volume of the sample.

The micropore volume of the powdered polymer sample was determined using BJH method, DH method, DR method, Horvath – Kawazoe (HK) method, Saito – Foley (SF) method and DFT method. The estimated micropore volumes of the powdered polymer sample using the methods mentioned above are given in Table 4.4..

Table 4.4: Micropore Volume Data for the Powdered PoPD

Analysis	**Micropore Volume** (cm^3/g)
BJH method (cumulative adsorption pore volume)	0.4766
DH method (cumulative adsorption pore volume)	0.4873
DR method (micropore volume)	0.3337
HK method (micropore volume)	0.1640
SF method (micropore volume)	0.0524
DFT (cumulative pore volume)	0.2720

BJH, DH and DFT methods presents cumulative adsorption pore volume while DR, HK and SF methods gave direct values of the micropore volumes based on their individual approaches. The values of the cumulative adsorption pore volume were slightly higher compare to those of direct values of the micropore volume.

The pore size of the powdered polymer sample was obtained using the methods mentioned above and are given in Table 4.5.

Table 4.5: Pore Size Data for the Powdered PoPD

Analysis	**Pore size** ($\boldsymbol{nm}$)
BJH method (adsorption pore diameter)	2.072
DH method (adsorption pore diameter)	2.072
DR method (micropore width)	5.555
HK method (pore diameter)	0.366
DA method (pore diameter)	2.740
SF method (pore diameter)	0.452
DFT (pore diameter)	2.647

BJH and DH measured the adsorption pore diamater of the adsorbent while DR method gave micropore width of adsorbent. DA, HK, SF and DFT methods measured the pore diameter of the adsorbent.

All these semi - empirical methods tend to underestimate the porosity except for density functional theory (DFT) which can describe accurately the configuration of the adsorbed phase at the molecular level. It is considered to be superior and provide a more reliable approach to porosity analysis. According to the density functional theory result, the micropore volume is $0.272\ cm^3/g$ and the pore diameter is $2.647\ nm$. The pore diameter of 2.647 nm according to DFT method suggest that the powdered polymer is made up of mesopores because the value falls within the range of 2 nm and 50 nm which is the standard widths for mesopores (Borislav *et al*., 2007). Figure 4.29 shows the Dubinin – Radushkavich (DR) plot of the powdered polymer

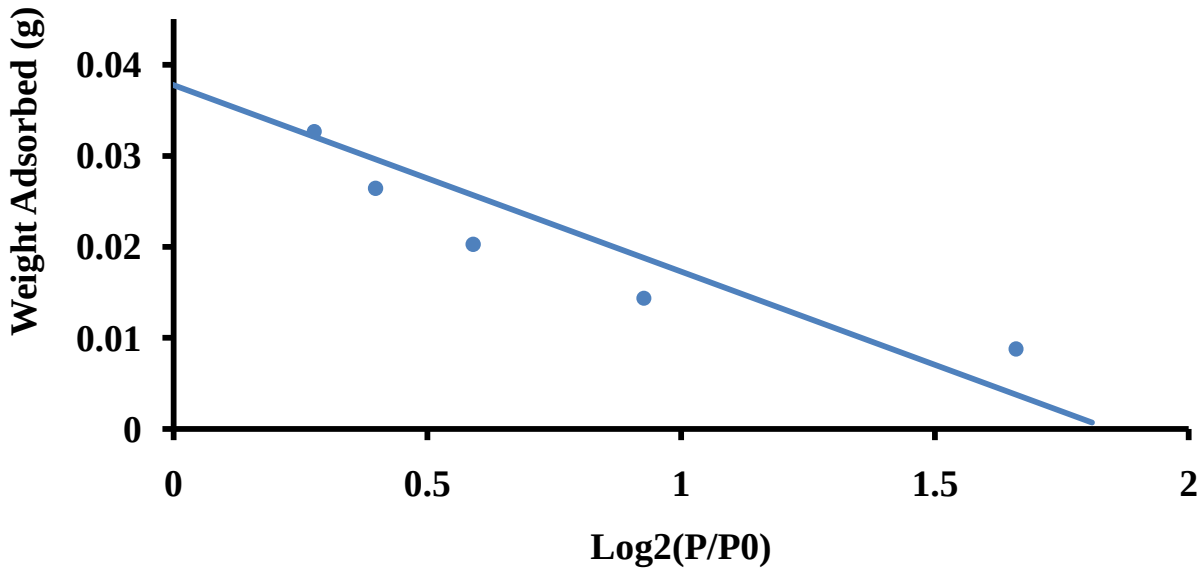

Figure 4.29: Dubinin – Radushkavich (DR) plot of the powdered PoPD sample.

Figure 4.29 shows the Dubinin – Radushkavish (D- R) plot of the powdered PoPD sample. The result shows that the slope of the graph is $-3.995 \times 10^{-1} g$ while the intercept on $y - axis$ is $3.775 \times 10^{-2} g$ and the correlation coefficient obtained is 0.983. Average pore width obtained using the (D – R) plot is 5.555 nm while the adsorption energy is 4.680 KJ/mol. The micropore volume obtained is $3.34 \times 10^{-1}\ cm^3/g$ and the micropore surface area of the powdered PoPD sample is 939.0 m^2/g.

CHAPTER FIVE

SUMMARY, CONCLUSION AND RECOMMENDATION

5.1 Summary of findings

The synthesis of poly (o-phenylenediamine) in HCl medium with potassium dichromate as an oxidizing agent using chemical method was successfully achieved. Also poly (o-phenylenediamine)thin films have been successfully deposited on FTO substrates at different pH values of reaction medium, using electropolymerization technique.

An UV- spectroscopy was used to determine the optical properties of the PoPD thin films. The morphology of the samples was done using scanning electron microscopy (SEM) and the structural properties of the samples were determined using X-ray diffractometry (XRD) and raman spectroscopy. Thermogravimetric analysis (TGA) was used to determine the thermal properties (stability) of the prepared PoPD and a four point probe to determine the electrical properties of the PoPD thin films. Surface area, porosity and micropore volume analysis of the PoPD were also done using Brunauer - Emmett – Teller (BET) and stylus profilometer to determine the thickness of the thin films. The pH values used for the deposition of the thin films are pH1.0, pH1.5, pH2.0 and pH9.0.

It was observed from the spectroscopic analysis that the synthesized PoPD film has a head to tail type arrangement with the benzenoid and quinoid structures in the phenazine – like backbone.The absorbance spectra of the films showed that the absorption bands of deposited PoPD slightly shifted to longer wavelength (lower energy) commonly known as red shift or Bathochromic shift. The transmittance of the polymer films increases slightly as the wavelength increase. The transmittance of the films is found to decrease as pH of the medium tends towards the alkaline region. Film deposited at a pH of 1.0 has the highest value of transmittance within

all regions of the spectrum while film deposited at pH of 9.0 has the least value of transmittance. This suggests that PoPD films with higher transmittive power could best be produced under acidic condition while PoPD films with lower transmittive power could best be produced under alkaline condition. The results also show that the reflectance of the PoPD film is generally low (between 0.9 % and 20.5 %). The patterns of the reflectance spectra for films deposited at pH values of 1.5, 2.0 and 9.0 are similar. Film deposited at strong acidic condition of pH of 1.0 has the least reflective power. Therefore, pH values of the reaction medium affect reflective power of the film produced in such medium.

The direct band gap energies of grown films were found to be $3.25\ eV$ for film deposited at pH of 1.0, $2.65\ eV$ for film deposited at pH of 1.5, $2.5\ eV$ for film deposited at pH of 2.0 and $2.20\ eV$ for film deposited at pH of 9.0 which shows that the energy band gaps of deposited PoPD films decrease as the pH of the reaction increase.

The optical transmittance spectra showed the coloured and bleached state of the PoPD thin film with pH of 1.5 in the wavelength range from 300 nm to 1100 nm. The optical transmittance of the coloured and bleached (T_c and T_b) state at the wavelength of 685nm are $T_c = 49.53$ % and $T_b = 93.93$ % respectively. The optical transmittance difference $\Delta T = T_b - T_c = 44.40$ %. The optical density (ΔOD) was determined as 0.64 and the contrast ratio (CR) at a 685 nm was calculated as approximately 1.9. The values of the ΔT, ΔOD and CR make the sample a potential material for use in electrochromic devices. With an optical density (ΔOD) above 0.3, the PoPD is suitable for monitors and smart glasses / windows and display applications.

The results of the SEM analysis of poly (o-phenylenediamine) samples look rough and show few spaces that were not properly coated in the case of thin film polymers coated on the FTO conducting glasses. More unevenly dispersed particles of the Poly (o - phenylenediamine)

polymer were observed. The particle sizes of the polymer samples increase as pH value moves towards low acid region from 1.0 to 1.5, reaching an optimal grain size ranging from ($200\ \mu m - 50\ \mu m$) at pH of 1.5, then it decreases to grain size range of ($20\ \mu m - 1\ \mu m$)as the pH of the reaction medium moves towards weak alkaline medium of pH value of 9.0.

The result of the XRD revealed that the samples are amorphous in nature. The shift in the pH values from highly acidic to weakly basic caused an increase in the intensity of the X – ray radiation. The powdered polymer sample has similar XRD pattern with that of the thin films with difference only in the intensity of the XRD pattern. X – ray intensity of the powdered polymer is higher than that of the thin film samples which confirms the formation of PoPD particles with good structural arrangement compare to the thin films of the same polymer.

The thermogravimetric analysis (TGA) results show that a weight loss occurred. It shows a weight loss of moisture content of 8.0% (0.908 mg) of actual sample used and a weight loss (thermal decomposition or pyrolysis) of 85.0% (9.649 mg) of the original sample with the percentage weight of the remaining residual of 7.0% (0.795 mg). The weight loss as a result of the thermal energy applied to the polymer sample is 9.649 mg which is 85.0% of the original polymer sample. The point of the greatest rate of change on the weight loss curve (point of inflection) is found to be 275 ^{0}C and is the peak temperature of the degradation of the PoPD.

The results obtained from the Raman spectra confirmed that the PoPD powdered and thin film polymer samples consist of predominantly quinoid, benzenoid rings, and primary and secondary diamine functional group which confirmed that the polymer fabricated contained phenazine ring ladder – structure made of quinoids and benzenoids imine units. The thicknesses of the deposited thin films obtained from stylus profilometry tool are 1100 Å, 5500 Å, 3800 Å, and 1000 Å for pH1.0, pH1.5, pH2.0 and pH9.0 respectively. The thickness of the film is found to decrease as the pH medium tends towards the alkaline region.

The values of the electrical conductivity show that the PoPD samples fabricated are conducting polymers. The electrical conductivity of the PoPD films increases towards strong acid medium and also increases as the pH moves towards weak alkaline medium. The resistivity of the film decreases towards strong acid medium and also decreases as the pH moves towards weak alkaline medium.

The results from the density functional theory (DFT) which is a more reliable approach to porosity analysis show that the micropore volume is 0.272 cm^3/g and the pore diameter is 2.647 nm. The pore diameter of 2.647 nm according to DFT method suggests that the powdered polymer is made up of mesopores.

5.2 Conclusion

It has been demonstrated that PoPD can be synthesized by chemical oxidation and electropolymerization techniques. Characterization of the synthesized samples showed that the synthesized PoPD film has a head to tail type arrangement with the benzenoid and quinoid structures in the phenazine – like backbone. Also, the PoPD films with higher transmittive power could best be produced under acidic condition while PoPD films with lower transmittive power could best be produced under alkaline condition and the transmittance of the polymer films increases slightly as the wavelength increases..The deposited films generally showed low reflectance and the film deposited at strong acidic condition of pH of 1.0 has the least reflective power. The direct energy band gaps of deposited PoPD films decrease as the pH of the reaction moves towards alkaline condition.The optical density (ΔOD) of the PoPD was determined as 0.64 which revealed that the polymer is electrochromic and is suitable for monitors and display applications.

More unevenly dispersed particles of the Poly (o - phenylenediamine) polymer were observed from the SEM images. The result of the XRD revealed that the samples are amorphous in nature. The thermogravimetric analysis (TGA) results showed that a weight loss occurred and the point of inflection is found to be 275 ^{0}C which is the peak temperature of the degradation of the PoPD. The results obtained from the Raman spectra confirmed that the PoPD powdered and polymer thin film samples contain phenazine ring ladder – structure made of quinoids and benzenoids imine units.

The film fabricated at pH1.5 has the highest thickness of 5500 Å which also revealed the electrochromic performance of conductive PoPD thin films. The values of the electrical conductivity showed that the PoPD samples fabricated are conducting polymers. The electrical conductivity of the PoPD films increases towards strong acidic medium and as the pH moves towards weak alkaline medium. The powdered polymer is made up of mesopores

5.3 Contribution to Knowledge

Having successfully synthesized poly (o- phenylenediamine) by chemical oxidation method using potassium dichromate, and electropolymerized the polymer using phosphate buffer with FTO substrates, the following are contributions to knowledge;

1. The electrochromic performance of the poly (o- phenylenediamine) reported in this research is novel
2. Determination of the point of inflection of PoPD studied in this research is also novel.
3. The electropolymerization of poly (o- phenylenediamine) at different pH values of the medium using phosphate buffer and FTO substrates has not been reported, therefore is also new.

5.4 Recommendation

Having successfully polymerized and electropolymerized PoPD on FTO substrates, the following recommendations are made for further studies;

i. Use of other types of conducting substrate such as ITO, for the deposition of these films so as to know the effect of the nature of the substrates on the properties of these polymer films fabricated in this work.

ii. Use of different acid other than H_3PO_4 for the electrodeposition of PoPD thin films.

iii. Use of different buffer solution other than phosphate buffer used in this work, and results compare with the results of this work.

REFERENCES

Abdul, M. (2017). Methodology of Nanotechnology. *Department of Physics, Majmaah University, Saudi Arabia.*

Abramoff, M.D., Magalhaes, P.J. and Ram, S.J. (2004). Image processing with ImageJ. *Biophotonic International, 11(7), 36 – 42.*

Aga, R.S. and Mu, R.R. (2010). Doping of polymers with ZnO nanostructures for optoelectronic and sensor applications. In L. Nicoleta (Ed.), *Nanowires Science and Technology* (pp. 205-222). Romania: National Institute of Research and Development for Technical Physics.

Agbor, N. E., Petty, M. C. and Monkman,f A. P. (1995). Polyaniline thin films for gas – sensing. *Sens. Actuators B, 28, 173 – 179.*

Aisha, G. (2014). Anticorrosive properties of poly (O-phenylenediamine)/ZnO nanocomposites coated stainless steel. *Journal of Nanomaterials, 2014, 1-8.*

Alias, A. N., Zabidi, Z. M., Ali, A. M., Harun, M. K.and Yahya, M.Z. (2013). Optical characterization and properties of polymeric materials for optoelectronic and photonic applications. *International Journal of Applied Science and Technology, 3 (5), 11.*

Archana, S. and Jaya, S. R. (2014). Synthesis and characterization of poly (p-phenylenediamine) in the presence of sodium dodecyl sulfate. *Research Journal of Chemical Science, 4(2), 60 – 67.*

Baibarac, M., Baltog, I., Smaranda, I., Scocioreanu, M. and Lefrant, S. (2011). Hybrid organic–inorganic materials based on poly(o-phenylenediamine)and polyoxometallate functionalized carbon nanotubes. *Journal of Molecular Structure, 985, 211–218.*

Bamfield, P. (2001). Chromic phenomena: The technological applications of colour chemistry, 2nd ed., p.8, Cambridge: Royal Society of Chemistry.

Borislav, D. Z., Jin, J.C., Martin, S. and Josef, J. (2007). Pore classsification in the characterization of porous materials: A perspective. *Central European Journal of Chemistry, 5 (2),* 385 – 395.

Bosch, O. C. and Sanchez, R. (2004). Recent development s in derivative ultraviolet /visible absorption spectrophotometry. *Analytical Chimica Acta, 518 (102), 1 – 24.*

Brady, S., Lau, K. T., Megill, W., Wallace, G. G. and Diamond, D (2005). The development and characterization of conducting polymeric-based sensing devices. *Synth. Met., 154, 25 – 28.*

Brunauer, S., Emmett, P.H. and Teller, E. (1938). Absorption of gases in multimolecular layers. *Journal of American Chemical Society, 60 (2), 309 – 319.*

Cai, G., Cui, M., Kumar, V., Darmawan, P., Wang, J., Wang, X, Lee-Sie Eh, A., Qian, K. and Lee P. S. (2016). Ultra-large optical modulation of electrochromicporous WO_3 film and the local monitoring of redoxactivity. *Chemical Science,7,1373 – 1382.*

Cao, Y., Smith, P. and Heeger, A. (1992). Counter-ion induced processibility of conducting polyaniline and of conducting polyblends of aniline in bulk polymers. *Synth. Met. 48, 91 - 97.*

Carquigny, S., Segut, O., Lakard, B., Lallemand, F. and Fiebet, P. (2008). Effect of electrolyte solvent on the morphology of polypyrrole films: Application to the use of polyprrole in pH sensors. *Synth Met. 158, 453 – 461.*

Chandra, H., Allen, W. S., Oberloier, W. S., Bihari, N., Gwamuri, J. and Pearce, M. J. (2017). Open source automated mapping four point probe. *Materials, 10 (2), 110.*

Chen, W. M., Huang, Y. H. and Yuan, L. X.(2011). Self-assembly LiFePO4/polyaniline composite cathode materials with inorganic acids as dopants for lithium-ion batteries. *Journal of Electroanal. Chem., 660, 108-113.*

Chiang, C. K., Finchee, C. R,, Park, Y. W., Heeger, A. J., Lewis, E. J., Gan, S. C. and MacDiarmid, A. G. (1977). Electrical conductivity in doped polyacetylene, *Physics Review Letter, 39, 1098.*

Chiang, C., Druy, M., Gau, S., Heeger, A., Louis, E., MacDiarmid, A. and Shirakawa, H. (1978). Synthesis of highly conducting films of derivatives of poly acetylene (CH)x. *Journal of the American Chemical Society, 100 (3), 1013 -1015.*

Cho, J. H., Yu, J. B., Kim, J. S., Sohn, S. O., Lee, D. D. and Huh, J. S. (2005). Sensing behaviours of polypyrrole sensor under humidity condition. *Sens. Actuators B, 108, 389 – 392.*

Colley, R. A., Budd, P. M., Owen, J. R. and Balderson, S. (2000). Poly [oxyymethylene-oligo(oxyethylene)] for use in subambient temperature electrochromic devices. *Polym. Int., 49, 371 -376.*

Cosnier, S. (2007). Recent advances in biological sensors based on electrogenerated polymers: A review. *Anal. Lett., 40, 1260-1279.*

Deepa, J. and Shanthi, J. R. (2017). Electrical conductivities of synthesized poly o-phenylemediamine) and its nanocomposites. *International Journal of Advanced Research. (IJAR) 5(5), 1274 – 1281.*

Deepa, J. and Shanthi, J. R. (2017). Comparison of electrical and photoluminescence properties of synthesized poly o- phenylenediamine) and its SiO_2 nanocomposites. *Research Journal of Chemical Science, 7(9), 1 – 7.*

Dinh, H. N. and Birss, V. I. (2000). Effect of substrate on polyaniline film properties: A cyclic voltammetry and impedance study. Journal of Electrochemi. Soc., 147, 3775 – 3784.

Dyer, L. A., Grenier, R. C. and Reynolds, R. J. (2007). A poly 3, 4-alkylenedioxythiophene. Electrochromic variable optical attenuator with near infra red

reflectivity tuned independently of the visible region. *Advanced Functional Materials, 17 (9), 1480 – 1486.*

Erokhin, V., Berzina, T., Camorani, P. and Fontana, M. (2006). Conducting polymer solid electrolyte fibrilla composite material for adaptive networks. *Soft matter, 2, 870-874.*

Gardiner, D. J. (1989). Practical Raman spectroscopy Springer .Berlin : New York : Springer-Verlag.

Granqvist, C.G. (2002). Handbook of inorganic electrochromic materials, Amsterdam, New York: Elsevier.

Granqvist, C.G. (1995). Handbook of inorganic electrochromic materials, Amsterdam, New York: Elsevier

Green, M. (1996). The promise of electronic systems. Chem. Ind. 17, 641 – 644.

Gopalakrishnan, K., Elango, M. and Thamilsevan, M. (2012). 0ptical studies on nano-structured conducting polyaniline prepared by oxidation method. *Archives of Phys. Research 3, 315 – 319.*

Gupta, G., Birbilis, N., Cook, A. B. and Khanna, A. S. (2013). Polyaniline – Lignosulfonate/epoxy coating for corrosion protection of AA 2024 T3 *Corros. Sci., 67, 256 - 267.*

Guo, X., Baumgarten, M. and Mullen, K. (2013). Designing conjugated Polymers for organic electronics. *Prog. Polym. Sci 38, 1832 – 1908.*

Guo, Y. P. and Zhou, Y. (2007). Polyaniline nanofibers fabricated by electrochemical polymerization: A mechanistic study. *European Polymer Journal, 43, 2292 – 2297.*

Hasanov, R., Bilgic, S. and Gece, G. (2011). Experimental and theoretical studies on the corrosion properties of some conducting polymer coating. *Journal of Solid State Electrochem, 15, 1063 – 1070.*

Haynes, W.M. (2010). *Handbook of chemistry and physics*.Boca Raton: CRC Press.

Hirase, R., Shikata, T. and Shirai, M. (2004). Selective formation of polyanline on wool by chemical polymerization, using potassium iodate. *Synth. Met., 146, 73 – 77.*

Hosseini, M., Bagheri, R. and Najjar, R. (2011). Electropolymerization of polypyrrole and polypyrrole-ZnO nanocomposites on mild steel and its corrosion protection performance. *Journal of Applied Polymer Science, 121, 3159 -3166.*

Hrehorova, E., Bliznyuk, V. V., Pud, A. A., Shevchenko, V. V. and Fatyeyeva. (2007). Electrical properties and fractal behaviour of Polyurethane elastomer/polyaniline composites under mechanical deformation polymer, 48; 4429 - 4437.

Hu, D., Duan, X., Xu, J., Zhang, L. and Zang, K. (2014). Synthesis of novel chiral l-leucine grafted PEDOT derivatives with excellent electrochromic performances. RSC Advances 4(67), 35597 – 35608.

Huisheng, P., Xuemei, S., Wei, W. and Xin, F. (2017). Structure and property of electronic polymers. In P. Huisheng, S. Xumei, W. Wei and F. Xin (Eds.), *Polymer Materials for Energy and Electronic Applications* (pp. 63-106), Amsterdam: Elsevier.

Jaymand, M. (2013). Recent progress in chemical modification of polyaniline. *Prog. Polym. Sci., 38,1287 – 1306.*

Jin, Z., Pramods, K.P., Auk, G. and Gosh, S.H. (2001). Dynamic mechanical behavioural of melt-processed multi- walled carbon nanotubes (poly methyl methacrylate) composites. *Chemical Physics Letters, 333, 43*

Josh, M., Bhattacharyya, A. and Ali, S. W. (2008). Characterization techniques for nanotechnology applications in textiles. *Indian Journal of Fiber and Textile Research, 33, 304 – 317.*

Khan, I., Ali, S., Mansha, M. and Qurashi, A. (2017). Sonochemical assisted hydrothermal

synthesis of pseudo-flower shaped Bismuth vanadate (BiO4) and their solar-driven water splitting application. *Ultrason Sonochem, 36, 386 – 392.*

Kim, B. C., Too, C. O., Kwon, J. S., Ko, J. M. and Wallace, G. G. (2011). A flexible capacitor based on conducting polymer electrodes. *Synth. Met, 161, 1130-1132.*

Knoll, M. and Thamer, M. (2011). An enhancement - mode electrochemical organic field effect transistor. *Electrochem. Comm., 13, 597-599.*

Kong, Y., Li, W., Wang, Z., Yao, C. and Tao, Y. (2013). Electrosorption behavior of copper ions with poly m phenylenediamine paper electrode. *Electrochem Comm., 26, 59-62.*

Kraft, A. (2019). Electrochromism: a fascinating branch of electrochemistry. The textbook *Journal of Chemistry (ChemTexts), 5(1), 1 – 18.*

Krishnam K.S and Rama C.V.(1928). The Negative Absorption of Radiation. Nature 122(3062):12-13

Lakard, B., Magnin, D., Deschaume, O., Vanlancker, G., Glinel, K., Demoustier-Champague, S., Nysten, B., Jonas, A. M., Bertrand, P. and Yunus, S. (2011). Urea potentiometric enzymatic biosensor based on charged biopolymers and electrodeposited polyanilne. *Biosens Bioelectron, 26, 4139-4145.*

Lakouraj, M. M., Zare, E. N. and Moghadam, P. N. (2014), Synthesis of Novel Conductive Poly(p-phenylenediamine)/ Fe3O4 Nanocomposite via Emulsion Polymerization and Investigation of Antioxidant Activity. *Advances in Polymer Technology, 33 (1), 1 – 7.*

Lamouri, S.,Bendahgane, S. and Oudia, A. (2014). The Preparation and Analytical Study of Conducting Polyaniline ThinFilms. *Journal of Petroleum & Environmental Biotechnology, 5(2), 1 – 5.*

Lange, U. and Mirsky, V. (2011). Chemiresistors based on conducting polymers.A review on measurement techniques Anal. *Chim. Acta, 687, 105-113.*

Leventis, N. (2002). Electrochromic devices. In A. Phillips (Ed.), *McGraw-Hill Encyclopedia of Science and Technology*, (pp. 153-156). New York:McGraw-Hill.

Lewis, R. J. (1996). *Sax's dangerous properties of industrial materials.*NewYork : Van Nostrand Peinhold, 2654.

Liang, L., Liu, J., Windisch, C. F., Exarhos, G. J. and Lin, Y. H. (2002). Direct assembly of large arrays of oriented conducting polymer nanowires, *Angew. Chem. Int. Ed. 41, 3665 – 3668.*

Li, T., Yuan, C., Zhao, Y., Chen, Q., Wei, M. and Wang, Y. (2013). Facile synthesis and characterization of *poly (o-phenylenediamine)* submicrospheres doped with glycine. *Journal of macromolecular Science, Part A, Pure and Applied Chemistry, 50 (3), 330-333.*

Liu, X. and Yu, W. (2006). Evaluating the thermal stability of high performance fibers by TGA. *Journal of Applied Polymer Science, 99, 937 – 944.*

Li, W., Li, D, Xiao, H. and He, B. (2015). Facile preparation of gold nanoparticles decorated poly(o-phenylenediamine) hollow microspheres and their applications for the detection of dopamine. *High Performance Polymers,1–10.*

Li, G. F., Martinez, C. and Semancik, S. (2005). Controlled electrophoretic patterning of polyaniline from a colloidal suspension. *Journal of American Chem. Soc.,127, 4903 – 4909.*

Lu, G. W., Qu, L. T. and Shi, G. Q. (2005). Electrochemical fabrication of neuro-type networks based on crystalline oligopyrene nanosheets. *Electrochem. Acta, 51, 340 – 346.*

Mabrook, M. F., Pearson, C. and Petty, M. C. (2006). Inkjet-printed polypyrrole thinfilms for vapour sensing. *Sens. Actuator B, 115, 547 – 551.*

Maiyalagan, T. (2008). Electrochemical synthesis, characterization and electro oxidation of methanol on platinum nanoparticles supported poly o-phenyhenediamine nanotubes.

Journal of Power Sources, 179(2), 443 – 450.

Majeed, K., Jawaid, M., Hassan, A., Bakar, A. Khali, H., Salema, A. and Inuwa, I. (2013). Potential materials for food packaging from nanoclay/natural fibres filled hybrid composites, *Materials and Design, 46, 391 -410.*

Mallick, K., Witcomb, M. J. and Scurrell, M. S. (2006). Palladium Nanoparticles in Poly(o-phenylenediamine): Synthesis of a Nanostructured 'Metal-Polymer' CompositeMaterial. *Journal of Macromolecular Science, Part A: Pure and Applied Chemistry, 43(9), 1469 – 1476.*

McGovern, S. T., Spinks, G. M. and Wallace, G. G (2005). Micro-humidity sensors based on a processable polyaniline blend. *Sens. Actuators B, 107, 657 – 665.*

Melad, O. (2016). Chemical oxidative synthesis of characterization of poly o-phenylenediamine doped with different acids. *European Journal of Chemistry. 7(4), 463 - 467.*

Molape, K., Nlangili, P. M. and Ajayi, R. F. (2012). Electronics of conjugated polymers: Polyaniline. *Int. Journal of Electrochem. Sci., 7, 11859 - 11875.*

Moon, Y., Yun, J. and Kim, H. (2013). Synergetic improvement in electromagnetic interference shielding characteristics of polyaniline-coated graphite oxide/γ-Fe2O3/BaTiO3 nanocompositer. *Journal of Ind. Chem., 19, 493 - 497.*

Monk, P. M. S., Mortimer, R. J. and Rosseinsky, D. R. (1995). Electrochromism: Fundamentals and applications. *Angewandte Chemie, 108(7), 853 – 854.*

Mortimer, R. J. and Rowley, N. M. (2004). Metal complexes as dyes for optical data storage and

electrochromic materials. In J.A. McCleverty and T.J. Meyer (Eds.), *Comprehensive coordination chemistry – II: From Biology to Nano technology* (pp. 581-619).Oxford: Elsevier.

Mortimer, R. J (1999). Organic electrochronic materials. *Electrochim. Acta, 44, 2971 – 2981.*

Mortimer, R. J., Dyer, A. L. and Reynolds, J. R. (2006). Electrochromic organic and polymeric materials for display applications. *Displays Elsevier, 27, 2 – 18.*

Muthirulan, P., Kannan, N. and Meenakshisundaram, M. (2013). Synthesis and Corrosion Protection properties of Poly o- phenylenediamine nanofibers. *Journal of advanced research, 4, 385 - 392.*

Nayak, J., Mahadeva, S. K., Chen, Y., Kang, K. S., and Kim, J. (2010) Effect of ionic liquid dispersion on performance of a conducting polymer based schottky diode. *Thin solid films, 518, 5626-5628.*

Omar, M. and Mariam, J. (2017). Copolymerization of poly o-phenylenediamine-co-o/p-Toluidine via the chemical oxidative technique. Synthesis and characterization. *Materials and Technology, 51 (2), 283-288.*

Pacios, R., Marcilla, R., Pozo-Gonalo, C., Pomposo, J. A., Grande, H., Aizpurua, J. and Mecerreyes, D. (2007). Combined electrochronic and plasmonic optical responses in conducting polymer/metal nanoparticle films. *Journal of Nanoscience and Nanotechnology, 7 (7), 1 - 4.*

Pages, H., Topart, P. and Lemordant, D. (2001). Wide band electrochromic displays based on thin conducting polymer films. *Electrochim Acta, 46, 2137-2143.*

Patois, T., Lakard, B., Monney, S., Roizard, X. and Fievet, P. (2011). Characterization of the surface properties of polypyrrole films: Influence of electrodeposition parameters. *Synth Met, 161, 2498 – 2505.*

Paulraj, P., Manikandan, A., Manikandan, E., Pandian, K., Moodley, M. K., Roro, K., and Murugan, K. (2018). Solid-State Synthesis of POPD@AgNPsNanocomposites for Electrochemical Sensors. *Journal of Nanoscience and Nanotechnology,18, 3991–3999.*

Porro, T. J. and Terharr, D. A. (1976). Double- beam fluorescence spectrophotometry. *Analytical chemistry, 48(13), 1103A-1107A.*

Prasad, G. K., Radhakrishnan, T. P., Kumar, D. S. and Krishna, M. G. (2005). Ammonia sensing characteristics of thin films based on polyelectrolyte templated polyanilijne. *Sens. Actuators B, 106, 626 – 631.*

Radoslav B. B. (1996) A study of effects of LiClO4 on poly(Ethylene Oxide), (PEO) melt dynamic behavior using fabry-perot interferometry. *(Master's Thesis),Department of Physics, Sofia University, Sofia, Bulgaria, 82.*

Ram, M. K., Yavuz, O., Lahsangah, V. and Aldissi, M. (2005). CO gas sensing from ultrathin nano-composite conducting polymer film. *Sens. Actuators B, 106, 750 – 757.*

Reemts, J., Parisi, J. and Schlettwein, D. (2004). Electrochemical growth of gas-sensitive polyaniline thin films across an insulating gap. *Thin Solid Films, 466, 320 – 325.*

Reiter, J., Krejza, O. and Sedlarikova, M. (2009). Electrochromic devices employing methcrylate-based polymer electrolytes. *Solar Energy Materials and Solar Cells, 93 (2), 249 – 255.*

Robert, A. S. (2002). Phenylene and Toluenediam. Ullmann's Encychopedia of Industrial Chemistry, Wiley VCH, Weinheim.

Rosanny, C. S., Marina, V. S., Roselena, F., Roger, J. M. and Adriana, S. R. (2016). Electrochromic properties of polyaniline based hybrid organic/inorganic material. *Journal of Brazilian Chemical Society, 27(10), 1847-1857.*

Rosseinsky, D. R. and Mortimer, R. J. (2001). Electrochromic systems and the prospects for devices. *Advanced Materials 13(11), 783 – 793.*

Rowley, N. M. and Mortimer, R. J. (2002). New electrochromic materials. *Science Progress, 85, 243 – 262.*

Ruangchuag, L., Sirivat, A. and Schwank, J. (2004). Selective conductivity response of polypyrrole-based sensor on flammable chemicals. *React. Funct. Polym., 61, 11 – 22.*

Salma, B. L., Anwar-ul-Haq, A. S. and Rudolf, H. (2011). Spectroelectrochemistry of poly (o-phenylenediamine: polyaniline-like segments in the polymer structure. *Eletrochim Acta, 56, 3353 – 3358.*

Samanta, S., Roy, P. and Kar, P., (2015). Influence of pH of the Reaction Medium on the and Property of Conducting Poly (o – phenylenediaine). *Materials Today: Proceedings, 2, 1301 – 1308.*

Samanta, S., Roy, P. and Kar, P. (2016). Synthesis of poly(o-phenylenediamine) nanofiber with novel structure and properties.*Polymer Advanced Technologies, 28(7), 797 – 804.*

Sandberg, H. G. O., Backlund, T. G., Osterbacka, R., Jussila, S., Makela, T. and Stubb, H. (2005). Applications of an all-polymer solution-processed high performance transistor. *Synth. Met., 155, 662 – 665.*

Sanjeev, K. G. and Jamil, A. (2011). Thermal oxidation of silicon carbide (SiC)- Experimentally observed facts. In M. Mukherjee (Ed.), *Silicon Carbide - Materials, Processing and Applications in Electronic Devices*(pp. 207-230). United Kingdom: Intech.

Saxens, D., Dwivedi, V. and Mishra, P. K. (2013). Dielectric study of polyaniline in frequency range 100Hz to 500Hz at Temperature 200^{o}C and 300^{o}C. *Research Journal of Chemical Science, 3(2), 16-19.*

Sayyah, S. M., Khahiel, A. B., Ahmed, A. A. and Mohamed, S. M. (2014). Chemical polymerization kinetics of *poly (o-phenylenediamine)* and characterization of the obtained polymer in aqueous hydrochloric acid solution using K2Cr2O7 as oxidizing agent. *International Journal of Polymer Science, 2014, 1-16.*

Segut, O., Lakard, B., Herlem, G., Rauch, J., Jeannot, J., Robert, L. and Fahys, B.(2007). Development of miniaturized pH biosensors based on electrosynthesized polymer films. *Anal. Chim. Acta, 597, 313-321.*

Sequeira, C. A. C. and Santos, D. M. F. (2010). Polymer electrolytes:Fundamentals and applications. *Wood publishing series in Electronic and optical materials, 3 - 61.*

Shanthi, T. and Rajendran, S. (2013). Influence of polyvinyl pyrolidone on corrosionresistance of mild steel simulated concrete pore solution prepared in well water. *Research Journal of Chemical Science, 3(9), 39-44.*

Siddhartha, S., Poulomi, R. and Pradip, K. (2015). Influence of pH of the reaction medium on the structure and property of conducting poly o-phenylenediamine. *Proceedings of 4th International Conference on Materials Processing and Characterization, 2, 1301 – 1308.*

Siddhartha, S., Poulomi, R. and Pradip, K. (2016). Structure and properties of conducting poly o-phenylenediamine synthesized in different inorganic acid medium. *Macromolecular Research, 24 (4),342 – 349.*

Silverstern, M. S., Tai, H. W., Sergienko, A., Lumelsky, Y. L. and Pavlovsky, S. (2005). PolyHIPE: IPNs, hybrids, nanoscale porosity, silica monoliths and ICP-basedsensors. Polymer, 46, 6682 – 6694.

Siva, T., Kamaraj, K., karpakam, V. Sathiyanarayanan, S. (2013). Poly o- phenylenediamine nanotubes and its application in self healing coatings. *Progress in organic coatings, 76 (4), 581 – 588.*

Skoog, A., Holler, F. J. and Crouch, S. R. (2007). *Principles of instrumental analysis.* Belmont,CA: Thomson Brooks /Cole.

Stafstrom, S., Bredas, J. L., Epstein, A. J., Woo, H. S., Tanner, D. B., Huang, W. S. and Mac Diarmind, A. C. (1987). Polaron Lattice in highly conducting polyaniline, theoretical and optical studies. *Physical Review Letters B, 59, 1464 – 1467.*

Stussi, E., Cella, S., Serra, G. and Venier, G. S (1996). Fabrication of conducting polymer patterns for gas sensing by a dry technique. *Mater. Sci. Eng. C-Biometric Mater. Sens. Sys., 4, 27 – 33.*

Suresh, K. V., Venkatraman, B. R., Shobana, V. and Subramania, A. (2012). Polythiophene Naphthosulphonic acid: New and effective corrosion inhibitor for carbon steel in acid solution. *Research Journal of Chemical Science, 2(10), 87-94.*

Tao, Z., Jin J., Yang, S., Hu, D., Li, G. and Jiang, G. J. (2009). Synthesis andcharacterization of fluorinated PBO with high thermal stability and low dielectric constant. *Journal of Macromolecular Science, Part B, 48, 1114 – 1124.*

Tkacheno, N. V. (2006). *Optical spectroscopy: Methods and instrumentations.*Amsterdam: Elsevier.

Tongpool, R. and Yoriya, S. (2005). Kinetics of nitrogen dioxides exposure in lead pythalocyanine sensors. *Thin Solid Films, 477, 148 – 152.*

Ullah, H., Khan, I., Yamani, Z. H. and Qurashi, A. (2017). Sonochemical-driven ultrafast facile synthesis of SnO2 nanoparticles: growth mechanism structural electrical and hydrogen gas sensing properties. *Ultrason Sonochem, 34, 484 – 490.*

Wang, C., Zheng, W., Yue, Z., Too, C. O. and Wallace, G. (2011). Buckled, stretchable polypyrrole electrodes for battery applications. *Adv. Mater, 23 3580-3584.*

Wang, H., Zhang, C., Wang, X., Huo, X. and Wang, G. (2013). Direct electrosynthesis of poly

o-phenylenediamine bulk materials for supercapacitor application. *Electrochim. Acta, 91, 144 – 151.*

Wang, H., Huang, M. and Li, X. (2007). Synthesis, film forming and electronic properties of o-phenylenediamine copolymers, displaying an uncommon tricolor. *Macromolecules, 40 (5), 1489.*

Wang, Z. and Liao, F. (2012). Synthesis of poly ortho-phenylenediamine fluffy microspheres and application for the removal of Cr(VI). *Journal of Nanomaterials, 2012, 1-7.*

Ward, M. D. and McCleverty, J. A. (2002). Non-innocent behavior in nanonuclear and polynuclear complexes: consequences for redox and electronic spectroscopic properties. *Journal of Chem. Soc. Dalton Trans, 275 – 288.*

Wu, T. Y., Li, W. B., Kuo, C. W., Chou, C. F., Liao, J. W., Chen, H. R. and Tseng, C. G. (2013). Study of poly (methyl methacrylate - based gel electrolyte for electrochromic device. *International Journal of Electrochemical Science, 8, 10720 - 10732.*

Wu, Z. C., Chen, Z. H., Du, X., Logan, J. M., Sippel, J., Nikolou, M., Kamaras, K., Reynolds, J. R.Tanner, D. B., Hebard, A. F. and Rinzler, A. G. (2004) Transparent, conductive carbon nanotube films. *Science, 305, 1273 – 1276.*

Xiang, C., Xie, Q., Hu, J. and Yao, S. (2006). Studies on electrochemical copolymerization of aniline with o-phenylenediamine and degradation of the resultant copolymers via electrochemical quartz crystal microbalance and scanning electrochemical microscope. *Synth. Met., 156, 444-453.*

Yan, H., Tomizawa, K.,, Ohno, H. and Toshima, N. (2003). All solid actuator consisting of polyaniline film & solid polymer electrolyte. *Macromol. Mater Eng., 288, 578 – 584.*

Yadegari, H., Heli, H. and Jabbari, A. (2013). Graphene/poly (ortho phenylenediamine) nanocompobite material for electrochemical super capacitor. *Journal of Solid State*

Electrochemistry, 17(8), 2203 – 2212.

Young, H.D and Freedman, R.A (2008). University Physics. (12th ed). New York: Pearson Addison Wesley, pp. 1095.

Yuan, J. H., Han, D. X., Zhang, Y. I., Shen, Y. F., Wang, Z. J., Zhang, Q. X. and Niu,. L. (2007). Electrostatic assembly of polyaniline and platinum-poly (amidoamine) dendrimers hybrid nanocomposite multilayer and its electrocatalysis towards CO &O2. *Journal of Electroanal. Chem, 599, 127-135.*

Yuan, C., Liu, X., Jia, M., Luo, Z. and Yao, J. (2014). Facile preparation of N- and O- doped hollow carbon spheres derived from *poly (o-phenylenediamine)* for supercapacitors. *Journal of Material Chemistry A, 3, 3409 - 3415.*

Zhao, Y., Si, S., and Liao, C. (2013). A single flow Zinc/ polyaniline suspension rechargeable battery. *Journal of Power Sources, 241, 449 – 453.*

Zhou, H. H., Jiao, S. Q., Chen, H. J., Wei, W. Z. and Kuang, Y. F. (2004). Relationship between preparation conditions, morphology and electrochemical properties of polyaniline prepared by pulse galvanostatic method (PGM). *Thin Solid Films, 450, 233 – 239.*

APPENDICES

A: Optical Properties

1. Optical Properties of PoPD Fabricated at pH value of 1.0

Wavelength (nm)	Absorbance	Transmittance (%)	Reflectance (%)	Photon Energy(eV)	αhυ	$(\alpha h\upsilon)^2$
300	0.14	72.19	13.66	4.15	1.96	3.84
302	0.21	61.27	17.46	4.11	2.89	8.36
305	0.18	66.65	15.73	4.07	2.35	5.52
308	0.24	57.25	18.53	4.04	3.17	10.07
311	0.25	55.73	18.88	4.00	3.27	10.68
314	0.25	56.85	18.62	3.96	3.10	9.61
316	0.26	55.12	19.01	3.93	3.21	10.32
319	0.27	54.03	19.23	3.89	3.26	10.65
322	0.29	51.79	19.63	3.86	3.43	11.74
325	0.28	51.93	19.61	3.83	3.35	11.25
328	0.29	51.10	19.74	3.80	3.38	11.41
330	0.28	52.65	19.49	3.76	3.17	10.08
333	0.29	51.32	19.71	3.73	3.25	10.53
336	0.29	50.91	19.77	3.70	3.23	10.43
339	0.27	53.35	19.36	3.67	2.96	8.75
341	0.26	54.90	19.06	3.64	2.78	7.71
344	0.27	54.14	19.21	3.61	2.80	7.81
347	0.26	55.38	18.95	3.58	2.65	7.02
350	0.24	56.92	18.61	3.55	2.49	6.18
353	0.24	57.47	18.47	3.53	2.41	5.78
355	0.23	58.67	18.17	3.50	2.28	5.20
358	0.23	59.32	18.00	3.47	2.20	4.83
361	0.22	59.74	17.89	3.44	2.13	4.56
364	0.22	60.32	17.73	3.42	2.06	4.25
367	0.22	60.43	17.69	3.39	2.02	4.09
369	0.22	60.31	17.73	3.37	2.00	4.01
372	0.22	60.21	17.76	3.34	1.98	3.91
375	0.22	60.72	17.61	3.32	1.92	3.67
378	0.22	60.47	17.69	3.29	1.90	3.62
380	0.21	60.96	17.54	3.27	1.85	3.41
383	0.21	61.40	17.42	3.24	1.79	3.21
386	0.21	61.93	17.26	3.22	1.74	3.01
389	0.21	62.37	17.13	3.20	1.69	2.84
392	0.20	63.03	16.92	3.17	1.62	2.64
394	0.20	63.49	16.78	3.15	1.58	2.49

Wavelength (nm)	Absorbance	Transmittance (%)	Reflectance (%)	Photon Energy(eV)	αhυ	$(\alpha h\upsilon)^2$
397	0.19	64.19	16.56	3.13	1.52	2.30
400	0.19	65.08	16.27	3.11	1.45	2.10
403	0.18	65.51	16.12	3.09	1.41	1.98
406	0.18	66.29	15.85	3.07	1.35	1.82
408	0.18	66.83	15.67	3.04	1.30	1.70
411	0.17	67.51	15.43	3.02	1.25	1.57
414	0.17	67.89	15.29	3.00	1.22	1.49
417	0.16	68.46	15.08	2.98	1.18	1.39
420	0.16	68.81	14.96	2.96	1.15	1.32
422	0.16	69.11	14.85	2.94	1.12	1.25
425	0.16	69.37	14.75	2.92	1.09	1.19
428	0.16	69.58	14.67	2.91	1.07	1.14
431	0.16	69.54	14.68	2.89	1.06	1.12
433	0.16	69.48	14.71	2.87	1.05	1.09
436	0.17	67.54	15.42	2.85	1.11	1.24
439	0.17	67.34	15.49	2.83	1.11	1.23
442	0.17	67.25	15.52	2.81	1.10	1.20
445	0.17	67.13	15.56	2.80	1.09	1.18
447	0.17	67.17	15.55	2.78	1.07	1.15
450	0.17	67.15	15.55	2.76	1.06	1.13
453	0.17	67.46	15.44	2.74	1.04	1.07
456	0.16	69.45	14.72	2.73	0.95	0.90
459	0.15	70.19	14.44	2.71	0.91	0.83
461	0.15	71.31	14.01	2.69	0.86	0.74
464	0.14	72.64	13.48	2.68	0.80	0.64
467	0.13	73.90	12.97	2.66	0.75	0.56
470	0.12	75.04	12.49	2.65	0.70	0.49
472	0.12	75.91	12.12	2.63	0.67	0.44
475	0.12	76.70	11.78	2.62	0.63	0.40
478	0.11	77.17	11.57	2.60	0.61	0.37
481	0.11	77.56	11.40	2.59	0.59	0.35
484	0.11	77.93	11.24	2.57	0.58	0.33
486	0.11	78.20	11.12	2.56	0.56	0.32
489	0.10	78.54	10.97	2.54	0.54	0.30
492	0.10	78.89	10.81	2.53	0.53	0.28
495	0.10	79.38	10.59	2.51	0.51	0.26
498	0.10	79.76	10.42	2.50	0.49	0.24
500	0.09	80.45	10.10	2.48	0.47	0.22
503	0.09	81.09	9.81	2.47	0.45	0.20
506	0.09	81.77	9.49	2.46	0.42	0.18

Wavelength (nm)	Absorbance	Transmittance (%)	Reflectance (%)	Photon Energy(eV)	αhυ	$(\alpha h\upsilon)^2$
509	0.08	82.44	9.17	2.44	0.40	0.16
511	0.08	83.15	8.84	2.43	0.38	0.14
514	0.08	84.11	8.38	2.42	0.35	0.12
517	0.07	85.22	7.84	2.40	0.32	0.10
520	0.07	86.06	7.42	2.39	0.30	0.09
523	0.06	87.02	6.94	2.38	0.27	0.08
525	0.06	87.98	6.46	2.37	0.25	0.06
528	0.05	88.84	6.02	2.35	0.23	0.05
531	0.05	89.81	5.52	2.34	0.21	0.04
534	0.04	90.89	4.96	2.33	0.18	0.03
537	0.04	91.52	4.63	2.32	0.17	0.03
539	0.04	91.98	4.39	2.30	0.16	0.02
542	0.03	92.43	4.15	2.29	0.14	0.02
545	0.03	93.30	3.69	2.28	0.13	0.02
548	0.03	93.53	3.57	2.27	0.12	0.01
551	0.03	93.40	3.63	2.26	0.12	0.01
553	0.03	93.63	3.51	2.25	0.12	0.01
556	0.03	93.75	3.45	2.24	0.11	0.01
559	0.03	93.81	3.41	2.22	0.11	0.01
562	0.03	93.85	3.40	2.21	0.11	0.01
564	0.03	93.89	3.37	2.20	0.11	0.01
567	0.03	93.90	3.37	2.19	0.11	0.01
570	0.03	93.90	3.37	2.18	0.10	0.01
573	0.03	93.93	3.35	2.17	0.10	0.01
576	0.03	93.86	3.39	2.16	0.10	0.01
578	0.03	93.83	3.40	2.15	0.10	0.01
581	0.03	93.81	3.41	2.14	0.10	0.01
584	0.03	93.83	3.41	2.13	0.10	0.01
587	0.03	93.83	3.40	2.12	0.10	0.01
590	0.03	93.96	3.34	2.11	0.10	0.01
592	0.03	94.02	3.30	2.10	0.09	0.01
595	0.03	94.13	3.24	2.09	0.09	0.01
598	0.03	94.26	3.17	2.08	0.09	0.01
601	0.03	94.36	3.12	2.07	0.09	0.01
603	0.02	94.58	3.00	2.06	0.08	0.01
606	0.02	94.78	2.89	2.05	0.08	0.01
609	0.02	94.86	2.85	2.04	0.08	0.01
612	0.02	95.19	2.67	2.03	0.07	0.01
615	0.02	95.43	2.54	2.02	0.07	0.00
617	0.02	95.62	2.44	2.01	0.06	0.00

Wavelength (nm)	Absorbance	Transmittance (%)	Reflectance (%)	Photon Energy(eV)	αhυ	$(\alpha h\upsilon)^2$
620	0.02	95.82	2.32	2.00	0.06	0.00
623	0.02	96.06	2.19	2.00	0.06	0.00
626	0.02	96.28	2.08	1.99	0.05	0.00
629	0.02	96.43	1.99	1.98	0.05	0.00
631	0.01	96.70	1.84	1.97	0.05	0.00
634	0.01	96.83	1.77	1.96	0.04	0.00
637	0.01	97.11	1.61	1.95	0.04	0.00
640	0.01	97.43	1.44	1.94	0.03	0.00
642	0.01	97.65	1.32	1.93	0.03	0.00
645	0.01	97.88	1.19	1.93	0.03	0.00
648	0.01	98.09	1.07	1.92	0.02	0.00
651	0.01	98.20	1.01	1.91	0.02	0.00
654	0.01	98.24	0.99	1.90	0.02	0.00
656	0.01	98.22	1.00	1.89	0.02	0.00
659	0.01	98.26	0.98	1.89	0.02	0.00
662	0.01	98.32	0.94	1.88	0.02	0.00
665	0.01	98.33	0.94	1.87	0.02	0.00
668	0.01	98.32	0.95	1.86	0.02	0.00
670	0.01	98.34	0.93	1.85	0.02	0.00
673	0.01	98.34	0.93	1.85	0.02	0.00
676	0.01	98.31	0.95	1.84	0.02	0.00
679	0.01	98.24	0.99	1.83	0.02	0.00
681	0.01	98.27	0.97	1.82	0.02	0.00
684	0.01	98.25	0.98	1.82	0.02	0.00
687	0.01	98.21	1.01	1.81	0.02	0.00
690	0.01	98.17	1.03	1.80	0.02	0.00
693	0.01	98.12	1.06	1.79	0.02	0.00
695	0.01	98.00	1.12	1.79	0.02	0.00
698	0.01	97.91	1.17	1.78	0.02	0.00
701	0.01	97.88	1.19	1.77	0.02	0.00
704	0.01	97.86	1.20	1.77	0.02	0.00
707	0.01	97.72	1.28	1.76	0.02	0.00
709	0.01	97.65	1.32	1.75	0.03	0.00
712	0.01	97.55	1.37	1.75	0.03	0.00
715	0.01	97.47	1.42	1.74	0.03	0.00
718	0.01	97.36	1.48	1.73	0.03	0.00
721	0.01	97.31	1.50	1.73	0.03	0.00
723	0.01	97.18	1.58	1.72	0.03	0.00
726	0.01	97.01	1.67	1.71	0.03	0.00
729	0.01	96.92	1.72	1.71	0.03	0.00

Wavelength (nm)	Absorbance	Transmittance (%)	Reflectance (%)	Photon Energy(eV)	αhυ	$(\alpha h\upsilon)^2$
732	0.01	96.79	1.79	1.70	0.03	0.00
734	0.01	96.71	1.84	1.69	0.03	0.00
737	0.02	96.57	1.91	1.69	0.03	0.00
740	0.02	96.54	1.93	1.68	0.03	0.00
743	0.02	96.41	2.00	1.67	0.04	0.00
746	0.02	96.29	2.07	1.67	0.04	0.00
748	0.02	96.12	2.16	1.66	0.04	0.00
751	0.02	96.09	2.18	1.65	0.04	0.00
754	0.02	96.02	2.22	1.65	0.04	0.00
757	0.02	95.92	2.27	1.64	0.04	0.00
760	0.02	95.84	2.31	1.64	0.04	0.00
762	0.02	95.67	2.41	1.63	0.04	0.00
765	0.02	95.56	2.47	1.62	0.04	0.00
768	0.02	95.45	2.53	1.62	0.04	0.00
771	0.02	95.51	2.49	1.61	0.04	0.00
773	0.02	95.54	2.48	1.61	0.04	0.00
776	0.02	95.51	2.50	1.60	0.04	0.00
779	0.02	95.60	2.45	1.60	0.04	0.00
782	0.02	95.63	2.43	1.59	0.04	0.00
785	0.02	95.59	2.45	1.58	0.04	0.00
787	0.02	95.60	2.44	1.58	0.04	0.00
790	0.02	95.76	2.36	1.57	0.04	0.00
793	0.02	95.85	2.31	1.57	0.04	0.00
796	0.02	95.92	2.27	1.56	0.04	0.00
799	0.02	96.00	2.22	1.56	0.03	0.00
801	0.02	96.04	2.21	1.55	0.03	0.00
804	0.02	96.08	2.18	1.55	0.03	0.00
807	0.02	96.17	2.14	1.54	0.03	0.00
810	0.02	96.28	2.07	1.54	0.03	0.00
812	0.02	96.38	2.02	1.53	0.03	0.00
815	0.02	96.51	1.95	1.52	0.03	0.00
818	0.02	96.55	1.92	1.52	0.03	0.00
821	0.01	96.65	1.87	1.51	0.03	0.00
824	0.01	96.75	1.82	1.51	0.03	0.00
826	0.01	96.86	1.76	1.50	0.03	0.00
829	0.01	96.98	1.69	1.50	0.02	0.00
832	0.01	97.11	1.62	1.49	0.02	0.00
835	0.01	97.17	1.58	1.49	0.02	0.00
838	0.01	97.25	1.54	1.48	0.02	0.00
840	0.01	97.36	1.48	1.48	0.02	0.00

Wavelength (nm)	Absorbance	Transmittance (%)	Reflectance (%)	Photon Energy(eV)	αhυ	$(\alpha h\upsilon)^2$
843	0.01	97.49	1.41	1.47	0.02	0.00
846	0.01	97.53	1.38	1.47	0.02	0.00
849	0.01	97.63	1.33	1.46	0.02	0.00
852	0.01	97.74	1.27	1.46	0.02	0.00
854	0.01	97.70	1.29	1.46	0.02	0.00
857	0.01	97.73	1.27	1.45	0.02	0.00
860	0.01	97.86	1.20	1.45	0.02	0.00
863	0.01	97.91	1.17	1.44	0.02	0.00
865	0.01	98.01	1.12	1.44	0.01	0.00
868	0.01	98.09	1.07	1.43	0.01	0.00
871	0.01	98.07	1.08	1.43	0.01	0.00
874	0.01	98.13	1.05	1.42	0.01	0.00
877	0.01	98.19	1.02	1.42	0.01	0.00
879	0.01	98.26	0.98	1.41	0.01	0.00
882	0.01	98.29	0.96	1.41	0.01	0.00
885	0.01	98.27	0.97	1.40	0.01	0.00
888	0.01	98.38	0.91	1.40	0.01	0.00
891	0.01	98.34	0.93	1.40	0.01	0.00
893	0.01	98.36	0.92	1.39	0.01	0.00
896	0.01	98.31	0.95	1.39	0.01	0.00
899	0.01	98.39	0.91	1.38	0.01	0.00
902	0.01	98.39	0.91	1.38	0.01	0.00
904	0.01	98.36	0.92	1.37	0.01	0.00
907	0.01	98.41	0.90	1.37	0.01	0.00
910	0.01	98.40	0.90	1.37	0.01	0.00
913	0.01	98.38	0.91	1.36	0.01	0.00
916	0.01	98.36	0.92	1.36	0.01	0.00
918	0.01	98.36	0.92	1.35	0.01	0.00
921	0.01	98.35	0.93	1.35	0.01	0.00
924	0.01	98.39	0.90	1.35	0.01	0.00
927	0.01	98.34	0.94	1.34	0.01	0.00
930	0.01	98.30	0.95	1.34	0.01	0.00
932	0.01	98.21	1.01	1.33	0.01	0.00
935	0.01	98.22	1.00	1.33	0.01	0.00
938	0.01	98.16	1.03	1.33	0.01	0.00
941	0.01	98.09	1.07	1.32	0.01	0.00
943	0.01	98.07	1.09	1.32	0.01	0.00
946	0.01	97.96	1.14	1.31	0.01	0.00
949	0.01	97.94	1.15	1.31	0.01	0.00
952	0.01	97.94	1.16	1.31	0.01	0.00

Wavelength (nm)	Absorbance	Transmittance (%)	Reflectance (%)	Photon Energy(eV)	αhυ	$(\alpha h\upsilon)^2$
955	0.01	97.93	1.16	1.30	0.01	0.00
957	0.01	98.00	1.12	1.30	0.01	0.00
960	0.01	97.92	1.16	1.29	0.01	0.00
963	0.01	97.87	1.20	1.29	0.01	0.00
966	0.01	97.77	1.25	1.29	0.01	0.00
969	0.01	97.71	1.28	1.28	0.01	0.00
971	0.01	97.54	1.38	1.28	0.01	0.00
974	0.01	97.51	1.40	1.28	0.01	0.00
977	0.01	97.38	1.47	1.27	0.02	0.00
980	0.01	97.34	1.49	1.27	0.02	0.00
982	0.01	97.14	1.60	1.27	0.02	0.00
985	0.01	96.98	1.69	1.26	0.02	0.00
988	0.01	96.78	1.80	1.26	0.02	0.00
991	0.01	96.62	1.89	1.25	0.02	0.00
994	0.02	96.42	2.00	1.25	0.02	0.00
996	0.02	96.17	2.14	1.25	0.02	0.00
999	0.02	95.92	2.27	1.24	0.02	0.00
1002	0.02	95.59	2.45	1.24	0.02	0.00
1005	0.02	95.23	2.65	1.24	0.03	0.00
1008	0.02	94.74	2.91	1.23	0.03	0.00
1010	0.03	94.33	3.14	1.23	0.03	0.00
1013	0.03	93.79	3.42	1.23	0.03	0.00
1016	0.03	93.18	3.75	1.22	0.04	0.00
1019	0.03	92.39	4.17	1.22	0.04	0.00
1022	0.04	91.68	4.55	1.22	0.04	0.00
1024	0.04	90.79	5.02	1.21	0.05	0.00
1027	0.05	89.91	5.47	1.21	0.05	0.00
1030	0.05	89.07	5.90	1.21	0.06	0.00
1033	0.05	88.36	6.27	1.20	0.06	0.00
1035	0.06	87.68	6.61	1.20	0.07	0.00
1038	0.06	87.14	6.88	1.20	0.07	0.00
1041	0.06	86.76	7.07	1.19	0.07	0.01
1044	0.06	86.36	7.27	1.19	0.07	0.01
1047	0.07	85.99	7.45	1.19	0.07	0.01
1049	0.07	85.75	7.58	1.18	0.08	0.01
1052	0.07	85.51	7.69	1.18	0.08	0.01
1055	0.07	85.30	7.79	1.18	0.08	0.01
1058	0.07	85.04	7.92	1.18	0.08	0.01
1061	0.07	84.82	8.03	1.17	0.08	0.01
1063	0.07	84.67	8.10	1.17	0.08	0.01

Wavelength (nm)	Absorbance	Transmittance (%)	Reflectance (%)	Photon Energy(eV)	αhυ	$(\alpha h\upsilon)^2$
1066	0.07	84.29	8.29	1.17	0.08	0.01
1069	0.07	84.29	8.29	1.16	0.08	0.01
1072	0.07	84.14	8.36	1.16	0.08	0.01
1074	0.08	84.04	8.41	1.16	0.08	0.01
1077	0.08	83.83	8.51	1.15	0.08	0.01
1080	0.08	83.71	8.57	1.15	0.08	0.01
1083	0.08	83.37	8.73	1.15	0.08	0.01
1086	0.08	83.25	8.79	1.15	0.08	0.01
1088	0.08	82.88	8.96	1.14	0.09	0.01
1091	0.08	82.85	8.98	1.14	0.09	0.01
1094	0.08	82.58	9.11	1.14	0.09	0.01
1097	0.08	82.35	9.22	1.13	0.09	0.01
1100	0.09	81.99	9.39	1.13	0.09	0.01

2. Optical Properties of PoPD Fabricated at pH value of 1.5

Wavelength (nm)	Absorbance	Transmittance (%)	Reflectance (%)	Photon Energy(eV)	αhυ	$(\alpha h\upsilon)^2$
300	0.36	43.67	20.35	4.15	4.98	24.80
302	0.37	42.69	20.34	4.11	5.02	25.23
305	0.38	41.98	20.32	4.07	5.03	25.29
308	0.38	41.59	20.31	4.04	4.99	24.92
311	0.40	40.11	20.22	4.00	5.10	26.06
314	0.41	39.14	20.12	3.96	5.15	26.51
316	0.42	37.81	19.95	3.93	5.24	27.51
319	0.44	35.97	19.62	3.89	5.42	29.36
322	0.46	35.03	19.41	3.86	5.46	29.85
325	0.47	34.02	19.15	3.83	5.52	30.46
328	0.46	34.39	19.25	3.80	5.37	28.85
330	0.46	34.73	19.34	3.76	5.23	27.38
333	0.45	35.14	19.44	3.73	5.09	25.89
336	0.45	35.30	19.48	3.70	4.98	24.82
339	0.44	35.90	19.61	3.67	4.82	23.24
341	0.44	36.00	19.63	3.64	4.73	22.38
344	0.44	35.90	19.61	3.61	4.67	21.77
347	0.44	36.15	19.66	3.58	4.56	20.81
350	0.44	36.52	19.73	3.55	4.44	19.74
353	0.44	36.41	19.71	3.53	4.39	19.24
355	0.44	36.52	19.73	3.50	4.30	18.53
358	0.44	36.55	19.74	3.47	4.23	17.93

Wavelength (nm)	Absorbance	Transmittance (%)	Reflectance (%)	Photon Energy(eV)	αhυ	$(\alpha h\upsilon)^2$
361	0.44	36.62	19.75	3.44	4.16	17.32
364	0.43	36.82	19.79	3.42	4.08	16.62
367	0.43	37.18	19.85	3.39	3.98	15.80
369	0.43	37.31	19.87	3.37	3.90	15.22
372	0.42	37.75	19.94	3.34	3.80	14.42
375	0.42	38.05	19.98	3.32	3.71	13.78
378	0.42	38.24	20.01	3.29	3.64	13.23
380	0.41	38.66	20.07	3.27	3.54	12.56
383	0.41	38.95	20.1	3.24	3.47	12.01
386	0.41	39.20	20.13	3.22	3.39	11.51
389	0.40	39.46	20.16	3.20	3.32	11.02
392	0.40	39.67	20.18	3.17	3.25	10.59
394	0.40	39.72	20.18	3.15	3.20	10.27
397	0.40	40.01	20.21	3.13	3.13	9.82
400	0.40	40.12	20.22	3.11	3.08	9.50
403	0.40	40.17	20.22	3.09	3.04	9.21
406	0.40	40.22	20.22	3.07	2.99	8.94
408	0.40	40.27	20.23	3.04	2.94	8.67
411	0.39	40.45	20.24	3.02	2.89	8.36
414	0.39	40.47	20.24	3.00	2.85	8.12
417	0.39	40.57	20.25	2.98	2.80	7.87
420	0.39	40.68	20.26	2.96	2.76	7.61
422	0.39	40.74	20.26	2.94	2.72	7.39
425	0.40	39.91	20.2	2.92	2.74	7.53
428	0.40	40.01	20.21	2.91	2.70	7.30
431	0.40	39.90	20.2	2.89	2.67	7.15
433	0.42	38.13	20	2.87	2.77	7.68
436	0.42	38.13	20	2.85	2.73	7.48
439	0.41	39.03	20.11	2.83	2.64	6.95
442	0.40	39.94	20.2	2.81	2.54	6.44
445	0.39	40.57	20.25	2.80	2.46	6.07
447	0.38	41.44	20.3	2.78	2.38	5.65
450	0.38	41.55	20.31	2.76	2.34	5.48
453	0.38	41.76	20.32	2.74	2.30	5.28
456	0.38	42.02	20.33	2.73	2.25	5.08
459	0.37	42.44	20.34	2.71	2.20	4.84
461	0.37	42.97	20.35	2.69	2.14	4.59
464	0.36	43.55	20.35	2.68	2.08	4.34
467	0.36	44.05	20.34	2.66	2.03	4.12

Wavelength (nm)	Absorbance	Transmittance (%)	Reflectance (%)	Photon Energy(eV)	αhυ	$(\alpha h\upsilon)^2$
470	0.35	44.39	20.34	2.65	1.99	3.95
472	0.35	44.71	20.33	2.63	1.95	3.79
475	0.35	44.89	20.32	2.62	1.91	3.66
478	0.35	45.00	20.32	2.60	1.89	3.56
481	0.35	45.07	20.32	2.59	1.86	3.46
484	0.35	45.11	20.32	2.57	1.84	3.38
486	0.35	45.08	20.32	2.56	1.82	3.30
489	0.35	45.13	20.32	2.54	1.79	3.22
492	0.35	45.16	20.32	2.53	1.77	3.14
495	0.34	45.21	20.31	2.51	1.75	3.07
498	0.34	45.28	20.31	2.50	1.73	2.99
500	0.34	45.38	20.31	2.48	1.70	2.90
503	0.34	45.50	20.3	2.47	1.68	2.82
506	0.34	45.62	20.3	2.46	1.66	2.74
509	0.34	45.79	20.29	2.44	1.63	2.66
511	0.34	46.04	20.27	2.43	1.60	2.56
514	0.33	46.26	20.26	2.42	1.57	2.48
517	0.33	46.48	20.25	2.40	1.55	2.39
520	0.33	46.77	20.23	2.39	1.52	2.30
523	0.33	47.01	20.21	2.38	1.49	2.23
525	0.33	47.25	20.19	2.37	1.47	2.15
528	0.32	47.50	20.17	2.35	1.44	2.07
531	0.32	47.74	20.15	2.34	1.42	2.00
534	0.32	47.93	20.13	2.33	1.39	1.94
537	0.32	48.12	20.11	2.32	1.37	1.88
539	0.32	48.29	20.1	2.30	1.35	1.83
542	0.32	48.36	20.09	2.29	1.33	1.78
545	0.31	48.46	20.08	2.28	1.32	1.73
548	0.31	48.54	20.07	2.27	1.30	1.69
551	0.31	48.63	20.06	2.26	1.28	1.65
553	0.31	48.68	20.05	2.25	1.27	1.61
556	0.31	48.73	20.05	2.24	1.26	1.58
559	0.31	48.76	20.05	2.22	1.24	1.54
562	0.31	48.78	20.04	2.21	1.23	1.51
564	0.31	48.78	20.04	2.20	1.22	1.48
567	0.31	48.81	20.04	2.19	1.20	1.45
570	0.31	48.82	20.04	2.18	1.19	1.42
573	0.31	48.86	20.04	2.17	1.18	1.39
576	0.31	48.80	20.04	2.16	1.17	1.37

Wavelength (nm)	Absorbance	Transmittance (%)	Reflectance (%)	Photon Energy(eV)	αhυ	$(\alpha h\upsilon)^2$
578	0.31	48.79	20.04	2.15	1.16	1.34
581	0.31	48.80	20.04	2.14	1.15	1.32
584	0.31	48.79	20.04	2.13	1.14	1.29
587	0.31	48.77	20.05	2.12	1.13	1.27
590	0.31	48.79	20.04	2.11	1.11	1.24
592	0.31	48.79	20.04	2.10	1.10	1.22
595	0.31	48.80	20.04	2.09	1.09	1.20
598	0.31	48.76	20.05	2.08	1.08	1.18
601	0.31	48.78	20.04	2.07	1.07	1.15
603	0.31	48.82	20.04	2.06	1.06	1.13
606	0.31	48.82	20.04	2.05	1.05	1.11
609	0.31	48.83	20.04	2.04	1.04	1.09
612	0.31	48.88	20.03	2.03	1.03	1.07
615	0.31	48.91	20.03	2.02	1.02	1.04
617	0.31	48.91	20.03	2.01	1.01	1.03
620	0.31	48.95	20.03	2.00	1.00	1.01
623	0.31	48.98	20.02	2.00	0.99	0.99
626	0.31	49.02	20.02	1.99	0.98	0.97
629	0.31	49.05	20.01	1.98	0.97	0.95
631	0.31	49.15	20	1.97	0.96	0.93
634	0.31	49.10	20.01	1.96	0.96	0.91
637	0.31	49.20	20	1.95	0.94	0.89
640	0.31	49.29	19.99	1.94	0.93	0.87
642	0.31	49.33	19.98	1.93	0.92	0.85
645	0.31	49.39	19.97	1.93	0.91	0.84
648	0.31	49.51	19.96	1.92	0.90	0.82
651	0.31	49.52	19.96	1.91	0.90	0.80
654	0.31	49.51	19.96	1.90	0.89	0.79
656	0.31	49.47	19.96	1.89	0.88	0.78
659	0.31	49.47	19.96	1.89	0.87	0.76
662	0.31	49.50	19.96	1.88	0.87	0.75
665	0.31	49.51	19.96	1.87	0.86	0.74
668	0.31	49.52	19.96	1.86	0.85	0.72
670	0.31	49.49	19.96	1.85	0.85	0.71
673	0.31	49.53	19.96	1.85	0.84	0.70
676	0.31	49.54	19.96	1.84	0.83	0.69
679	0.31	49.52	19.96	1.83	0.82	0.68
681	0.31	49.54	19.96	1.82	0.82	0.67
684	0.31	49.53	19.96	1.82	0.81	0.66

Wavelength (nm)	Absorbance	Transmittance (%)	Reflectance (%)	Photon Energy(eV)	αhυ	$(\alpha h\upsilon)^2$
687	0.31	49.54	19.96	1.81	0.80	0.65
690	0.30	49.56	19.95	1.80	0.80	0.63
693	0.31	49.54	19.96	1.79	0.79	0.62
695	0.31	49.50	19.96	1.79	0.79	0.62
698	0.31	49.46	19.97	1.78	0.78	0.61
701	0.31	49.47	19.96	1.77	0.77	0.60
704	0.31	49.48	19.96	1.77	0.77	0.59
707	0.31	49.44	19.97	1.76	0.76	0.58
709	0.31	49.42	19.97	1.75	0.76	0.57
712	0.31	49.46	19.97	1.75	0.75	0.56
715	0.31	49.39	19.97	1.74	0.75	0.56
718	0.31	49.37	19.98	1.73	0.74	0.55
721	0.31	49.36	19.98	1.73	0.73	0.54
723	0.31	49.35	19.98	1.72	0.73	0.53
726	0.31	49.26	19.99	1.71	0.73	0.53
729	0.31	49.27	19.99	1.71	0.72	0.52
732	0.31	49.25	19.99	1.70	0.71	0.51
734	0.31	49.21	20	1.69	0.71	0.50
737	0.31	49.23	19.99	1.69	0.70	0.50
740	0.31	49.16	20	1.68	0.70	0.49
743	0.31	49.12	20.01	1.67	0.70	0.48
746	0.31	49.07	20.01	1.67	0.69	0.48
748	0.31	49.06	20.01	1.66	0.69	0.47
751	0.31	49.01	20.02	1.65	0.68	0.47
754	0.31	48.99	20.02	1.65	0.68	0.46
757	0.31	48.92	20.03	1.64	0.67	0.45
760	0.31	48.93	20.03	1.64	0.67	0.45
762	0.31	48.84	20.04	1.63	0.67	0.44
765	0.31	48.82	20.04	1.62	0.66	0.44
768	0.31	48.80	20.04	1.62	0.66	0.43
771	0.31	48.77	20.05	1.61	0.65	0.43
773	0.31	48.75	20.05	1.61	0.65	0.42
776	0.31	48.71	20.05	1.60	0.64	0.42
779	0.31	48.73	20.05	1.60	0.64	0.41
782	0.31	48.69	20.05	1.59	0.64	0.40
785	0.31	48.68	20.05	1.58	0.63	0.40
787	0.31	48.66	20.06	1.58	0.63	0.39
790	0.31	48.67	20.06	1.57	0.62	0.39
793	0.31	48.67	20.06	1.57	0.62	0.38
796	0.31	48.69	20.05	1.56	0.61	0.38

Wavelength (nm)	Absorbance	Transmittance (%)	Reflectance (%)	Photon Energy(eV)	αhυ	$(\alpha h\upsilon)^2$
799	0.31	48.67	20.06	1.56	0.61	0.37
801	0.31	48.62	20.06	1.55	0.61	0.37
804	0.31	48.63	20.06	1.55	0.60	0.36
807	0.31	48.59	20.06	1.54	0.60	0.36
810	0.31	48.61	20.06	1.54	0.59	0.35
812	0.31	48.61	20.06	1.53	0.59	0.35
815	0.31	48.62	20.06	1.52	0.59	0.34
818	0.31	48.60	20.06	1.52	0.58	0.34
821	0.31	48.61	20.06	1.51	0.58	0.33
824	0.31	48.62	20.06	1.51	0.57	0.33
826	0.31	48.62	20.06	1.50	0.57	0.32
829	0.31	48.62	20.06	1.50	0.57	0.32
832	0.31	48.66	20.06	1.49	0.56	0.32
835	0.31	48.68	20.06	1.49	0.56	0.31
838	0.31	48.66	20.06	1.48	0.55	0.31
840	0.31	48.69	20.05	1.48	0.55	0.30
843	0.31	48.70	20.05	1.47	0.55	0.30
846	0.31	48.68	20.06	1.47	0.54	0.30
849	0.31	48.71	20.05	1.46	0.54	0.29
852	0.31	48.73	20.05	1.46	0.54	0.29
854	0.31	48.64	20.06	1.46	0.53	0.28
857	0.31	48.65	20.06	1.45	0.53	0.28
860	0.31	48.71	20.05	1.45	0.53	0.28
863	0.31	48.71	20.05	1.44	0.52	0.27
865	0.31	48.74	20.05	1.44	0.52	0.27
868	0.31	48.75	20.05	1.43	0.51	0.26
871	0.31	48.75	20.05	1.43	0.51	0.26
874	0.31	48.75	20.05	1.42	0.51	0.26
877	0.31	48.78	20.04	1.42	0.50	0.25
879	0.31	48.78	20.04	1.41	0.50	0.25
882	0.31	48.82	20.04	1.41	0.50	0.25
885	0.31	48.83	20.04	1.40	0.49	0.24
888	0.31	48.83	20.04	1.40	0.49	0.24
891	0.31	48.81	20.04	1.40	0.49	0.24
893	0.31	48.81	20.04	1.39	0.49	0.24
896	0.31	48.79	20.04	1.39	0.48	0.23
899	0.31	48.82	20.04	1.38	0.48	0.23
902	0.31	48.84	20.04	1.38	0.48	0.23
904	0.31	48.80	20.04	1.37	0.47	0.22
907	0.31	48.82	20.04	1.37	0.47	0.22

Wavelength (nm)	Absorbance	Transmittance (%)	Reflectance (%)	Photon Energy(eV)	αhυ	$(\alpha h\upsilon)^2$
910	0.31	48.79	20.04	1.37	0.47	0.22
913	0.31	48.78	20.04	1.36	0.47	0.22
916	0.31	48.80	20.04	1.36	0.46	0.21
918	0.31	48.77	20.05	1.35	0.46	0.21
921	0.31	48.78	20.04	1.35	0.46	0.21
924	0.31	48.81	20.04	1.35	0.45	0.21
927	0.31	48.78	20.04	1.34	0.45	0.20
930	0.31	48.75	20.05	1.34	0.45	0.20
932	0.31	48.73	20.05	1.33	0.45	0.20
935	0.31	48.71	20.05	1.33	0.44	0.20
938	0.31	48.67	20.06	1.33	0.44	0.20
941	0.31	48.66	20.06	1.32	0.44	0.19
943	0.31	48.68	20.05	1.32	0.44	0.19
946	0.31	48.65	20.06	1.31	0.43	0.19
949	0.31	48.67	20.06	1.31	0.43	0.19
952	0.31	48.69	20.05	1.31	0.43	0.18
955	0.31	48.70	20.05	1.30	0.43	0.18
957	0.31	48.70	20.05	1.30	0.42	0.18
960	0.31	48.70	20.05	1.29	0.42	0.18
963	0.31	48.68	20.05	1.29	0.42	0.18
966	0.31	48.64	20.06	1.29	0.42	0.17
969	0.31	48.63	20.06	1.28	0.41	0.17
971	0.31	48.57	20.07	1.28	0.41	0.17
974	0.31	48.58	20.07	1.28	0.41	0.17
977	0.31	48.52	20.07	1.27	0.41	0.17
980	0.31	48.48	20.08	1.27	0.41	0.17
982	0.32	48.40	20.08	1.27	0.41	0.16
985	0.32	48.32	20.09	1.26	0.40	0.16
988	0.32	48.26	20.1	1.26	0.40	0.16
991	0.32	48.19	20.11	1.25	0.40	0.16
994	0.32	48.09	20.12	1.25	0.40	0.16
996	0.32	48.01	20.12	1.25	0.40	0.16
999	0.32	47.91	20.13	1.24	0.40	0.16
1002	0.32	47.75	20.15	1.24	0.40	0.16
1005	0.32	47.65	20.16	1.24	0.40	0.16
1008	0.32	47.44	20.17	1.23	0.40	0.16
1010	0.33	47.24	20.19	1.23	0.40	0.16
1013	0.33	47.04	20.21	1.23	0.40	0.16
1016	0.33	46.80	20.22	1.22	0.40	0.16
1019	0.33	46.47	20.25	1.22	0.40	0.16

Wavelength (nm)	Absorbance	Transmittance (%)	Reflectance (%)	Photon Energy(eV)	αhυ	$(\alpha h\upsilon)^2$
1022	0.34	46.19	20.26	1.22	0.40	0.16
1024	0.34	45.86	20.28	1.21	0.40	0.16
1027	0.34	45.54	20.3	1.21	0.40	0.16
1030	0.34	45.26	20.31	1.21	0.40	0.16
1033	0.35	45.01	20.32	1.20	0.40	0.16
1035	0.35	44.78	20.33	1.20	0.40	0.16
1038	0.35	44.59	20.33	1.20	0.40	0.16
1041	0.35	44.54	20.33	1.19	0.40	0.16
1044	0.35	44.49	20.34	1.19	0.40	0.16
1047	0.35	44.47	20.34	1.19	0.40	0.16
1049	0.35	44.39	20.34	1.18	0.40	0.16
1052	0.35	44.44	20.34	1.18	0.40	0.16
1055	0.35	44.47	20.34	1.18	0.39	0.15
1058	0.35	44.40	20.34	1.18	0.39	0.15
1061	0.35	44.39	20.34	1.17	0.39	0.15
1063	0.35	44.45	20.34	1.17	0.39	0.15
1066	0.35	44.43	20.34	1.17	0.39	0.15
1069	0.35	44.54	20.33	1.16	0.38	0.15
1072	0.35	44.55	20.33	1.16	0.38	0.14
1074	0.35	44.51	20.34	1.16	0.38	0.14
1077	0.35	44.50	20.34	1.15	0.38	0.14
1080	0.35	44.59	20.33	1.15	0.37	0.14
1083	0.35	44.63	20.33	1.15	0.37	0.14
1086	0.35	44.67	20.33	1.15	0.37	0.14
1088	0.35	44.65	20.33	1.14	0.37	0.14
1091	0.35	44.69	20.33	1.14	0.37	0.13
1094	0.35	44.63	20.33	1.14	0.36	0.13
1097	0.35	44.63	20.33	1.13	0.36	0.13
1100	0.35	44.59	20.33	1.13	0.36	0.13

3. Optical Properties of PoPD Fabricated at pH value of 1.5 (- 0.7 V)

Wavelength (nm)	Absorbance	Transmittance (%)	Reflectance (%)	Photon Energy(eV)	αhυ	$(\alpha h\upsilon)^2$
300	0.66	21.71	11.95	4.15	9.19	84.53
302	0.68	21.09	11.32	4.11	9.20	84.58
305	0.76	17.48	6.78	4.08	10.12	102.4
308	0.74	18.03	7.566	4.04	9.76	95.27

Wavelength (nm)	Absorbance	Transmittance (%)	Reflectance (%)	Photon Energy (eV)	$\alpha h\upsilon$	$(\alpha h\upsilon)^2$
311	0.69	20.43	10.6	4.00	8.89	78.95
313	0.64	23.08	13.24	3.97	8.06	64.97
316	0.61	24.29	14.26	3.93	7.64	58.39
319	0.59	25.47	15.13	3.90	7.26	52.67
322	0.59	25.90	15.43	3.86	7.05	49.65
325	0.58	26.28	15.69	3.83	6.85	46.92
327	0.57	26.88	16.06	3.80	6.62	43.85
330	0.56	27.35	16.35	3.77	6.42	41.27
333	0.55	28.45	16.96	3.73	6.13	37.52
336	0.54	29.00	17.24	3.70	5.93	35.19
338	0.52	30.07	17.74	3.67	5.66	32.09
341	0.51	30.55	17.95	3.64	5.50	30.24
344	0.50	31.78	18.44	3.61	5.23	27.36
347	0.49	32.27	18.61	3.58	5.08	25.79
350	0.48	32.78	18.78	3.56	4.93	24.28
352	0.48	33.34	18.96	3.53	4.78	22.83
355	0.47	33.57	19.02	3.50	4.67	21.84
358	0.47	33.65	19.05	3.47	4.59	21.08
361	0.47	33.97	19.14	3.45	4.48	20.08
363	0.46	34.38	19.25	3.42	4.36	19.05
366	0.46	34.88	19.38	3.39	4.24	17.97
369	0.45	35.40	19.5	3.37	4.12	16.95
372	0.44	36.10	19.65	3.34	3.98	15.84
375	0.43	36.76	19.78	3.32	3.85	14.83
377	0.43	37.38	19.88	3.29	3.73	13.92
380	0.42	38.10	19.99	3.27	3.61	13
383	0.41	38.68	20.07	3.25	3.50	12.23
386	0.41	39.35	20.14	3.22	3.38	11.46
388	0.40	39.84	20.19	3.20	3.29	10.84
391	0.39	40.29	20.23	3.18	3.21	10.28
394	0.39	40.67	20.26	3.15	3.13	9.789
397	0.39	41.17	20.29	3.13	3.04	9.262
400	0.38	41.47	20.3	3.11	2.98	8.856
402	0.38	41.73	20.31	3.09	2.91	8.493
405	0.38	42.03	20.33	3.07	2.85	8.128
408	0.37	42.28	20.33	3.05	2.79	7.801
411	0.37	42.58	20.34	3.03	2.73	7.466
413	0.37	42.97	20.35	3.01	2.67	7.113
416	0.36	43.37	20.35	2.99	2.60	6.775
419	0.36	43.75	20.35	2.97	2.54	6.46
422	0.35	44.22	20.34	2.95	2.48	6.13
425	0.35	44.66	20.33	2.93	2.41	5.827
427	0.35	44.96	20.32	2.91	2.36	5.584

Wavelength (nm)	Absorbance	Transmittance (%)	Reflectance (%)	Photon Energy(eV)	αhυ	$(\alpha h\upsilon)^2$
430	0.34	45.42	20.3	2.89	2.30	5.303
433	0.34	45.81	20.29	2.87	2.25	5.055
436	0.34	46.12	20.27	2.85	2.20	4.844
438	0.33	46.45	20.25	2.83	2.15	4.634
441	0.33	46.79	20.23	2.82	2.11	4.435
444	0.33	47.17	20.2	2.80	2.06	4.232
447	0.32	47.50	20.17	2.78	2.01	4.052
450	0.32	47.85	20.14	2.76	1.97	3.875
452	0.32	48.33	20.09	2.75	1.92	3.678
455	0.31	49.00	20.02	2.73	1.86	3.455
458	0.30	49.83	19.92	2.71	1.79	3.215
461	0.29	50.94	19.77	2.70	1.72	2.942
464	0.28	52.02	19.6	2.68	1.64	2.697
466	0.27	53.19	19.39	2.67	1.57	2.457
469	0.27	54.11	19.22	2.65	1.51	2.271
472	0.26	54.91	19.06	2.63	1.45	2.113
475	0.26	55.42	18.95	2.62	1.41	2.001
477	0.25	55.73	18.88	2.60	1.38	1.917
480	0.25	55.95	18.83	2.59	1.36	1.848
483	0.25	56.09	18.8	2.57	1.34	1.791
486	0.25	56.21	18.77	2.56	1.32	1.737
489	0.25	56.37	18.74	2.54	1.30	1.682
491	0.25	56.54	18.69	2.53	1.28	1.626
494	0.25	56.76	18.64	2.52	1.25	1.568
497	0.24	57.09	18.57	2.50	1.23	1.502
500	0.24	57.49	18.47	2.49	1.20	1.433
502	0.24	57.99	18.34	2.47	1.17	1.358
505	0.23	58.58	18.19	2.46	1.13	1.279
508	0.23	59.34	18	2.45	1.09	1.192
511	0.22	60.19	17.76	2.43	1.05	1.104
514	0.21	61.18	17.48	2.42	1.01	1.012
516	0.20	62.39	17.12	2.41	0.96	0.912
519	0.20	63.79	16.69	2.39	0.90	0.811
522	0.18	65.33	16.18	2.38	0.84	0.712
525	0.17	67.14	15.56	2.37	0.78	0.61
527	0.16	69.13	14.84	2.36	0.72	0.513
530	0.15	71.19	14.05	2.34	0.65	0.426
533	0.13	73.32	13.2	2.33	0.59	0.348
536	0.12	75.45	12.32	2.32	0.53	0.281
539	0.11	77.41	11.47	2.31	0.48	0.227

Wavelength (nm)	Absorbance	Transmittance (%)	Reflectance (%)	Photon Energy(eV)	αhυ	$(\alpha h\upsilon)^2$
541	0.10	79.24	10.65	2.30	0.43	0.184
544	0.09	80.79	9.945	2.28	0.39	0.151
547	0.09	82.12	9.325	2.27	0.36	0.126
550	0.08	83.18	8.82	2.26	0.33	0.108
552	0.08	84.06	8.4	2.25	0.31	0.094
555	0.07	84.80	8.041	2.24	0.29	0.083
558	0.07	85.34	7.775	2.23	0.27	0.076
561	0.07	85.67	7.611	2.22	0.27	0.07
564	0.07	86.02	7.44	2.21	0.26	0.066
566	0.06	86.45	7.226	2.19	0.25	0.06
569	0.06	86.30	7.302	2.18	0.25	0.06
572	0.06	86.25	7.326	2.17	0.24	0.06
575	0.06	86.19	7.356	2.16	0.24	0.059
577	0.07	86.06	7.419	2.15	0.24	0.059
580	0.06	86.10	7.399	2.14	0.24	0.058
583	0.06	86.12	7.389	2.13	0.24	0.056
586	0.07	86.10	7.402	2.12	0.24	0.055
589	0.06	86.14	7.378	2.11	0.23	0.054
591	0.06	86.18	7.362	2.10	0.23	0.053
594	0.06	86.28	7.312	2.09	0.23	0.051
597	0.06	86.31	7.296	2.08	0.22	0.05
600	0.06	86.54	7.184	2.07	0.22	0.047
603	0.06	86.67	7.117	2.06	0.21	0.045
605	0.06	86.81	7.046	2.05	0.21	0.043
608	0.06	86.88	7.012	2.04	0.21	0.042
611	0.06	87.05	6.929	2.04	0.20	0.04
614	0.06	87.26	6.823	2.03	0.20	0.038
616	0.06	87.53	6.685	2.02	0.19	0.036
619	0.06	87.83	6.532	2.01	0.18	0.033
622	0.05	88.18	6.355	2.00	0.18	0.031
625	0.05	88.54	6.174	1.99	0.17	0.028
628	0.05	88.83	6.026	1.98	0.16	0.026
630	0.05	89.08	5.897	1.97	0.16	0.025
633	0.05	89.61	5.625	1.96	0.15	0.022
636	0.04	90.60	5.114	1.95	0.13	0.017
639	0.04	91.61	4.587	1.95	0.12	0.013
641	0.03	92.38	4.18	1.94	0.10	0.011
644	0.03	92.87	3.917	1.93	0.10	0.009
647	0.03	93.22	3.732	1.92	0.09	0.008
650	0.03	93.34	3.669	1.91	0.09	0.008

Wavelength (nm)	Absorbance	Transmittance (%)	Reflectance (%)	Photon Energy(eV)	αhυ	$(\alpha h\upsilon)^2$
653	0.03	93.44	3.611	1.90	0.09	0.007
655	0.03	93.61	3.523	1.90	0.08	0.007
658	0.03	93.66	3.495	1.89	0.08	0.007
661	0.03	93.71	3.466	1.88	0.08	0.006
664	0.03	93.77	3.439	1.87	0.08	0.006
666	0.03	93.79	3.426	1.87	0.08	0.006
669	0.03	93.87	3.38	1.86	0.08	0.006
672	0.03	93.91	3.361	1.85	0.08	0.006
675	0.03	93.92	3.358	1.84	0.07	0.006
678	0.03	93.89	3.369	1.83	0.07	0.005
680	0.03	93.89	3.371	1.83	0.07	0.005
683	0.03	93.93	3.349	1.82	0.07	0.005
686	0.03	93.89	3.371	1.81	0.07	0.005
689	0.03	93.83	3.404	1.81	0.07	0.005
691	0.03	93.89	3.373	1.80	0.07	0.005
694	0.03	93.78	3.434	1.79	0.07	0.005
697	0.03	93.72	3.465	1.78	0.07	0.005
700	0.03	93.66	3.496	1.78	0.07	0.005
703	0.03	93.60	3.526	1.77	0.07	0.005
705	0.03	93.53	3.564	1.76	0.07	0.005
708	0.03	93.40	3.637	1.76	0.07	0.005
711	0.03	93.32	3.68	1.75	0.07	0.005
714	0.03	93.18	3.754	1.74	0.07	0.006
716	0.03	93.03	3.831	1.73	0.08	0.006
719	0.03	92.89	3.905	1.73	0.08	0.006
722	0.03	92.77	3.971	1.72	0.08	0.006
725	0.03	92.62	4.05	1.72	0.08	0.006
728	0.03	92.47	4.131	1.71	0.08	0.006
730	0.03	92.31	4.215	1.70	0.08	0.007
733	0.04	92.15	4.299	1.70	0.08	0.007
736	0.04	91.99	4.385	1.69	0.08	0.007
739	0.04	91.82	4.471	1.68	0.08	0.007
742	0.04	91.65	4.565	1.68	0.09	0.007
744	0.04	91.45	4.666	1.67	0.09	0.008
747	0.04	91.34	4.726	1.66	0.09	0.008
750	0.04	91.15	4.824	1.66	0.09	0.008
753	0.04	90.99	4.911	1.65	0.09	0.008
755	0.04	90.75	5.033	1.65	0.09	0.008
758	0.04	90.60	5.115	1.64	0.09	0.009
761	0.04	90.34	5.249	1.63	0.09	0.009

Wavelength (nm)	Absorbance	Transmittance (%)	Reflectance (%)	Photon Energy(eV)	αhυ	$(\alpha h\upsilon)^2$
764	0.04	90.23	5.304	1.63	0.10	0.009
767	0.04	90.17	5.338	1.62	0.10	0.009
769	0.05	90.15	5.344	1.62	0.09	0.009
772	0.05	90.15	5.344	1.61	0.09	0.009
775	0.04	90.21	5.316	1.60	0.09	0.009
778	0.04	90.26	5.291	1.60	0.09	0.008
780	0.04	90.33	5.251	1.59	0.09	0.008
783	0.04	90.39	5.221	1.59	0.09	0.008
786	0.04	90.47	5.178	1.58	0.09	0.008
789	0.04	90.55	5.137	1.58	0.09	0.007
792	0.04	90.58	5.125	1.57	0.09	0.007
794	0.04	90.63	5.096	1.56	0.08	0.007
797	0.04	90.69	5.064	1.56	0.08	0.007
800	0.04	90.77	5.024	1.55	0.08	0.007
803	0.04	90.95	4.928	1.55	0.08	0.006
805	0.04	90.95	4.93	1.54	0.08	0.006
808	0.04	91.05	4.879	1.54	0.08	0.006
811	0.04	91.15	4.826	1.53	0.08	0.006
814	0.04	91.26	4.766	1.53	0.07	0.006
817	0.04	91.43	4.681	1.52	0.07	0.005
819	0.04	91.58	4.601	1.52	0.07	0.005
822	0.04	91.71	4.533	1.51	0.07	0.005
825	0.04	91.87	4.445	1.51	0.07	0.005
828	0.04	92.02	4.37	1.50	0.07	0.004
830	0.04	92.16	4.292	1.50	0.06	0.004
833	0.03	92.32	4.209	1.49	0.06	0.004
836	0.03	92.43	4.152	1.49	0.06	0.004
839	0.03	92.62	4.05	1.48	0.06	0.003
842	0.03	92.76	3.974	1.48	0.06	0.003
844	0.03	92.92	3.892	1.47	0.06	0.003
847	0.03	93.07	3.813	1.47	0.05	0.003
850	0.03	93.21	3.738	1.46	0.05	0.003
853	0.03	93.39	3.64	1.46	0.05	0.003
855	0.03	93.51	3.577	1.45	0.05	0.002
858	0.03	93.67	3.488	1.45	0.05	0.002
861	0.03	93.77	3.439	1.44	0.05	0.002
864	0.03	93.89	3.372	1.44	0.05	0.002
867	0.03	93.99	3.319	1.43	0.04	0.002
869	0.03	94.09	3.267	1.43	0.04	0.002
872	0.03	94.13	3.24	1.43	0.04	0.002

Wavelength (nm)	Absorbance	Transmittance (%)	Reflectance (%)	Photon Energy(eV)	αhυ	$(\alpha h\upsilon)^2$
875	0.03	94.26	3.171	1.42	0.04	0.002
878	0.03	94.33	3.134	1.42	0.04	0.002
881	0.03	94.39	3.103	1.41	0.04	0.002
883	0.02	94.45	3.072	1.41	0.04	0.002
886	0.02	94.47	3.059	1.40	0.04	0.002
889	0.02	94.53	3.026	1.40	0.04	0.001
892	0.02	94.57	3.004	1.39	0.04	0.001
894	0.02	94.66	2.957	1.39	0.04	0.001
897	0.02	94.60	2.991	1.39	0.04	0.001
900	0.02	94.62	2.977	1.38	0.04	0.001
903	0.02	94.61	2.985	1.38	0.04	0.001
906	0.02	94.60	2.988	1.37	0.04	0.001
908	0.02	94.62	2.977	1.37	0.04	0.001
911	0.02	94.62	2.979	1.36	0.04	0.001
914	0.02	94.64	2.97	1.36	0.04	0.001
917	0.02	94.54	3.022	1.36	0.04	0.001
919	0.02	94.56	3.008	1.35	0.04	0.001
922	0.02	94.53	3.026	1.35	0.04	0.001
925	0.02	94.47	3.059	1.34	0.04	0.001
928	0.03	94.40	3.098	1.34	0.04	0.001
931	0.03	94.38	3.108	1.34	0.04	0.001
933	0.03	94.27	3.167	1.33	0.04	0.001
936	0.03	94.12	3.246	1.33	0.04	0.001
939	0.03	94.08	3.271	1.32	0.04	0.001
942	0.03	94.04	3.29	1.32	0.04	0.001
944	0.03	94.24	3.185	1.32	0.04	0.001
947	0.03	94.26	3.172	1.31	0.04	0.001
950	0.03	94.33	3.134	1.31	0.03	0.001
953	0.03	94.39	3.102	1.30	0.03	0.001
956	0.03	94.40	3.099	1.30	0.03	0.001
958	0.03	94.33	3.133	1.30	0.03	0.001
961	0.03	94.27	3.17	1.29	0.03	0.001
964	0.03	94.10	3.258	1.29	0.04	0.001
967	0.03	94.04	3.289	1.29	0.04	0.001
969	0.03	93.80	3.422	1.28	0.04	0.001
972	0.03	93.68	3.483	1.28	0.04	0.001
975	0.03	93.36	3.657	1.27	0.04	0.002
978	0.03	93.17	3.756	1.27	0.04	0.002
981	0.03	92.85	3.926	1.27	0.04	0.002
983	0.03	92.69	4.013	1.26	0.04	0.002

Wavelength (nm)	Absorbance	Transmittance (%)	Reflectance (%)	Photon Energy(eV)	αhυ	$(\alpha h\upsilon)^2$
986	0.03	92.27	4.235	1.26	0.04	0.002
989	0.04	91.99	4.383	1.26	0.05	0.002
992	0.04	91.53	4.627	1.25	0.05	0.002
994	0.04	91.06	4.871	1.25	0.05	0.003
997	0.04	90.58	5.124	1.25	0.05	0.003
1000	0.05	89.95	5.449	1.24	0.06	0.003
1003	0.05	89.31	5.782	1.24	0.06	0.004
1006	0.05	88.50	6.195	1.24	0.07	0.004
1008	0.06	87.60	6.651	1.23	0.07	0.005
1011	0.06	86.64	7.13	1.23	0.08	0.006
1014	0.07	85.51	7.691	1.23	0.08	0.007
1017	0.07	84.31	8.276	1.22	0.09	0.008
1020	0.08	83.15	8.836	1.22	0.10	0.009
1022	0.09	82.12	9.327	1.22	0.10	0.01
1025	0.09	80.99	9.851	1.21	0.11	0.012
1028	0.10	80.16	10.24	1.21	0.11	0.013
1031	0.10	79.39	10.59	1.21	0.12	0.014
1033	0.10	78.85	10.83	1.20	0.12	0.014
1036	0.11	78.44	11.01	1.20	0.12	0.015
1039	0.11	78.13	11.15	1.20	0.12	0.015
1042	0.11	77.95	11.23	1.19	0.12	0.015
1045	0.11	77.68	11.35	1.19	0.12	0.016
1047	0.11	77.46	11.45	1.19	0.13	0.016
1050	0.11	77.32	11.51	1.18	0.13	0.016
1053	0.11	77.23	11.55	1.18	0.13	0.016
1056	0.11	77.09	11.61	1.18	0.13	0.016
1058	0.11	76.97	11.66	1.17	0.13	0.016
1061	0.11	76.82	11.73	1.17	0.13	0.016
1064	0.11	76.74	11.76	1.17	0.13	0.016
1067	0.12	76.61	11.82	1.17	0.13	0.016
1070	0.12	76.50	11.87	1.16	0.13	0.016
1072	0.12	76.45	11.89	1.16	0.13	0.016
1075	0.12	76.27	11.97	1.16	0.13	0.016
1078	0.12	76.15	12.02	1.15	0.13	0.016
1081	0.12	75.86	12.14	1.15	0.13	0.016
1083	0.12	75.76	12.18	1.15	0.13	0.016
1086	0.12	75.34	12.36	1.14	0.13	0.017
1089	0.12	75.11	12.46	1.14	0.13	0.017
1092	0.13	74.86	12.57	1.14	0.13	0.017
1095	0.13	74.71	12.63	1.14	0.13	0.017

Wavelength (nm)	Absorbance	Transmittance (%)	Reflectance (%)	Photon Energy(eV)	αhυ	$(\alpha h\upsilon)^2$
1097	0.13	74.26	12.81	1.13	0.13	0.018

4. Optical Properties of PoPD Fabricated at pH value of 2.0

Wavelength (nm)	Absorbance	Transmittance (%)	Reflectance (%)	Photon Energy(eV)	αhυ	$(\alpha h\upsilon)^2$
300	0.32	47.90	20.13	4.15	4.42	19.58
302	0.33	46.89	20.22	4.11	4.47	19.97
305	0.32	47.49	20.17	4.07	4.31	18.62
308	0.41	38.93	20.1	4.04	5.37	28.81
311	0.44	35.97	19.62	4.00	5.71	32.65
314	0.45	35.21	19.46	3.96	5.73	32.84
316	0.47	33.96	19.14	3.93	5.83	33.93
319	0.49	32.23	18.6	3.89	6.00	36.00
322	0.50	31.29	18.25	3.86	6.05	36.62
325	0.51	31.07	18.17	3.83	5.98	35.80
328	0.52	30.35	17.87	3.80	6.00	36.00
330	0.53	29.70	17.57	3.76	6.01	36.08
333	0.52	30.06	17.74	3.73	5.85	34.19
336	0.54	29.14	17.31	3.70	5.90	34.81
339	0.53	29.66	17.56	3.67	5.72	32.71
341	0.53	29.43	17.45	3.64	5.66	32.07
344	0.54	29.06	17.27	3.61	5.63	31.68
347	0.52	29.98	17.7	3.58	5.40	29.16
350	0.52	30.14	17.77	3.55	5.29	27.99
353	0.52	29.92	17.68	3.53	5.24	27.44
355	0.52	30.08	17.75	3.50	5.13	26.36
358	0.52	29.97	17.7	3.47	5.07	25.71
361	0.52	29.93	17.68	3.44	5.00	24.97
364	0.52	29.89	17.66	3.42	4.93	24.27
367	0.53	29.79	17.62	3.39	4.87	23.68
369	0.53	29.64	17.55	3.37	4.81	23.17
372	0.52	29.99	17.71	3.34	4.70	22.05
375	0.52	30.22	17.81	3.32	4.60	21.12
378	0.52	30.37	17.88	3.29	4.51	20.33
380	0.51	30.71	18.02	3.27	4.40	19.38
383	0.51	30.94	18.11	3.24	4.31	18.59
386	0.51	31.14	18.19	3.22	4.23	17.86
389	0.50	31.35	18.27	3.20	4.14	17.16

Wavelength (nm)	Absorbance	Transmittance (%)	Reflectance (%)	Photon Energy(eV)	αhυ	$(\alpha h\upsilon)^2$
392	0.50	31.51	18.33	3.17	4.06	16.52
394	0.50	31.55	18.35	3.15	4.00	16.03
397	0.50	31.78	18.44	3.13	3.92	15.38
400	0.50	31.87	18.47	3.11	3.86	14.89
403	0.50	31.90	18.48	3.09	3.80	14.45
406	0.50	31.94	18.5	3.07	3.75	14.03
408	0.50	31.99	18.51	3.04	3.69	13.62
411	0.49	32.13	18.56	3.02	3.63	13.15
414	0.49	32.15	18.57	3.00	3.58	12.79
417	0.49	32.22	18.59	2.98	3.52	12.39
420	0.49	32.31	18.62	2.96	3.47	12.01
422	0.49	32.36	18.64	2.94	3.42	11.67
425	0.50	31.69	18.4	2.92	3.43	11.79
428	0.50	31.73	18.42	2.91	3.39	11.46
431	0.50	31.73	18.42	2.89	3.34	11.17
433	0.50	31.75	18.42	2.87	3.30	10.87
436	0.50	31.77	18.43	2.85	3.25	10.58
439	0.50	31.89	18.48	2.83	3.20	10.25
442	0.50	31.95	18.5	2.81	3.16	9.96
445	0.49	32.08	18.54	2.80	3.11	9.64
447	0.49	32.16	18.57	2.78	3.06	9.36
450	0.49	32.25	18.6	2.76	3.01	9.09
453	0.49	32.42	18.66	2.74	2.96	8.79
456	0.48	33.38	18.97	2.73	2.85	8.13
459	0.47	33.71	19.07	2.71	2.79	7.79
461	0.47	34.13	19.18	2.69	2.73	7.44
464	0.46	34.59	19.31	2.68	2.66	7.08
467	0.46	34.99	19.4	2.66	2.60	6.76
470	0.45	35.26	19.47	2.65	2.55	6.51
472	0.45	35.51	19.53	2.63	2.50	6.27
475	0.45	35.66	19.56	2.62	2.46	6.07
478	0.45	35.75	19.58	2.60	2.43	5.91
481	0.45	35.80	19.59	2.59	2.40	5.75
484	0.45	35.83	19.6	2.57	2.37	5.61
486	0.45	35.81	19.59	2.56	2.34	5.49
489	0.45	35.85	19.6	2.54	2.31	5.36
492	0.45	35.87	19.6	2.53	2.29	5.23
495	0.44	35.91	19.61	2.51	2.26	5.10
498	0.44	35.97	19.62	2.50	2.23	4.97
500	0.44	36.04	19.64	2.48	2.20	4.84

Wavelength (nm)	Absorbance	Transmittance (%)	Reflectance (%)	Photon Energy(eV)	αhυ	$(\alpha h\upsilon)^2$
503	0.44	36.14	19.66	2.47	2.17	4.71
506	0.44	36.24	19.68	2.46	2.14	4.58
509	0.44	36.37	19.7	2.44	2.11	4.45
511	0.44	36.57	19.74	2.43	2.08	4.31
514	0.43	36.74	19.77	2.42	2.04	4.18
517	0.43	36.92	19.81	2.40	2.01	4.05
520	0.43	37.15	19.85	2.39	1.98	3.91
523	0.43	37.34	19.88	2.38	1.95	3.79
525	0.43	37.53	19.91	2.37	1.92	3.67
528	0.42	37.73	19.94	2.35	1.89	3.56
531	0.42	37.92	19.97	2.34	1.86	3.45
534	0.42	38.07	19.99	2.33	1.83	3.35
537	0.42	38.23	20.01	2.32	1.80	3.25
539	0.42	38.36	20.03	2.30	1.78	3.16
542	0.42	38.42	20.04	2.29	1.76	3.09
545	0.41	38.49	20.05	2.28	1.74	3.01
548	0.41	38.56	20.05	2.27	1.72	2.94
551	0.41	38.63	20.06	2.26	1.69	2.87
553	0.41	38.67	20.07	2.25	1.68	2.81
556	0.40	39.61	20.17	2.24	1.62	2.61
559	0.39	40.47	20.24	2.22	1.56	2.45
562	0.39	40.67	20.26	2.21	1.54	2.37
564	0.39	40.81	20.27	2.20	1.52	2.31
567	0.39	40.91	20.27	2.19	1.50	2.25
570	0.39	40.98	20.28	2.18	1.48	2.20
573	0.39	41.06	20.28	2.17	1.46	2.15
576	0.39	41.06	20.28	2.16	1.45	2.10
578	0.39	41.12	20.29	2.15	1.43	2.06
581	0.39	41.14	20.29	2.14	1.42	2.02
584	0.39	41.17	20.29	2.13	1.40	1.97
587	0.39	41.20	20.29	2.12	1.39	1.93
590	0.38	41.26	20.29	2.11	1.38	1.89
592	0.38	41.31	20.3	2.10	1.36	1.85
595	0.38	41.39	20.3	2.09	1.34	1.81
598	0.38	41.44	20.3	2.08	1.33	1.77
601	0.38	41.49	20.3	2.07	1.32	1.73
603	0.38	41.59	20.31	2.06	1.30	1.69
606	0.38	41.68	20.31	2.05	1.29	1.65
609	0.38	41.77	20.32	2.04	1.27	1.61
612	0.38	41.89	20.32	2.03	1.26	1.58

Wavelength (nm)	Absorbance	Transmittance (%)	Reflectance (%)	Photon Energy(eV)	αhυ	$(\alpha h\upsilon)^2$
615	0.38	42.00	20.32	2.02	1.24	1.54
617	0.38	42.10	20.33	2.01	1.23	1.50
620	0.37	42.22	20.33	2.00	1.21	1.46
623	0.37	42.32	20.33	2.00	1.20	1.43
626	0.37	42.42	20.34	1.99	1.18	1.40
629	0.37	42.52	20.34	1.98	1.17	1.37
631	0.37	42.62	20.34	1.97	1.16	1.33
634	0.37	42.78	20.34	1.96	1.14	1.30
637	0.37	43.02	20.35	1.95	1.12	1.26
640	0.36	43.30	20.35	1.94	1.10	1.22
642	0.36	43.50	20.35	1.93	1.09	1.19
645	0.36	43.64	20.35	1.93	1.08	1.16
648	0.36	43.77	20.35	1.92	1.06	1.13
651	0.36	43.83	20.35	1.91	1.05	1.11
654	0.36	43.88	20.35	1.90	1.04	1.08
656	0.36	43.89	20.35	1.89	1.03	1.06
659	0.36	43.89	20.35	1.89	1.02	1.05
662	0.36	43.96	20.35	1.88	1.01	1.03
665	0.36	43.97	20.35	1.87	1.00	1.01
668	0.36	44.03	20.34	1.86	0.99	0.99
670	0.36	44.00	20.35	1.85	0.99	0.97
673	0.36	44.03	20.34	1.85	0.98	0.96
676	0.36	44.05	20.34	1.84	0.97	0.94
679	0.36	44.03	20.34	1.83	0.96	0.92
681	0.36	44.04	20.34	1.82	0.95	0.91
684	0.36	44.06	20.34	1.82	0.94	0.89
687	0.36	44.07	20.34	1.81	0.94	0.88
690	0.36	44.07	20.34	1.80	0.93	0.86
693	0.36	44.07	20.34	1.79	0.92	0.85
695	0.36	44.04	20.34	1.79	0.92	0.84
698	0.36	44.04	20.34	1.78	0.91	0.82
701	0.36	44.04	20.34	1.77	0.90	0.81
704	0.36	44.06	20.34	1.77	0.89	0.80
707	0.36	44.07	20.34	1.76	0.89	0.79
709	0.36	44.02	20.35	1.75	0.88	0.78
712	0.36	44.00	20.35	1.75	0.87	0.76
715	0.36	43.99	20.35	1.74	0.87	0.75
718	0.36	43.96	20.35	1.73	0.86	0.74
721	0.36	43.97	20.35	1.73	0.85	0.73
723	0.36	43.96	20.35	1.72	0.85	0.72

Wavelength (nm)	Absorbance	Transmittance (%)	Reflectance (%)	Photon Energy(eV)	αhυ	$(\alpha h\upsilon)^2$
726	0.36	43.90	20.35	1.71	0.84	0.71
729	0.36	43.91	20.35	1.71	0.84	0.70
732	0.36	43.89	20.35	1.70	0.83	0.69
734	0.36	43.87	20.35	1.69	0.82	0.68
737	0.36	43.86	20.35	1.69	0.82	0.67
740	0.36	43.88	20.35	1.68	0.81	0.66
743	0.36	43.87	20.35	1.67	0.81	0.65
746	0.36	43.86	20.35	1.67	0.80	0.64
748	0.36	43.82	20.35	1.66	0.80	0.63
751	0.36	43.84	20.35	1.65	0.79	0.62
754	0.36	43.84	20.35	1.65	0.78	0.61
757	0.36	43.79	20.35	1.64	0.78	0.61
760	0.36	43.83	20.35	1.64	0.77	0.60
762	0.36	43.79	20.35	1.63	0.77	0.59
765	0.36	43.77	20.35	1.62	0.76	0.58
768	0.36	43.76	20.35	1.62	0.76	0.57
771	0.36	43.80	20.35	1.61	0.75	0.56
773	0.36	43.84	20.35	1.61	0.74	0.55
776	0.36	43.87	20.35	1.60	0.74	0.55
779	0.36	43.93	20.35	1.60	0.73	0.54
782	0.36	43.95	20.35	1.59	0.73	0.53
785	0.36	43.97	20.35	1.58	0.72	0.52
787	0.36	43.98	20.35	1.58	0.72	0.51
790	0.36	44.05	20.34	1.57	0.71	0.50
793	0.36	44.09	20.34	1.57	0.70	0.49
796	0.35	44.17	20.34	1.56	0.70	0.49
799	0.35	44.18	20.34	1.56	0.69	0.48
801	0.35	44.16	20.34	1.55	0.69	0.47
804	0.35	44.20	20.34	1.55	0.68	0.46
807	0.35	44.21	20.34	1.54	0.68	0.46
810	0.35	44.24	20.34	1.54	0.67	0.45
812	0.35	44.30	20.34	1.53	0.67	0.44
815	0.35	44.34	20.34	1.52	0.66	0.44
818	0.35	44.35	20.34	1.52	0.66	0.43
821	0.35	44.39	20.34	1.51	0.65	0.42
824	0.35	44.40	20.34	1.51	0.65	0.42
826	0.35	44.46	20.34	1.50	0.64	0.41
829	0.35	44.44	20.34	1.50	0.64	0.41
832	0.35	44.50	20.34	1.49	0.63	0.40
835	0.35	44.55	20.33	1.49	0.63	0.39

Wavelength (nm)	Absorbance	Transmittance (%)	Reflectance (%)	Photon Energy(eV)	αhυ	$(\alpha h\upsilon)^2$
838	0.35	44.54	20.34	1.48	0.62	0.39
840	0.35	44.57	20.33	1.48	0.62	0.38
843	0.35	44.60	20.33	1.47	0.61	0.38
846	0.35	44.58	20.33	1.47	0.61	0.37
849	0.35	44.63	20.33	1.46	0.60	0.37
852	0.35	44.66	20.33	1.46	0.60	0.36
854	0.35	44.65	20.33	1.46	0.60	0.36
857	0.35	44.63	20.33	1.45	0.59	0.35
860	0.35	44.68	20.33	1.45	0.59	0.35
863	0.35	44.68	20.33	1.44	0.58	0.34
865	0.35	44.68	20.33	1.44	0.58	0.34
868	0.35	44.71	20.33	1.43	0.58	0.33
871	0.35	44.70	20.33	1.43	0.57	0.33
874	0.35	44.71	20.33	1.42	0.57	0.32
877	0.35	44.74	20.33	1.42	0.57	0.32
879	0.35	44.73	20.33	1.41	0.56	0.32
882	0.35	44.74	20.33	1.41	0.56	0.31
885	0.35	44.74	20.33	1.40	0.55	0.31
888	0.35	44.76	20.33	1.40	0.55	0.30
891	0.35	44.74	20.33	1.40	0.55	0.30
893	0.35	44.76	20.33	1.39	0.54	0.30
896	0.35	44.74	20.33	1.39	0.54	0.29
899	0.35	44.74	20.33	1.38	0.54	0.29
902	0.35	44.72	20.33	1.38	0.53	0.29
904	0.35	44.76	20.33	1.37	0.53	0.28
907	0.35	44.74	20.33	1.37	0.53	0.28
910	0.35	44.72	20.33	1.37	0.52	0.28
913	0.35	44.70	20.33	1.36	0.52	0.27
916	0.35	44.70	20.33	1.36	0.52	0.27
918	0.35	44.68	20.33	1.35	0.52	0.27
921	0.35	44.65	20.33	1.35	0.51	0.26
924	0.35	44.70	20.33	1.35	0.51	0.26
927	0.35	44.68	20.33	1.34	0.51	0.26
930	0.35	44.65	20.33	1.34	0.50	0.25
932	0.35	44.64	20.33	1.33	0.50	0.25
935	0.35	44.61	20.33	1.33	0.50	0.25
938	0.35	44.58	20.33	1.33	0.50	0.25
941	0.35	44.57	20.33	1.32	0.49	0.24
943	0.35	44.60	20.33	1.32	0.49	0.24
946	0.35	44.53	20.34	1.31	0.49	0.24

Wavelength (nm)	Absorbance	Transmittance (%)	Reflectance (%)	Photon Energy(eV)	αhυ	$(\alpha h\upsilon)^2$
949	0.35	44.53	20.34	1.31	0.48	0.24
952	0.35	44.55	20.33	1.31	0.48	0.23
955	0.35	44.53	20.34	1.30	0.48	0.23
957	0.35	44.53	20.34	1.30	0.48	0.23
960	0.35	44.54	20.34	1.29	0.47	0.22
963	0.35	44.52	20.34	1.29	0.47	0.22
966	0.35	44.47	20.34	1.29	0.47	0.22
969	0.35	44.46	20.34	1.28	0.47	0.22
971	0.35	44.40	20.34	1.28	0.46	0.22
974	0.35	44.37	20.34	1.28	0.46	0.21
977	0.35	44.34	20.34	1.27	0.46	0.21
980	0.35	44.32	20.34	1.27	0.46	0.21
982	0.35	44.25	20.34	1.27	0.46	0.21
985	0.35	44.17	20.34	1.26	0.45	0.21
988	0.36	44.11	20.34	1.26	0.45	0.20
991	0.36	44.05	20.34	1.25	0.45	0.20
994	0.36	43.98	20.35	1.25	0.45	0.20
996	0.36	43.87	20.35	1.25	0.45	0.20
999	0.36	43.80	20.35	1.24	0.45	0.20
1002	0.36	43.66	20.35	1.24	0.45	0.20
1005	0.36	43.53	20.35	1.24	0.44	0.20
1008	0.36	43.37	20.35	1.23	0.44	0.20
1010	0.36	43.19	20.35	1.23	0.44	0.20
1013	0.37	43.00	20.35	1.23	0.44	0.20
1016	0.37	42.81	20.34	1.22	0.44	0.20
1019	0.37	42.51	20.34	1.22	0.45	0.20
1022	0.37	42.24	20.33	1.22	0.45	0.20
1024	0.38	41.97	20.32	1.21	0.45	0.20
1027	0.38	41.63	20.31	1.21	0.45	0.20
1030	0.38	41.32	20.3	1.21	0.45	0.20
1033	0.39	41.06	20.28	1.20	0.45	0.20
1035	0.39	40.85	20.27	1.20	0.45	0.20
1038	0.39	40.65	20.26	1.20	0.45	0.20
1041	0.39	40.55	20.25	1.19	0.45	0.20
1044	0.39	40.46	20.24	1.19	0.45	0.20
1047	0.39	40.36	20.24	1.19	0.45	0.20
1049	0.40	40.23	20.23	1.18	0.45	0.20
1052	0.40	40.20	20.22	1.18	0.44	0.20
1055	0.40	40.17	20.22	1.18	0.44	0.20
1058	0.40	40.08	20.21	1.18	0.44	0.19

Wavelength (nm)	Absorbance	Transmittance (%)	Reflectance (%)	Photon Energy(eV)	αhυ	$(\alpha h\upsilon)^2$
1061	0.40	40.01	20.21	1.17	0.44	0.19
1063	0.40	39.96	20.2	1.17	0.44	0.19
1066	0.40	39.78	20.19	1.17	0.44	0.19
1069	0.40	39.83	20.19	1.16	0.43	0.19
1072	0.40	39.78	20.19	1.16	0.43	0.19
1074	0.40	39.71	20.18	1.16	0.43	0.19
1077	0.40	39.62	20.17	1.15	0.43	0.19
1080	0.40	39.56	20.17	1.15	0.43	0.18
1083	0.40	39.47	20.16	1.15	0.43	0.18
1086	0.40	39.36	20.15	1.15	0.43	0.18
1088	0.41	39.21	20.13	1.14	0.43	0.18
1091	0.41	39.12	20.12	1.14	0.43	0.18
1094	0.41	38.93	20.1	1.14	0.43	0.18
1097	0.41	38.82	20.09	1.13	0.42	0.18
1100	0.41	38.54	20.05	1.13	0.43	0.18
1100	0.41	38.54	20.05	1.13	0.43	0.18

5. Optical Properties of PoPD Fabricated at pH value of 9.0

Wavelength (nm)	Absorbance	Transmittance (%)	Reflectance (%)	Photon Energy(eV)	αhυ	$(\alpha h\upsilon)^2$
300	0.34	45.55	20.3	4.15	4.73	22.35
302	0.61	24.39	14.33	4.11	8.33	69.33
305	0.58	26.54	15.85	4.07	7.69	59.09
308	0.64	22.79	12.98	4.04	8.41	70.80
311	0.65	22.19	12.42	4.00	8.41	70.80
314	0.65	22.63	12.84	3.96	8.16	66.51
316	0.66	21.95	12.19	3.93	8.18	66.90
319	0.67	21.51	11.75	3.89	8.14	66.32
322	0.69	20.62	10.81	3.86	8.22	67.62
325	0.68	20.68	10.87	3.83	8.07	65.10
328	0.69	20.34	10.5	3.80	8.01	64.21
330	0.68	20.96	11.18	3.76	7.73	59.77
333	0.69	20.43	10.6	3.73	7.73	59.70
336	0.69	20.27	10.41	3.70	7.64	58.32
339	0.67	21.24	11.47	3.67	7.29	53.17
341	0.66	21.86	12.1	3.64	7.04	49.57
344	0.67	21.55	11.8	3.61	6.99	48.87
347	0.66	22.05	12.29	3.58	6.78	45.93
350	0.64	22.66	12.87	3.55	6.55	42.89

Wavelength (nm)	Absorbance	Transmittance (%)	Reflectance (%)	Photon Energy(eV)	αhυ	$(\alpha h\upsilon)^2$
353	0.64	22.88	13.06	3.53	6.40	41.01
355	0.63	23.36	13.48	3.50	6.22	38.64
358	0.63	23.62	13.71	3.47	6.07	36.88
361	0.62	23.78	13.84	3.44	5.95	35.40
364	0.62	24.01	14.03	3.42	5.82	33.87
367	0.62	24.06	14.07	3.39	5.72	32.77
369	0.62	24.01	14.03	3.37	5.65	31.88
372	0.62	24.14	14.13	3.34	5.54	30.71
375	0.62	24.17	14.16	3.32	5.45	29.74
378	0.62	24.24	14.21	3.29	5.36	28.76
380	0.61	24.27	14.24	3.27	5.28	27.88
383	0.61	24.44	14.37	3.24	5.18	26.81
386	0.61	24.65	14.53	3.22	5.07	25.72
389	0.61	24.83	14.67	3.20	4.97	24.74
392	0.60	25.09	14.86	3.17	4.87	23.68
394	0.60	25.28	14.99	3.15	4.77	22.78
397	0.59	25.55	15.19	3.13	4.67	21.79
400	0.59	25.91	15.44	3.11	4.56	20.77
403	0.58	26.08	15.55	3.09	4.47	20.00
406	0.58	26.39	15.76	3.07	4.37	19.11
408	0.58	26.60	15.89	3.04	4.29	18.38
411	0.57	26.88	16.06	3.02	4.20	17.61
414	0.57	27.03	16.15	3.00	4.12	16.99
417	0.56	27.25	16.29	2.98	4.04	16.33
420	0.56	27.39	16.37	2.96	3.97	15.78
422	0.56	27.51	16.44	2.94	3.91	15.26
425	0.56	27.62	16.5	2.92	3.84	14.78
428	0.56	27.70	16.55	2.91	3.79	14.33
431	0.56	27.68	16.54	2.89	3.74	13.98
433	0.56	27.66	16.53	2.87	3.69	13.64
436	0.56	27.64	16.51	2.85	3.65	13.31
439	0.56	27.62	16.5	2.83	3.60	12.99
442	0.56	27.65	16.52	2.81	3.56	12.64
445	0.56	27.66	16.53	2.80	3.51	12.32
447	0.56	27.67	16.53	2.78	3.47	12.01
450	0.56	27.61	16.5	2.76	3.43	11.76
453	0.56	27.61	16.5	2.74	3.39	11.47
456	0.56	27.65	16.52	2.73	3.34	11.17
459	0.56	27.62	16.5	2.71	3.30	10.91
461	0.55	27.87	16.64	2.69	3.24	10.50

Wavelength (nm)	Absorbance	Transmittance (%)	Reflectance (%)	Photon Energy(eV)	αhυ	$(\alpha h\upsilon)^2$
464	0.54	28.59	17.03	2.68	3.14	9.85
467	0.54	28.75	17.11	2.66	3.09	9.53
470	0.53	29.19	17.34	2.65	3.01	9.08
472	0.52	30.22	17.81	2.63	2.89	8.38
475	0.52	30.53	17.94	2.62	2.84	8.04
478	0.51	30.72	18.02	2.60	2.79	7.77
481	0.51	30.88	18.09	2.59	2.74	7.53
484	0.51	31.03	18.15	2.57	2.70	7.30
486	0.51	31.13	18.19	2.56	2.66	7.09
489	0.50	31.27	18.24	2.54	2.62	6.88
492	0.50	31.41	18.3	2.53	2.58	6.67
495	0.50	31.60	18.37	2.51	2.54	6.46
498	0.50	31.75	18.43	2.50	2.50	6.26
500	0.49	32.03	18.53	2.48	2.46	6.03
503	0.49	32.28	18.61	2.47	2.41	5.82
506	0.49	32.55	18.71	2.46	2.37	5.60
509	0.48	32.82	18.79	2.44	2.32	5.40
511	0.48	33.10	18.88	2.43	2.28	5.20
514	0.48	33.48	19	2.42	2.23	4.99
517	0.47	33.93	19.13	2.40	2.18	4.77
520	0.47	34.26	19.22	2.39	2.14	4.58
523	0.46	34.64	19.32	2.38	2.10	4.39
525	0.46	35.03	19.41	2.37	2.05	4.21
528	0.45	35.37	19.49	2.35	2.01	4.04
531	0.45	35.75	19.58	2.34	1.97	3.88
534	0.44	36.19	19.67	2.33	1.93	3.71
537	0.44	36.43	19.72	2.32	1.89	3.58
539	0.44	36.62	19.75	2.30	1.86	3.48
542	0.43	36.80	19.78	2.29	1.84	3.37
545	0.43	37.14	19.85	2.28	1.80	3.24
548	0.43	37.23	19.86	2.27	1.78	3.16
551	0.43	37.18	19.85	2.26	1.76	3.11
553	0.43	37.28	19.87	2.25	1.74	3.03
556	0.43	37.32	19.87	2.24	1.72	2.96
559	0.43	37.35	19.88	2.22	1.70	2.90
562	0.43	37.36	19.88	2.21	1.68	2.84
564	0.43	37.38	19.88	2.20	1.67	2.78
567	0.43	37.38	19.88	2.19	1.65	2.73
570	0.43	37.38	19.88	2.18	1.63	2.67
573	0.43	37.39	19.89	2.17	1.62	2.62

Wavelength (nm)	Absorbance	Transmittance (%)	Reflectance (%)	Photon Energy(eV)	αhυ	$(\alpha h\upsilon)^2$
576	0.43	37.37	19.88	2.16	1.60	2.57
578	0.43	37.35	19.88	2.15	1.59	2.53
581	0.43	37.35	19.88	2.14	1.57	2.48
584	0.43	37.35	19.88	2.13	1.56	2.43
587	0.43	37.36	19.88	2.12	1.54	2.38
590	0.43	37.40	19.89	2.11	1.53	2.33
592	0.43	37.43	19.89	2.10	1.51	2.29
595	0.43	37.47	19.9	2.09	1.50	2.24
598	0.43	37.52	19.91	2.08	1.48	2.19
601	0.43	37.56	19.91	2.07	1.47	2.15
603	0.42	37.65	19.93	2.06	1.45	2.10
606	0.42	37.73	19.94	2.05	1.43	2.05
609	0.42	37.77	19.94	2.04	1.42	2.01
612	0.42	37.89	19.96	2.03	1.40	1.96
615	0.42	37.99	19.98	2.02	1.38	1.91
617	0.42	38.07	19.99	2.01	1.37	1.87
620	0.42	38.15	20	2.00	1.35	1.83
623	0.42	38.24	20.01	2.00	1.34	1.79
626	0.42	38.33	20.02	1.99	1.32	1.75
629	0.42	38.39	20.03	1.98	1.31	1.71
631	0.41	38.50	20.05	1.97	1.29	1.67
634	0.41	38.55	20.05	1.96	1.28	1.64
637	0.41	38.66	20.07	1.95	1.26	1.60
640	0.41	38.79	20.08	1.94	1.25	1.56
642	0.41	38.88	20.09	1.93	1.24	1.53
645	0.41	38.97	20.1	1.93	1.22	1.49
648	0.41	39.05	20.11	1.92	1.21	1.46
651	0.41	39.09	20.12	1.91	1.20	1.43
654	0.41	39.11	20.12	1.90	1.19	1.41
656	0.41	39.10	20.12	1.89	1.18	1.38
659	0.41	39.12	20.12	1.89	1.17	1.36
662	0.41	39.14	20.12	1.88	1.16	1.34
665	0.41	39.15	20.12	1.87	1.15	1.31
668	0.41	39.14	20.12	1.86	1.14	1.29
670	0.41	39.15	20.12	1.85	1.13	1.27
673	0.41	39.15	20.12	1.85	1.12	1.25
676	0.41	39.14	20.12	1.84	1.11	1.23
679	0.41	39.11	20.12	1.83	1.10	1.21
681	0.41	39.12	20.12	1.82	1.09	1.19
684	0.41	39.11	20.12	1.82	1.08	1.17

Wavelength (nm)	Absorbance	Transmittance (%)	Reflectance (%)	Photon Energy(eV)	αhυ	$(\alpha h\upsilon)^2$
687	0.41	39.10	20.12	1.81	1.07	1.15
690	0.41	39.08	20.12	1.80	1.07	1.14
693	0.41	39.06	20.11	1.79	1.06	1.12
695	0.41	39.01	20.11	1.79	1.05	1.10
698	0.41	38.98	20.1	1.78	1.04	1.09
701	0.41	38.97	20.1	1.77	1.04	1.07
704	0.41	38.96	20.1	1.77	1.03	1.06
707	0.41	38.90	20.1	1.76	1.02	1.04
709	0.41	38.88	20.09	1.75	1.01	1.03
712	0.41	38.83	20.09	1.75	1.01	1.01
715	0.41	38.80	20.08	1.74	1.00	1.00
718	0.41	38.76	20.08	1.73	0.99	0.99
721	0.41	38.74	20.08	1.73	0.99	0.97
723	0.41	38.69	20.07	1.72	0.98	0.96
726	0.41	38.62	20.06	1.71	0.97	0.95
729	0.41	38.59	20.06	1.71	0.97	0.94
732	0.41	38.53	20.05	1.70	0.96	0.92
734	0.41	38.50	20.05	1.69	0.96	0.91
737	0.42	38.45	20.04	1.69	0.95	0.90
740	0.42	38.43	20.04	1.68	0.94	0.89
743	0.42	38.38	20.03	1.67	0.94	0.88
746	0.42	38.33	20.02	1.67	0.93	0.87
748	0.42	38.27	20.02	1.66	0.93	0.86
751	0.42	38.25	20.01	1.65	0.92	0.85
754	0.42	38.23	20.01	1.65	0.91	0.83
757	0.42	38.18	20	1.64	0.91	0.82
760	0.42	38.16	20	1.64	0.90	0.81
762	0.42	38.09	19.99	1.63	0.90	0.80
765	0.42	38.04	19.98	1.62	0.89	0.79
768	0.42	38.00	19.98	1.62	0.89	0.78
771	0.42	38.02	19.98	1.61	0.88	0.77
773	0.42	38.04	19.98	1.61	0.87	0.76
776	0.42	38.02	19.98	1.60	0.87	0.75
779	0.42	38.06	19.99	1.60	0.86	0.74
782	0.42	38.07	19.99	1.59	0.85	0.73
785	0.42	38.06	19.99	1.58	0.85	0.72
787	0.42	38.06	19.99	1.58	0.84	0.71
790	0.42	38.12	20	1.57	0.83	0.70
793	0.42	38.16	20	1.57	0.83	0.68
796	0.42	38.19	20	1.56	0.82	0.67

Wavelength (nm)	Absorbance	Transmittance (%)	Reflectance (%)	Photon Energy(eV)	αhυ	$(\alpha h\upsilon)^2$
799	0.42	38.22	20.01	1.56	0.81	0.66
801	0.42	38.23	20.01	1.55	0.81	0.65
804	0.42	38.25	20.01	1.55	0.80	0.64
807	0.42	38.28	20.02	1.54	0.80	0.63
810	0.42	38.33	20.02	1.54	0.79	0.62
812	0.42	38.37	20.03	1.53	0.78	0.61
815	0.42	38.42	20.04	1.52	0.78	0.60
818	0.42	38.44	20.04	1.52	0.77	0.59
821	0.41	38.48	20.04	1.51	0.77	0.59
824	0.41	38.52	20.05	1.51	0.76	0.58
826	0.41	38.56	20.05	1.50	0.75	0.57
829	0.41	38.61	20.06	1.50	0.75	0.56
832	0.41	38.66	20.07	1.49	0.74	0.55
835	0.41	38.68	20.07	1.49	0.74	0.54
838	0.41	38.72	20.07	1.48	0.73	0.53
840	0.41	38.76	20.08	1.48	0.72	0.53
843	0.41	38.81	20.08	1.47	0.72	0.52
846	0.41	38.83	20.09	1.47	0.71	0.51
849	0.41	38.87	20.09	1.46	0.71	0.50
852	0.41	38.91	20.1	1.46	0.70	0.49
854	0.41	38.90	20.09	1.46	0.70	0.49
857	0.41	38.91	20.1	1.45	0.69	0.48
860	0.41	38.96	20.1	1.45	0.69	0.47
863	0.41	38.98	20.1	1.44	0.68	0.47
865	0.41	39.02	20.11	1.44	0.68	0.46
868	0.41	39.05	20.11	1.43	0.67	0.45
871	0.41	39.04	20.11	1.43	0.67	0.45
874	0.41	39.06	20.11	1.42	0.66	0.44
877	0.41	39.09	20.12	1.42	0.66	0.44
879	0.41	39.12	20.12	1.41	0.66	0.43
882	0.41	39.13	20.12	1.41	0.65	0.42
885	0.41	39.12	20.12	1.40	0.65	0.42
888	0.41	39.17	20.13	1.40	0.64	0.41
891	0.41	39.15	20.12	1.40	0.64	0.41
893	0.41	39.16	20.12	1.39	0.63	0.40
896	0.41	39.14	20.12	1.39	0.63	0.40
899	0.41	39.17	20.13	1.38	0.63	0.39
902	0.41	39.17	20.13	1.38	0.62	0.39
904	0.41	39.16	20.12	1.37	0.62	0.38
907	0.41	39.18	20.13	1.37	0.61	0.38

Wavelength (nm)	Absorbance	Transmittance (%)	Reflectance (%)	Photon Energy(eV)	αhυ	$(\alpha h\upsilon)^2$
910	0.41	39.17	20.13	1.37	0.61	0.37
913	0.41	39.17	20.12	1.36	0.61	0.37
916	0.41	39.16	20.12	1.36	0.60	0.36
918	0.41	39.16	20.12	1.35	0.60	0.36
921	0.41	39.15	20.12	1.35	0.60	0.36
924	0.41	39.17	20.13	1.35	0.59	0.35
927	0.41	39.15	20.12	1.34	0.59	0.35
930	0.41	39.14	20.12	1.34	0.59	0.34
932	0.41	39.10	20.12	1.33	0.58	0.34
935	0.41	39.10	20.12	1.33	0.58	0.34
938	0.41	39.08	20.12	1.33	0.58	0.33
941	0.41	39.05	20.11	1.32	0.57	0.33
943	0.41	39.04	20.11	1.32	0.57	0.33
946	0.41	39.00	20.11	1.31	0.57	0.32
949	0.41	38.99	20.11	1.31	0.56	0.32
952	0.41	38.99	20.11	1.31	0.56	0.32
955	0.41	38.99	20.11	1.30	0.56	0.31
957	0.41	39.01	20.11	1.30	0.55	0.31
960	0.41	38.98	20.1	1.29	0.55	0.30
963	0.41	38.96	20.1	1.29	0.55	0.30
966	0.41	38.92	20.1	1.29	0.55	0.30
969	0.41	38.90	20.09	1.28	0.54	0.30
971	0.41	38.83	20.09	1.28	0.54	0.29
974	0.41	38.82	20.09	1.28	0.54	0.29
977	0.41	38.77	20.08	1.27	0.54	0.29
980	0.41	38.75	20.08	1.27	0.53	0.28
982	0.41	38.67	20.07	1.27	0.53	0.28
985	0.41	38.61	20.06	1.26	0.53	0.28
988	0.41	38.53	20.05	1.26	0.53	0.28
991	0.41	38.47	20.04	1.25	0.53	0.28
994	0.42	38.38	20.03	1.25	0.52	0.27
996	0.42	38.29	20.02	1.25	0.52	0.27
999	0.42	38.18	20	1.24	0.52	0.27
1002	0.42	38.06	19.99	1.24	0.52	0.27
1005	0.42	37.91	19.97	1.24	0.52	0.27
1008	0.42	37.72	19.94	1.23	0.52	0.27
1010	0.43	37.55	19.91	1.23	0.52	0.27
1013	0.43	37.34	19.88	1.23	0.52	0.27
1016	0.43	37.09	19.84	1.22	0.52	0.27
1019	0.43	36.78	19.78	1.22	0.52	0.27

Wavelength (nm)	Absorbance	Transmittance (%)	Reflectance (%)	Photon Energy(eV)	αhυ	$(\alpha h\upsilon)^2$
1022	0.44	36.50	19.73	1.22	0.52	0.27
1024	0.44	36.14	19.66	1.21	0.52	0.27
1027	0.45	35.79	19.59	1.21	0.53	0.28
1030	0.45	35.46	19.51	1.21	0.53	0.28
1033	0.45	35.18	19.45	1.20	0.53	0.28
1035	0.46	34.91	19.38	1.20	0.53	0.28
1038	0.46	34.69	19.33	1.20	0.53	0.28
1041	0.46	34.54	19.29	1.19	0.53	0.28
1044	0.46	34.38	19.25	1.19	0.53	0.28
1047	0.47	34.23	19.21	1.19	0.53	0.28
1049	0.47	34.14	19.19	1.18	0.53	0.28
1052	0.47	34.04	19.16	1.18	0.53	0.28
1055	0.47	33.96	19.14	1.18	0.52	0.27
1058	0.47	33.86	19.11	1.18	0.52	0.27
1061	0.47	33.77	19.08	1.17	0.52	0.27
1063	0.47	33.71	19.07	1.17	0.52	0.27
1066	0.47	33.56	19.02	1.17	0.52	0.27
1069	0.47	33.56	19.02	1.16	0.52	0.27
1072	0.47	33.50	19	1.16	0.51	0.26
1074	0.48	33.46	18.99	1.16	0.51	0.26
1077	0.48	33.37	18.97	1.15	0.51	0.26
1080	0.48	33.33	18.95	1.15	0.51	0.26
1083	0.48	33.19	18.91	1.15	0.51	0.26
1086	0.48	33.14	18.9	1.15	0.51	0.26
1088	0.48	33.00	18.85	1.14	0.51	0.26
1091	0.48	32.98	18.85	1.14	0.50	0.25
1094	0.48	32.88	18.81	1.14	0.50	0.25
1097	0.48	32.78	18.78	1.13	0.50	0.25
1100	0.49	32.64	18.74	1.13	0.50	0.25